The
PHILOSOPHICAL
MAGAZINE

FIRST PUBLISHED IN 1798

L. 46 SEVENTH SERIES No. 375 April 1955

UNIVERSITY OF HAWAII
LIBRARY
JUN 2 '55

A Journal of
Theoretical Experimental
and Applied Physics

EDITOR
PROFESSOR N. F. MOTT, M.A., D.Sc., F.R.S.

EDITORIAL BOARD
SIR LAWRENCE BRAGG, O.B.E., M.C., M.A., D.Sc., F.R.S.
SIR GEORGE THOMSON, M.A., D.Sc., F.R.S.
PROFESSOR A. M. TYNDALL, C.B.E., D.Sc., F.R.S.

PRICE 15s. 0d.
Annual Subscription £8 0s. 0d. payable in advance

D AND PUBLISHED BY TAYLOR & FRANCIS LTD., RED LION COURT, FLEET ST., LONDON, E.C.4.

Commemoration Number

To mark the 150th Anniversary of the

PHILOSOPHICAL MAGAZINE

Natural Philosophy through the Eighteenth Century & Allied Topics

CONTENTS

The Philosophical Magazine. By ALLAN FERGUSON, M.A., D.Sc., and JOHN FERGUSON, M.A., B.D.

Astronomy through the Eighteenth Century. By Sir H. SPENCER-JONES, F.R.S.

Physics in the Eighteenth Century. By Prof. HERBERT DINGLE, D.Sc.

Chemistry through the Eighteenth Century. By Prof. J. R. PARTINGTON, D.Sc.

Mathematics through the Eighteenth Century. By J. F. SCOTT, Ph.D.

Engineering and Invention in the Eighteenth Century. By Engineer-Captain EDGAR C. SMITH, O.B.E., R.N.

Scientific Instruments in the Eighteenth Century. By ROBERT S. WHIPPLE, M.I.E.E., F.Inst.P.

The Scientific Periodical from 1665 to 1798. By DOUGLAS McKIE, D.Sc., Ph.D.

Scientific Societies to the end of the Eighteenth Century. By DOUGLAS McKIE, D.Sc., Ph.D.

The Teaching of the Physical Sciences at the end of the Eighteenth Century. By F. SHERWOOD TAYLOR, Ph.D.

ALERE FLAMMAM

viii + 164 pages

15/6

POST FREE

TAYLOR & FRANCIS, LTD.

RED LION COURT, FLEET ST., LONDON, E.C.4

PRINTERS & PUBLISHERS FOR OVER 150 YEARS

XLV. *The Effect of Discontinuous Space Charge on Rectifier Characteristics*

By G. G. Wiles
University of the Witwatersrand, Johannesburg*

[Received in revised form November 24, 1954]

Summary

The paper is theoretical. An expression is derived for the local current density in the blocking direction near any impurity centre that happens to be situated at an optimum distance from the metal. Numerical examples are given. The effects of these large local currents on the average current through the interface is evaluated in the case of a uniform distribution of impurity centres. When the semi-conductor has a dielectric constant of 10 the error at room temperature caused by assuming the usual continuous distribution of space charge is found to be very small with 10^{16} impurity centres per cm^3, but becomes appreciable at 10^{18}. The case of a random distribution is treated by a more approximate method but this is considered to be a more satisfactory method than that used by Schottky. The results are much the same as for the case of a uniform distribution.

§ 1. The Continuous Space-Charge Approximation

When a suitable metal and semi-conductor are in contact the well-known Schottky potential barrier (Schottky 1939) is formed by the charged impurity centres in the semi-conductor. The space charge is often regarded as a continuous uniform distribution of charge. When this approximation is made we have a field whose intensity F near the metal is given by

$$F^2=8\pi Ne(V_w+V_a)/\epsilon \qquad \text{. . . . . . (1)}$$

where N is the number of impurity centres per cm^3, e is the electronic charge, ϵ is the dielectric constant of the semi-conductor, V_a is the potential applied externally in the blocking direction, and eV_w is approximately the height of the barrier when no current is flowing. Throughout this paper the symbol F will denote the field defined by eqn. (1). If zero potential is chosen at the energy level of the bottom of the conduction band of the semi-conductor when this is isolated and uncharged, then the potential V at a distance x not too far from the metal is

$$V=Fx \qquad \text{. . . . . (2)}$$

as in fig. 1. The barrier reaches its maximum height at the interface $x=0$ and the potential there is $V=0$.

---

* Communicated by the Author.

On the diode theory of Bethe (1942) the electrons are considered to have a sufficiently long mean free path to pass right across the barrier without suffering collisions. When $eV_w \gg kT$, the current J per cm^2 is given by

$$2J/n_0ev_0=\exp(-eV_a/kT)-1 \qquad . \quad . \quad . \quad . \quad (3)$$

where k is Boltzmann's constant and T is the absolute temperature. The symbol v_0 is the average velocity of an electron in one direction in a Maxwellian distribution and so is equal to $(2kT/\pi m)^{1/2}$ where m is the mass of an electron. The symbol n_0 denotes the number of carriers per cm^3 in the conduction band at $x=0$.

Fig. 1

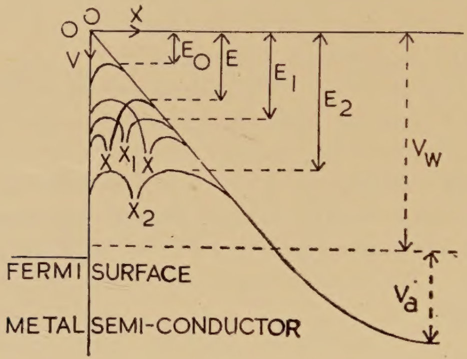

The top of the barrier due to a continuous uniform distribution of space charge is at the potential $V=0$. The image face lowers the barrier to E_0. An impurity centre in either of the positions $x=X$ lowers the barrier to E. An impurity centre at the optimum position X_1 lowers the barrier to E_1. Two impurity centres near X_2 lower the barrier to E_2.

On the diffusion theory of Mott (1939) the electrons are considered to have a short mean free path so that they suffer many collisions while passing across the barrier. In this case the current density J is given by

$$J/n_0ev_1F=\exp(-eV_a/kT)-1 \qquad . \quad . \quad . \quad . \quad (4)$$

where v_1 is the mobility of the electrons.

§ 2. The Effect of Lowering the Potential Barrier

The image force produces in effect a lowering of the top of the barrier from $V=0$ to $V=E_0$ as in figs. 1 and 2. An impurity centre situated near the interface produces a further lowering in its vicinity from $V=E_0$ to $V=E$.

This paper is concerned with single carrier theories of rectification. On the diode theory the effect of lowering the top of the barrier from 0 to E_0 is to increase the current density from the value J given in eqn. (3) to the value j_0 given by $j_0/J=\exp(eE_0/kT)$. The effect of lowering the top of the barrier from E_0 to E is to increase the local current density from j_0 to j given by

$$j/j_0=\exp\,[e(E-E_0)/kT]. \qquad (5)$$

On the diffusion theory the effect of lowering the top of the barrier from 0 to E_0 is to increase the current density from the value J given in eqn. (4) to the value j_0 given by

$$j_0/J=kT[eF\int \exp\,(-eV/kT)\,dx]^{-1} \qquad (6)$$

where the integration extends across the whole barrier. Similarly the effect of lowering the top of the barrier from E_0 to E is to increase the local current density from j_0 to j given by

$$j/J=kT[eF\int \exp\,(-eV/kT)\,dx]^{-1}. \qquad (7)$$

Equation (6) is derived by dividing the more familiar equation

$$j_0\int \exp\,(-eV/kT)\,dx=n_0v_1kT[\exp\,(-eV_a/kT)-1]$$

by eqn. (4). Equation (7) is derived similarly.

Fig. 2

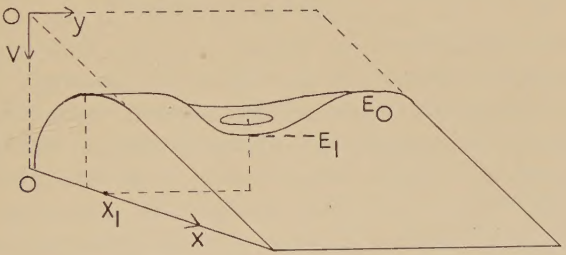

The potential barrier at points in a plane z=constant. An impurity centre lies in this plane at the optimum distance X_1 from the metal interface $x=0$.

The integral in eqn. (6) across the barrier lowered by image force has been considered by Landsberg (1951) and by Billig (1951). However, the barrier referred to in eqn. (7) is of a more general shape and will sometimes have two maxima as seen in figs. 1 and 2. We can find the order of magnitude of the integral across this barrier by using $V=E$ in the range $x=0$ to $x=E/F$, and $V=Fx$ from eqn. (2) in the range $x=E/F$ to $x=\infty$. Using this method of approximation in both (6) and (7) we can divide (7) by (6) and find

$$j/j_0\doteq a\exp\,[e(E-E_0)/kT] \qquad (8)$$

where a is the comparatively unimportant factor

$$a=(eE_0+kT)(eE+kT)^{-1}.$$

We conclude from eqns. (5) and (8) that as far as orders of magnitude are concerned the effect of lowering a barrier from the general level

$V=E_0$ to a local level $V=E$ in the vicinity of an impurity centre is to increase the current density from the general value j_0 to a local value j given by eqn. (5).

§ 3. THE EFFECT OF ONE IMPURITY CENTRE

Let a point be chosen on the interface between the metal and the semiconductor so that the normal from this point does not pass close to any impurity centre. Then fig. 1 shows how the maximum of the barrier along this normal is depressed by the image force from $V=0$ to $V=E_0$ giving rise to a current density j_0. Let another normal be chosen so as to pass through an impurity centre at a distance X from the interface. Figure 1 shows how the maximum of the barrier along this normal is depressed into two maxima, one on each side of the potential well at $x=X$. We denote the potential at the higher of the two maxima by E and the local current density there by j.

There is an optimum position $x=X_1$ for the impurity centre which makes the levels of the two maxima the same. We denote this level as $V=E_1$. This is the lowest level to which an impurity centre can depress the barrier. For if the impurity centre lies further from the metal then the barrier is higher than E_1 on the metal side of the well. If the impurity centre lies closer to the metal then the barrier is higher than E_1 on the side away from the metal. It follows that when the impurity centre lies at the optimum distance X_1 then the local current density has the largest value j_1 that is possible near a single impurity centre. Figure 1 indicates this situation and fig. 2 shows more detail. The interface is the plane $x=0$ and the barrier is shown for points in the plane $z=$constant that passes through the impurity centre. On this representation the effect of the impurity centre shows up as a saddle-shaped pass through the barrier with a well at the top of the pass. We shall now calculate the local current density j_1 due to electrons that make their way through the pass.

By analogy with eqn. (5) or (8) the current density j_1 is given in terms of the current j_0 by

$$j_1/j_0=\exp\left[e(E_1-E_0)/kT\right]. \quad . \quad . \quad . \quad . \quad (9)$$

To evaluate this we need expressions for E_0 and E_1. To find E_0 we add a term $e/4\epsilon x$ to the V of eqn. (2) so as to allow for the image force. The barrier has its maximum where V has its minimum, and this occurs at $x=(e/4\epsilon F)^{1/2}$. This gives at the maximum of the barrier the potential

$$E_0=(eF/\epsilon)^{1/2}. \quad . \quad . \quad . \quad . \quad . \quad . \quad . \quad . \quad (10)$$

To find E_1 we consider the potential along the normal that passes through the impurity centre at X_1. We regard the field near $x=0$ as consisting of two parts. Firstly there is the part $2e/\epsilon X_1^2$ due to the impurity centre at X_1 and its image at $-X_1$. Secondly there is the part F_1 due to all the other impurity centres and their images. In practical cases F_1 is not very different from F. The potential along the normal can now be written approximately as

$$V=(2e/\epsilon X_1^2+F_1)x+e/4\epsilon x, \qquad x<X_1,$$

$$V=e/\epsilon(x-X_1)+F_1x, \qquad x>X_1.$$

In the case $x<X_1$ the last term is the contribution due to the image force. This approximation for V is reasonable near the minimum of V although it breaks down when x approaches either 0 or X_1. In the case $x>X_1$ the terms due to the image force and due to the image of the impurity centre have been neglected. By equating the minimum of V when $x<X_1$ to the minimum of V when $x>X_1$ we find the optimum position X_1 to be $X_1=c_1(e/4\epsilon F_1)^{1/2}$ where c_1 is a solution of the quartic $c_1^4+8c_1^3+12c_1^2=32$ which gives the value $c_1=1{\cdot}18$. Since $(e/4\epsilon F)^{1/2}$ is the value of x where the barrier has its maximum when a continuous distribution of charge is assumed, we see that the optimum position X_1 for a single impurity centre is just beyond this maximum as shown in fig. 2. Using this value of X_1 we find the value of the potential at the maxima to be

$$E_1=(2+\tfrac{1}{2}c_1)(eF_1/\epsilon)^{1/2}. \qquad \ldots\ldots \quad (11)$$

We have derived the current j_1 near a single impurity centre lying at the optimum distance from the metal. If this centre is part of a uniform distribution of centres then the closest neighbours will be at a distance of about $N^{-1/3}$ or more. Hence we draw a sphere OA of volume $1/N$ that touches the interface at O with its diameter OA passing through the impurity centre at X_1. We assume that all the other impurity centres can be represented by a continuous uniform distribution of space charge outside the sphere. This space charge and its image produce the field F_1. Since the radius of the sphere is $(4\pi N/3)^{-1/3}$ the appropriate value for F_1 is

$$F_1=F-2(e/\epsilon)(4\pi N/3)^{2/3}. \qquad \ldots\ldots\ldots \quad (12)$$

Some numerical values calculated for a uniform distribution with $\epsilon=10$ at 17°C are shown in table 1. The first column gives the concentration of the impurity centres, N. The second gives approximately the applied voltage V_a. The third shows the optimum distance X_1 where the single impurity centre is lying so as to produce its maximum effect. This column also gives an idea of the size of the pass since the length of the pass across the well from one maximum to the other is about $2{\cdot}3X_1$. The width of the pass at the same energy level is much the same. The fourth column shows the depth of the pass from the crest of the barrier E_0 down to the mouth of the well E_1. This is about $1{\cdot}6E_0$. The last column shows j_1/j_0. Here we see the tremendous increase in the current density that can occur in the immediate neighbourhood of an impurity centre when this happens to lie at its optimum distance from the metal.

The values in table 1 refer of course only to the case $\epsilon=10$ at 17°C. Values of j_1/j_0 at other values of ϵ and at other temperatures can, however, be inferred from table 1. For the value of j_1/j_0 remains practically the same under different conditions provided $N(V_w+V_a)/\epsilon^3T^4$ remains the same. For example the value $j_1/j_0=6200$ given for $V_w+V_a=50$ volts will also be the value for $V_w+V_a=5$ volts if $N=10^{18}$ or if $\epsilon=4{\cdot}6$ or if $T=163$°K.

Table 1

N (per cm^3)	V_w+V_a (volts)	X_1 (angströms)	Depth of pass (electron volts)	j_1/j_0 —
10^{16}	1	30	0·07	6
	97	9	0·24	340
10^{17}	1	17	0·13	22
	20	8	0·28	990
	50	6	0·36	6200
10^{18}	1	10	0·22	200
	12	5	0·44	40000
	22	4	0·51	270000

§ 4. THE EFFECT OF A UNIFORM DISTRIBUTION OF IMPURITY CENTRES.

In view of the very large current density j_1 that can be obtained near an impurity centre, the question arises as to whether the average current density over a large area of interface is anywhere near equal to the current density j_0 calculated on the usual assumption of a continuous uniform distribution of space charge. In this section we shall examine the average current density j_u when the impurity centres are distributed uniformly through the semi-conductor. In § 5 we shall examine the average current density j_r when the impurity centres are distributed at random.

With either of these distributions we see from eqn. (5) that the ratio j_u/j_0 or j_r/j_0 is equal to

$$\frac{\text{average value of }\exp\,(eE/kT)}{\exp\,(eE_0/kT)} \quad . \quad . \quad . \quad . \quad . \quad (13)$$

where E is the minimum value of V along the normal drawn at each surface element of the interface. With either distribution we can choose any arbitrary point O on the interface and draw a sphere OA of volume $1/N$ to touch the interface at O (see figs. 3 and 4). We can then assume that as far as potentials in the neighbourhood of O are concerned, all the impurity centres outside the sphere can be treated as a continuous distribution of charge outside the sphere. Inside the sphere there may be no impurity centre, or one, or more than one. If the point O is allowed to move to many different points on the interface, the average number of impurity centres in the sphere will be one.

In this section we shall assume that the continuous distribution of charge outside the sphere OA is uniform so that it produces near the interface a constant field F_1 given by eqn. (12). We shall find the average current density j_u through those parts of the interface for which the number of impurity centres inside the sphere OA is one. We shall call j_u the average current density given by a uniform distribution of impurity centres for the following reason.

Fig. 3

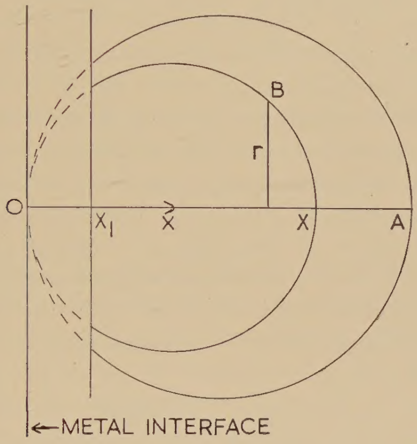

The sphere OA contains on the average one impurity centre. If this impurity centre lies anywhere on the surface XB it produces a barrier of the same height along the line OA.

Fig. 4

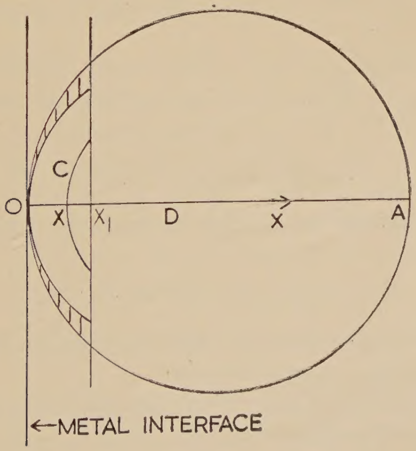

OA is the same sphere as in fig. 3. If an impurity centre lies anywhere on the surface XC it produces a barrier of the same height along the line OA. A centre in the shaded region does not affect the barrier height along OA appreciably.

The first approximation in existing theories is based on the assumption of a continuous uniform distribution of space charge. A better approximation is obtained by allowing the charge e distributed through the sphere OA to condense to a point charge e somewhere within the sphere. The limitations implied in this approximation are (a) that the field due to distant centres is constant over the interface, and (b) that only one centre contributes to the formation of each pass across the barrier. Now these are just the limitations that would be imposed by a distribution of centres that is uniform instead of random. For a distribution of points may be regarded as uniform when (a) there are no large scale fluctuations in the concentration of the points, and (b) no two points are separated by a distance of less than about $N^{-1/3}$.

It is assumed in the calculation of j_u that the probability of occupation by the impurity centre is the same for all points within the sphere OA. This is equivalent to a third limitation on the distribution of the centres, for it excludes distributions in which the centres are arranged in a regular pattern. If the centres were arranged in a regular pattern there would generally be an unduly large number or else an unduly small number of centres lying in the critical region near the plane $x=X_1$.

In the calculation of j_u/j_0 from the expression (13) the average value of $\exp\,(eE/kT)$ is

$$N \int \exp(eE/kT)\, dv \qquad \dots\dots \quad (14)$$

where E is the minimum value of V along the diameter OA when the impurity centre lies within the volume element dv. The integration extends through the sphere OA and the factor N comes in as the reciprocal of the volume of the sphere. To perform the integration it is convenient to consider firstly the part of the sphere beyond the plane $x=X_1$ as in fig. 3, and secondly the part between the interface and the plane $x=X_1$ as in fig. 4.

Firstly, then, the impurity centre lies in the sphere to the right of the plane $x=X_1$ as in fig. 3. When it lies on the line OA at a point $x=X$, then the field near O is $2e/\epsilon X^2+F_1$ so that the potential is

$$V=(2e/\epsilon X^2+F_1)x+e/4\epsilon x.$$

The minimum value of this is found with the help of the expression above for X_1 to be

$$E=(1+8X_1^2/c_1^2X^2)^{1/2}(eF_1/\epsilon)^{1/2}. \qquad \dots\dots \quad (15)$$

As a check we can use the quartic defining c_1 to find that when $X=X_1$, E reduces to E_1 given by (11) as it should.

When the impurity centre lies off the line OA at a distance r from OA it still gives with its image the same field at O provided it lies on the surface $r^2=X^{4/3}x^{2/3}-x^2$. This surface is very similar to the sphere $r^2=Xx-x^2$, both being surfaces of revolution about the line OA cutting OA normally at $x=0$ and $x=X$. Hence when the impurity centre lies to the right of the plane $x=X_1$ between two neighbouring spheres of diameters X and $X+dX$ then E is given by eqn. (15). The volume element between the spheres is

$$dv=(\pi/2)(X^2-X_1^2)\,dX.$$

The integration goes from $X=X_1$ to $X=\mathrm{OA}$. This contribution to the integral in (14) was evaluated numerically.

Secondly the impurity centre lies in the sphere OA to the left of the plane $x=X_1$ in fig. 4. When it lies on the line OA at any point $x=X$ we assume for the maximum of the barrier the linear relation

$$E=[1+(1+\tfrac{1}{2}c_1)X/X_1](eF_1/\epsilon)^{1/2}. \quad . \quad . \quad . \quad . \quad (16)$$

This relation was obtained from the following considerations. When $X=X_1$, E must reduce to the value E_1 given by eqn. (11). When $X=0$, the impurity centre and its image will give no contribution to the maximum of the barrier. Since the field is then F_1, E must reduce to $(eF_1/\epsilon)^{1/2}$ by analogy with eqn. (10). At intermediate values of X the assumption of a linear variation was found to be a reasonable approximation in particular numerical cases.

When the impurity centre lies off the line OA we take the locus of its positions that maintain the value of E in (16) to be the surface of a sphere that cuts OA at $x=X$ and that has its centre at D in fig. 4. The point D is at $x=(1+2/c_1)X_1$ so as to coincide with the second maximum of the barrier when the impurity centre is on OA at $x=X_1$. When X is near X_1 this locus is reasonable because the maximum of the barrier then occurs near D. Wherever the impurity centre may be on the locus, the potential at D remains at the value $e/\epsilon R+F_1(1+2/c_1)X_1$ where R is the radius of the locus. When X is not near X_1, any locus is reasonable since the impurity centre in such positions does not depress the barrier height along OA appreciably. The volume element between two neighbouring spheres that cut OA at X and $X+dX$ is

$$dv=2\pi[X^2-(2+2/c_1)X_1X+(1+2/c_1)X_1^2]\,dX.$$

The integration goes from $X=0$ to $X=X_1$. This contribution to the integral in (14) was integrated exactly.

To complete the integral in (14) we still have to consider the remaining volume that is shaded in fig. 4. When the impurity centre lies in this region its depression of the barrier along OA is negligible so that E has the constant value $(eF_1/\epsilon)^{1/2}$. The volume of the shaded region is

$$\pi(3/4\pi N)^{1/3}X_1^2-\pi(1+2/c_1)X_1^3.$$

This gives the final contribution to the integral in (14) for substitution into (13).

Some numerical values for the case $\epsilon=10$ at 17°C are shown in table 2. The values of j_u/j_0 are given in the third column, j_u being the current density in the blocking direction averaged over a large area of the interface when the distribution of centres is uniform, and j_0 being the corresponding current density calculated on the usual assumption of a continuous uniform distribution of space change. The values close to 1 show that when there are 10^{16} or 10^{17} impurity centres per cm^3 the approximation based on a continuous distribution of space change is a good one. But at a concentration of 10^{18} the approximation is not so good. At first sight one might expect the higher concentrations to behave more like a continuous distribution than the lower concentrations. But the reverse is seen to be true. The reason is that the higher concentrations provide more impurity centres in the critical region near the plane $x=X_1$ than the lower concentrations do.

A few values of j_u/j_0 in table 2 are less than 1. This may be an error due to the approximations used. On the other hand it seems possible in principle for j_u to be less than j_0. For the effect of averaging exp (eE/kT) as in eqn. (13) instead of averaging by the use of a continuous space change as in § 1 tends to make j_u exceed j_0. But the effect of introducing the image force before averaging as in eqn. (15) instead of introducing it afterwards as in § 2 tends to make j_u less than j_0.

The values in table 2 refer only to the case $\epsilon=10$ at 17°C. In the case of j_1/j_0 in table 1 we pointed out that the tabulated values can be adapted for other values of ϵ and T. Unfortunately this does not seem possible in the case of j_u/j_0. It seems that a separate numerical integration is required for every case.

Table 2

N (per cm^3)	V_w+V_a (volts)	j_u/j_0 accurate	j_u/j_0 approximate	j_r/j_0 approximate
10^{16}	1	0·99	1·00	1·00
	97	0·99	1·00	1·00
10^{17}	1	0·98	1·00	1·00
	20	1·00	1·00	1·01
	50	1·02	1·01	1·02
10^{18}	1	1·02	1·02	1·03
	12	1·63	1·49	1·67
	22	2·91	3·04	3·70

§ 5. THE EFFECT OF A RANDOM DISTRIBUTION OF IMPURITY CENTRES.

This problem was examined in § 10 of a paper by Schottky (1942). He discussed first the effect of a series of impurity centres arranged in a line. They were sufficiently close together to allow electrons to pass from one to the other through the barrier. He concluded that this arrangement of impurity centres would occur so seldom in a random distribution that it would have no appreciable effect on the general current.

He discussed next the effect of random fluctuations in the concentration of the impurity centres. A local increase in the concentration has the effect of reducing the width of the barrier in this locality. If the concentration increases everywhere by a factor r^2 then the width of the barrier decreases everywhere by a factor $1/r$. Accordingly Schottky assumed that a local increase in the concentration in the ratio r^2 decreases the local width of the barrier from the general width b to the local width b/r. He took the local region to be that part of the barrier that is enclosed in a cylinder having its axis normal to the interface and having an area of cross section equal to b^2. At the next stage of the argument a smaller cylinder with an area of cross section (b/r^2) is chosen within the original cylinder. A random increase in the concentration in the second cylinder in the ratio r^2 reduces the barrier width from the general value b/r over the first cylinder to the local value b/r^2 over the second cylinder. This argument is repeated for successive stages and at each stage a new cylinder is introduced within the previous one. After n stages the local width of the barrier has been reduced to b/r^n over an area $(b/r^{n-1})^2$. We arrive in effect at a cone with its base of area b^2 in the plane $x=b$ and its apex in the interface. The random fluctuations in the concentration of impurity centres within the cone reduces the local width of the barrier indefinitely until there is a break through of electrons at the apex due to the tunnel effect. The assumption has been made that the field near the apex of the cone is mainly due to the space charge within the cone. On the basis of a continuous uniform distribution of charge about 87% of this field is caused by charge outside the cone. Only the remaining 13% is affected by the increase of concentration within the cone. Therefore the decrease in the local width of the barrier has been overestimated.

Schottky used as an example the case $r=\frac{5}{4}$. He found it necessary to carry the process through about twenty stages in order to get a part of the barrier thin enough for a break through by the tunnel effect. He showed how to calculate the probability of such a fluctuation in the concentration on the basis of a Poisson distribution. In the earlier stages the cylinders are large enough to contain many impurity centres. But in the later stages the cylinders become too small for this condition to hold. For example in the seventeenth cylinder the width of the barrier is reduced from 35 to 28 angströms. This is caused by a random fluctuation that increases the number of impurity centres in the cylinder from 0·36 to 0·56. It becomes clear that there is a need for an analysis that deals with whole impurity centres.

In the earlier sections of this paper we used a sphere OA drawn at any point O on the interface, with a volume $1/N$ where N is the number of impurity centres per cm³. All the centres lying outside this sphere can be represented by a continuous distribution of space charge. In the case of a uniform distribution of impurity centres we assumed that there would be in effect only one centre within the sphere. In the case of a random distribution of impurity centres the sphere will often contain no impurity centre, often one, sometimes two, and occasionally three or more. When there are n impurity centres in the sphere they will be most effective when they are close together and acting like a single centre of charge ne at an optimum distance $x=X_n$. They will then depress the pass through the barrier to a potential $V=E_n$ and give rise to a local current density j_n. By generalizing the previous theory we find eqns. (9) and (11) replaced by

$$j_n/j_0=\exp\,[e(E_n-E_0)/kT] \qquad . \quad . \quad . \quad . \quad . \quad (17)$$

where

$$E_n=(2n^{1/2}+\tfrac{1}{2}c_n)(eF_1/\epsilon)^{1/2}. \qquad . \quad . \quad . \quad . \quad . \quad (18)$$

Here c_n is a solution of the quartic $c_n^4+8_n^{1/2}c_n^3+4(4n-1)c_n^2=32n$ giving the values shown in table 3.

Table 3

n	1	2	3	4	. . .	∞
c_n	1·18	1·22	1·24	1·25	. . .	$\sqrt{2}$

Incidentally the optimum distance X_n has the value

$$X_n=c_n(e/4\epsilon F_1)^{1/2}$$

so that the optimum position for a multiple centre is practically the same as the optimum position for a single centre.

The average current density j_r has been given in eqn. (13). The sphere OA can be used as before to find the average value of exp (eE/kT). There will be n impurity centres in the sphere with a relative frequency of $1/n\,!$. When $n=0$, $E=(eF_1/\epsilon)^{1/2}$ with F_1 given by (12). When $n=1$ we average by expression (14). When $n=2$ the integral (14) is replaced by a double integral, when $n=3$ by a triple integral, and so on. But this process involves the numerical integration of multiple integrals. In order to avoid the long computations this accurate method was abandoned and the following approximate method was used instead.

The comparatively large sphere OA was replaced by a small critical region near the optimum position X_1 opposite the fixed point O. A suitable volume for this region was found by trial and error to be $v=X_1^3/10$. The average current density at O is obtained by assuming that when n impurity centres lie within the critical region the current density is j_n given by (17) and (18), and when no impurity centres lie within the critical region the current density is simply j_0.

The method has been tested on the case of a uniform distribution of impurity centres with $\epsilon=10$ at 17°c. In this case there cannot be more than one impurity centre in the critical region and the probability of finding even one there is Nv. The appropriate value for F_1 is given by eqn. (12) and the values of j_n/j_0 obtained by this method are shown in the fourth column of table 2. They compare well with the accurate values in the third column.

When the method is applied to the case of a random distribution of impurity centres we have the number of centres in the critical region governed by a Poisson distribution. The average number of impurity centres in regions of volume v is Nv. Hence the probability of finding n impurity centres in the critical region is $(N^nv^n/n\,!)\exp\,(-Nv)$. The appropriate value for F_1 is $F_1=F$ since the volume v is too small for a correction of the type in eqn. (12) to be necessary. The values obtained for j_r/j_0 with $\epsilon=10$ at 17°C are given in the last column of table 2. It is seen that the ratios are a little higher than they are in the case of a uniform distribution, as we might expect.

It was demonstrated above that $v=X_1{}^3/10$ is a suitable volume for the critical region when this contains only one impurity centre. The question arises as to whether this is a suitable volume when there is more than one impurity centre in the critical region. The answer seems to be that it does not matter whether it is the correct volume or not in these cases. For when j_r/j_0 differs appreciably from j_u/j_0 an examination of the numerical work shows that the difference between the two is not due to clusters of impurity centres in the critical region. The clusters occur too seldom. Even double impurity centres account for only about 1% of the difference. The remaining 99% of the difference is due to the use of $F_1=F$ in one case and the use of F_1 corrected by eqn. (12) in the other case. Physically this means that when a single impurity centre lies in the critical region, which occurs comparatively often, its effect is enhanced when other centres are allowed to lie near it at random. In the pictorial representation of fig. 2 these other centres lower the pass indirectly. The pass is still caused by the single impurity centre in the critical region but the other centres lower the barrier in which the pass is made.

No allowance has been made in this paper for electrons that break through the barrier by the tunnel effect. When the distance from the metal to an impurity centre is a little greater than X_1, the barrier is higher on the metal side of the well than it is on the side away from the metal. In cases when X_1 is small (see table 1, column 3) the barrier on the metal side may be narrow enough for electrons to break through by the tunnel effect. Then the electrons contributing to the current need only sufficient energy to surmount the lower part of the barrier on the side away from the metal. This will give rise to local current densities greater than those indicated by j_1/j_0 in table 1, and to average current densities greater than those indicated by j_u/j_0 and j_r/j_0 in table 2.

ACKNOWLEDGMENTS

This work was started at the H.H. Wills Physical Laboratory, Bristol, and was continued at the University of the Witwatersrand, Johannesburg, South Africa. I wish to thank particularly Professor Mott who suggested this problem to me and discussed it on various occasions.

REFERENCES

BETHE, H. A., 1942, *M.I.T. Radiation Laboratory Report*, 43–12.
BILLIG, E., 1951, *Proc. Roy. Soc.* A, **207**, 156.
LANDSBERG, P. T., 1951, *Proc. Roy. Soc.* A, **206**, 463.
MOTT, N. F., 1939, *Proc. Roy. Soc.* A, **171**, 27.
MOTT, N. F., and SNEDDON, I. N., 1948, *Wave Mechanics and its Applications*, p, 230.
SCHOTTKY, W., 1939, *Z. f. Phys.*, **113**, 367 ; 1942, *Ibid.*, **118**, 574.

XLVI. *A Contribution to the Theory of Nuclei with a Diffuse Surface*

By Z. Janković*
CERN, † Theoretical Study Group ‡

[Received November 23, 1954]

The theory of neutron reactions has recently made significant advances by introduction of the complex square-well potential (Feshbach, Porter and Weisskopf 1953). In this connection it seems worth while to investigate the consequences of replacing the sharp nuclear surface by a potential which varies more gradually. The aim of this letter is to enumerate only some results which the author has obtained while a more systematic and detailed exposition will be given in a separate article.

The nuclear potential is assumed to vary continuously over a range, δ, from its exterior value $V=0$ to the interior value

$$V=-V_0(1+i\xi). \qquad \qquad (1)$$

For simplicity a linear variation of V in the surface region has been assumed (cf. fig. 1). From the solution of the Schroedinger equation the logarithmic derivative f and its derivative with respect to the energy have been determined. As in the region of low energies the s-neutrons play the most important part in nuclear reactions, we quote the logarithmic derivative for this case :

$$\left.\begin{aligned} \operatorname{Re}(f)&=\gamma(R+\delta)\,\frac{(F\bar{F}+G\bar{G})-\xi/3(\bar{F}G-F\bar{G})}{F^2+G^2} \\ \operatorname{Im}(f)&=\gamma(R+\delta)\,\frac{(\bar{F}G-F\bar{G})+\xi/3(F\bar{F}+G\bar{G})}{F^2+G^2} \end{aligned}\right\} \qquad (2)$$

with

$$\left.\begin{aligned} F&=-qJ_{1/3}(a)+p\xi gJ_{1/3}{}'(a)+\xi gJ_{1/3}{}''(a) \\ G&=pJ_{1/3}(a)+J_{1/3}{}'(a)+q\xi gJ_{1/3}{}'(a), \end{aligned}\right\} \qquad (3)$$

where $J_{1/3}$ is the Bessel function of order one third and the barred quantities contain the Bessel functions of order minus one third.

$$\left.\begin{aligned} p&=\frac{\cot\sqrt{(V_0)}R[\coth^2 b-1]}{\cot^2\sqrt{(V_0)}R+\coth^2 b}+\frac{1}{2\delta\sqrt{V_0}}, \\ q&=\frac{\coth b[\cot^2\sqrt{(V_0)}R+1]}{\cot^2\sqrt{(V_0)}R+\coth^2 b}+\frac{\xi}{4\delta\sqrt{V_0}}, \end{aligned}\right\} \qquad (4)$$

$$a=\tfrac{2}{3}\delta\sqrt{V_0},\ b=\xi/2\sqrt{(V_0)}R,\ g=\tfrac{1}{3}\delta\sqrt{V_0},\ \gamma=\frac{\sqrt[3]{3}}{3}\,\frac{\Gamma(2/3)}{\Gamma(4/3)}\,\frac{\sqrt{V_0}}{(\delta\sqrt{V_0})^{1/3}} \qquad (5)$$

(ξ is assumed to be a small quantity compared with unity).

---

* On leave from the Faculty of Science and the Institut za fiziku Rudjer Boskovic, Zagreb.

† European Council for Nuclear Research. This work has been performed at the Institute for Theoretical Physics, University of Copenhagen.

‡ Communicated by C. Møller.

On the basis of these expressions, Γ_n/D, σ_{sc}, σ_r, σ_t have been calculated by means of the well-known procedures (Blatt and Weisskopf 1952, Feshbach, Porter and Weisskopf, published 1954). The results of these calculations are summarized in the following diagrams, which plot the various quantities as a function of the radius R; the calculated cases have been chosen in such a way as to study the effect of independent variations of the several parameters occurring in the theory.

Fig. 1

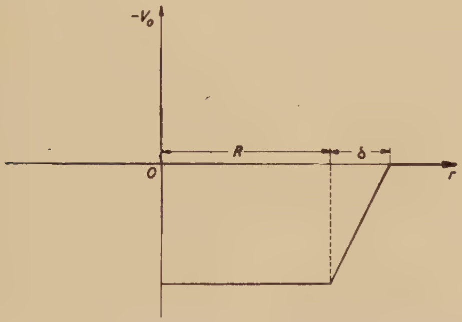

The assumed shape of the nuclear potential.

The data suggest that four maxima (Adair 1954) of the various cross sections occur in the range of the periodic system of the elements, i.e. between $0<R<10$, and that the fourth maximum is important for the description of the behaviour of the heavier nuclei. As could be seen from the theory, the parameter $\xi(\xi\ll 1)$ does not influence appreciably the position of the maxima in this range, and the $R_{\max}$ values (determined by the condition that for $R=R_{\max}$, $\mathrm{Re}(f)$ vanishes and $-\mathrm{Im}(f)$ is near its minimum value) could be determined from the requirement

$$\cot\sqrt{(V_0)}R_{\max}=-\frac{1}{2\delta\sqrt{V_0}}-\frac{J'_{-1/3}(a)}{J_{-1/3}(a)}. \quad . \quad . \quad . \quad (6)$$

These $R_{\max}$ values compared with the corresponding values for the case $\delta=0$ show a shift to smaller R values, the difference being greater than $\delta/2$ and increasing with V_0 and δ.

By comparing the corresponding diagrams the main qualitative effects of changing only one of the parameters V_0, δ, ξ may be obtained :

(*a*) V_0 : greater V_0 shifts the curves to the smaller R values, the distance between maxima becoming smaller and the width is decreased ; the influence on the value of maxima and minima is a small one.

(*b*) δ : greater δ shifts the curves to the smaller R values : all the cross sections are increased as is also the widths of the ' resonances '.

(*c*) ξ : increase of ξ does not shift the curves in the first approximation ; values near the minima are increased, but maxima are depressed and the width is enlarged.

Fig. 2

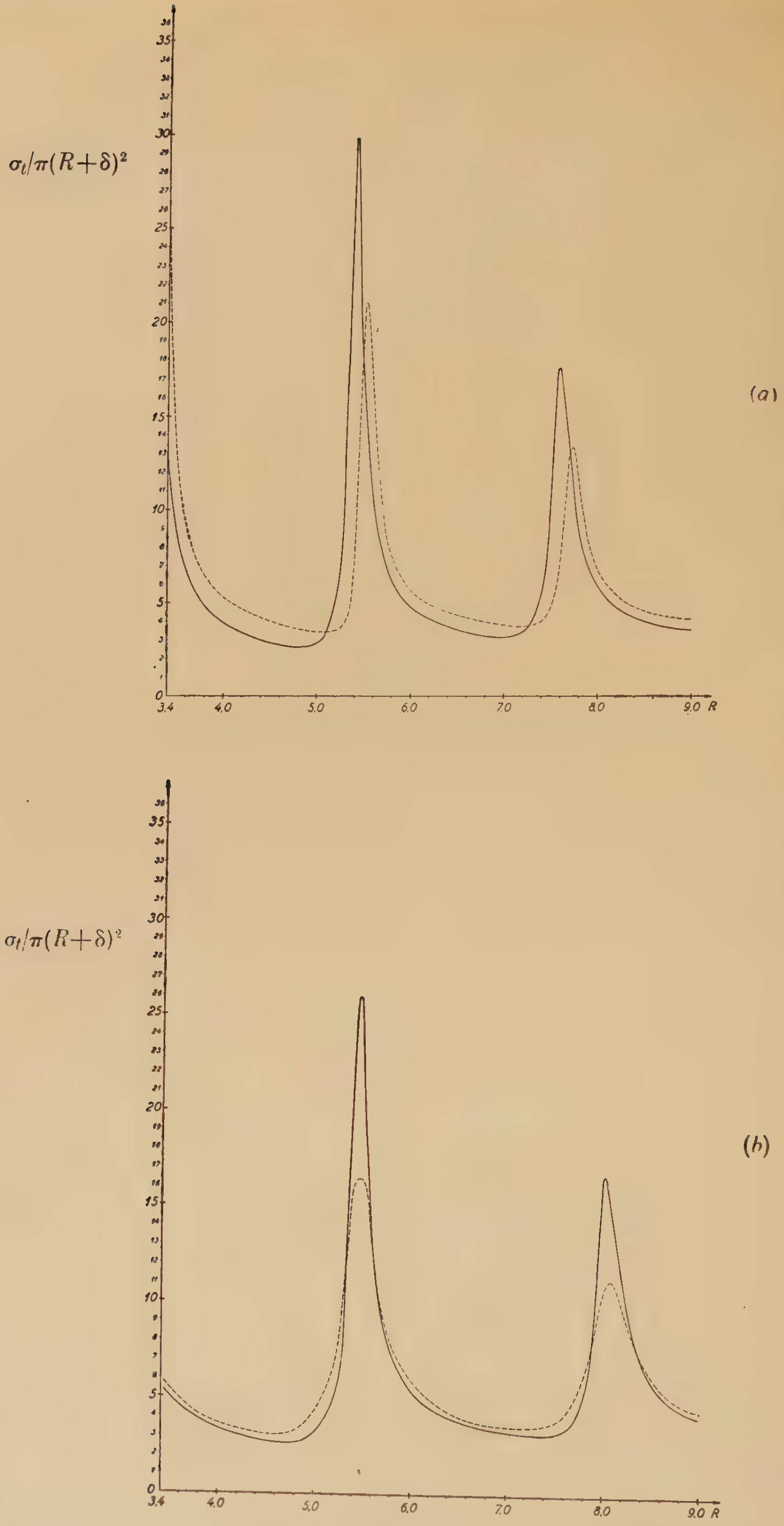

The calculated total cross section for incident s-wave neutrons is plotted as a function of the radius parameter R (in units of 10^{-13} cm). The curves refer to a neutron energy which varies with R so that $kR=0{\cdot}2$, where k is the wave number of the incident neutrons. The parameters of the potential are for (*a*) the dashed curve, $V_0=42$ MeV, $\delta=0$, $\xi=0{\cdot}03$; the solid curve, $V_0=42$ MeV, $\delta=2\times10^{-13}$ cm, $\xi=0{\cdot}03$ (the curve shifted for $\delta/2$ to the right); for (*b*) the dashed curve, $V_0=30$ MeV, $\delta=2\times10^{-13}$ cm, $\xi=0{\cdot}05$; the solid curve, $V_0=30$ MeV, $\delta=2\times10^{-13}$ cm, $\xi=0{\cdot}03$.

Fig. 3

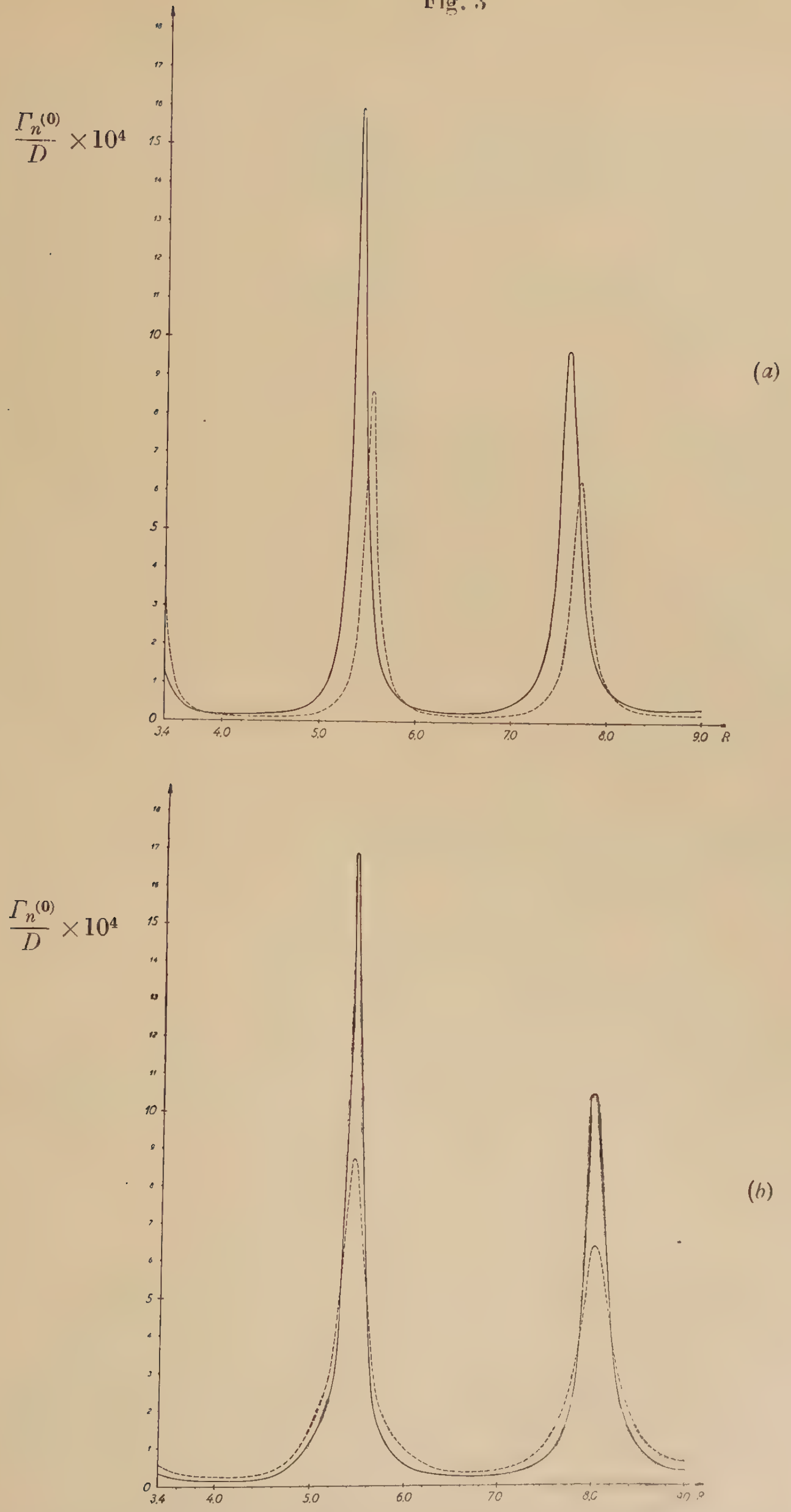

The ratio of neutron width $\Gamma_n^{(0)}$ (reduced to 1 ev neutron energy) to the level spacing D is plotted as a function of the radius parameter R (in units of 10^{-13} cm). The parameters of the potentials used are the same as for the corresponding curves in figs. 2 (*a*) and 2 (*b*).

In the diagrams, R was intentionally left as the independent variable, because of the several possible relations between this parameter and the atomic number A. Perhaps the best definition of the nuclear radius ρ in our case would be

$$\rho = R + \kappa \qquad \qquad (7)$$

(κ is a constant between zero and δ) and then assume ρ (or R) to be proportional to $A^{1/3}$

$$\rho(\text{or } R) = r_0 A^{1/3}. \qquad \qquad (8)$$

In either case we may remark that the maxima are at equal distances $\pi/\sqrt{V_0}$ from each other (irrespective of δ), i.e.

$$R_i - R_{i-1} = r_0(A_i^{1/3} - A_{i-1}^{1/3}) = \pi/\sqrt{V_0}. \qquad \qquad (9)$$

Thus, from A_4 and A_3 we can infer A_2 and also the value for $r_0\sqrt{V_0}$. Now, if either r_0 or V_0 is given, R_i can be determined from (8) and then δ from (6). The remaining parameter, ξ, should be adjusted to yield the experimentally observed peak to valley ratios of the cross sections (Feshbach, Porter and Weisskopf, published 1954).

Finally we may remark that the inclusion of the nuclear deformation may also be important in the analysis of the experimental data (A. Bohr and B. R. Mottelson 1953).

The author wishes to express his appreciation of the arrangements which made possible his participation in the CERN Theoretical Study Group in Copenhagen. He is very grateful to Dr. B. R. Mottelson and to Dr. A. Bohr for raising this question and for their interest regarding this work.

REFERENCES

ADAIR, R. K., 1954, *Phys. Rev.*, **94**, 737.
BLATT, J. M., and WEISSKOPF, V. F., 1952, *Theoretical Nuclear Physics* (J. Wiley).
BOHR, A., and MOTTELSON, B. R., 1953, *Dan. Mat. Fys. Medd.*, **27**, No. 16.
FESHBACH, H., PORTER, C. E., and WEISSKOPF, V. F., 1953, *Phys. Rev.*, **90**, 166; "Neutron Reactions and the Formation of the Compound Nucleus" (MIT), (unpublished); 1954, *Phys. Rev.*, **96**, 448.

XLVII. *The Disintegration of ^{7}Be by Slow Neutrons*

By R. C. Hanna
Atomic Energy Research Establishment, Harwell †

[Revised MS. received November 26, 1954]

Summary

The reaction ^{7}Be (n p) ^{7}Li has been identified for neutrons incident with thermal energies. The cross section has been measured as $5{\cdot}3\pm0{\cdot}8\times10^{-20}$ cm^2. The cross section for the reaction ^{7}Be (n α) ^{4}He does not exceed 1 barn. The results show the parity of ^{7}Be to be odd.

The activity of ^{7}Be source has been diminished by neutron bombardment. The cross section for all processes leading to the destruction of ^{7}Be is found to the $4{\cdot}8\pm0{\cdot}9\times10^{-20}$ cm^2.

A comparison of the ^{7}Be (n p)^{7}Li and ^{7}Li(p n)^{7}Be cross sections gives evidence for a level in ^{8}Be near the neutron threshold of width not exceeding 30 kev.

§ 1. Introduction

^{7}Be is a K capture body of half life 53 days ; in 11% of disintegrations the daughter nucleus, ^{7}Li, is left in an excited state at 478 kev and γ-radiation is emitted (Turner 1949, Richards and Williamson 1949).

From the energy balances of the reactions

$$^7\text{Li}+\text{p}={}^7\text{Be}+\text{n}-1{\cdot}65\ \text{Mev}$$

$$^7\text{Li}+\text{p}={}^8\text{Be}+\gamma+17{\cdot}2\ \text{Mev}$$

$$^8\text{Be}=2\alpha+80\ \text{kev}$$

the following reaction may be expected to occur when ^{7}Be is bombarded with thermal neutrons :

$$^7\text{Be}+\text{n}={}^7\text{Li}+\text{p}+1{\cdot}65\ \text{Mev}$$

$$^7\text{Be}+\text{n}={}^7\text{Li}^*+\text{p}+1.17\ \text{Mev}$$

$$^7\text{Be}+\text{n}=2\alpha+18{\cdot}9\ \text{Mev}.$$

The mode of disintegration of the excited ^{8}Be compound nucleus is determined by its parity. A ^{8}Be nucleus of even parity and spin can split into two α particles, and the energy release for this reaction is so much greater than for proton emission that it would be expected to predominate. A ^{8}Be nucleus of odd parity will de-excite by proton emission ; competition from γ-ray emission would be expected to be small. Cross sections for neutrons of thermal energies are appreciable only for the incident neutron wave of zero angular momentum. Thus the parity of the compound ^{8}Be nucleus will be the same as that of the ground state of ^{7}Be. A determination of the relative magnitudes of the cross sections for the np and nα reactions thus leads to an assignment of parity to the ground state of ^{7}Be.

---

† Communicated by the Author.

The measurement of the proportion of protons which leave the ^{7}Li nucleus excited is not readily interpreted (cf. ^{10}B (n α) ^{7}Li).

From the reciprocity theorem the cross sections for the reactions ^{7}Be (n p) ^{7}Li and ^{7}Li (p n) ^{7}Be for the same excitation of the compound nucleus are in the ratio

$$\sigma(\mathrm{n\ p})/\sigma(\mathrm{p\ n}) = P_{\mathrm{p}}{}^2(2J_{\mathrm{Li}}+1)(2J_{\mathrm{p}}+1)/P_{\mathrm{n}}{}^2(2J_{\mathrm{Be}}+1)(2J_{\mathrm{n}}+1).$$

In principle, therefore, the spin of ^{7}Be can be determined. From measurements of the cross sections for the ^{7}Be (n α) and ^{7}Be (n p) reactions both the spin and parity of the ^{7}Be nucleus in its ground state can be deduced.

§ 2. STUDIES ON ^{7}Be+n BY PARTICLE COUNTING

2.1. *Preparation and Assaying of* ^{7}Be *Samples*

^{7}Be was prepared by bombardment of a block of pile graphite with the 175 MEV internal proton beam of the Harwell cyclotron. After chemical separation the ^{7}Be was deposited on platinum sheet as a ‘weightless’ source.

The mass of ^{7}Be was determined from the counting rate due to 478 kev γ-rays detected in an organic scintillation crystal relative to the rate due to 411 kev γ-rays from a source of ^{198}Au; the source strength of the latter was determined by coincidence counting. Corrections were made for internal conversion and the presence of harder radiation in the spectrum of ^{198}Au (Cavanagh 1951). The difference of crystal detection efficiency for ^{198}Au and ^{7}Be γ-rays was calculated from the Klein–Nishina formula.

Pulse height spectra taken with a sodium iodide detector, and half-life measurements, showed the ^{7}Be source to be radioactively pure. The absolute activity was found to be $5{\cdot}4 \pm 0{\cdot}1 \times 10^6$ γ-rays/second, which corresponds to a mass of $3{\cdot}76 \pm 0{\cdot}40 \times 10^{-9}$ g ^{7}Be. The error is largely due to the 10% uncertainty in the value of the branching ratio in ^{7}Be decay.

2.2. *The* ^{7}Be (n p) *Reaction*

2.2.1. *Method*

The ^{7}Be was mounted on the source electrode of a parallel plate gridded ionization chamber, and bombarded with a collimated beam of thermal neutrons from the Harwell pile B.E.P.O. A linear amplifier and four channel pulse amplitude analyser were used to study the spectrum of pulses from electron collection in the chamber.

With the very small mass of target material available, the observation of disintegration particles of the expected energy was necessary but not sufficient evidence for the occurrence of the ^{7}Be (n p) reaction. At sufficiently reduced pressures of the chamber filling gas, the reaction products pass out of the collecting volume of the chamber and the associated pulses are reduced in height. From a study of pulse height spectra as a function of gas filling pressure, both the energy and the range of the particles responsible for a peak in the spectrum could be found, and thus the type of particle identified.

A definite identification of the ^{7}Be (n p) reaction was made from the following observations.

1. The spectrum of pulses showed a peak at an energy of 1·44 MeV when the ^{7}Be was present in the chamber. In its absence there was no peak.
2. The variation in the shape of the spectrum as the gas filling pressure was reduced showed that the peak was due to protons.

Fig. 1

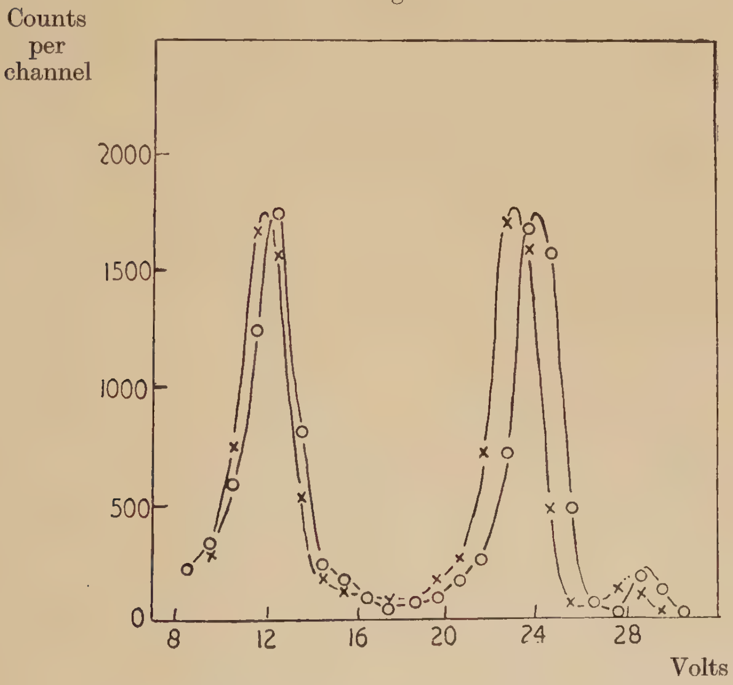

Pulse height spectra from the reaction B^{10}(n α)^{7}Li.
o 76 cm of mercury filling pressure
x 11 cm of mercury filling pressure

3. Cadmium difference curves showed that the peak was due to incident thermal neutrons.
4. Since the proton energy was greater than the energy corresponding to the neutron proton mass difference (0·78 MeV) the target nucleus must have been heavier than the product nucleus i.e. unstable against K-capture. ^{7}Be is the only neutron deficient product of the proton bombardment of carbon to give the correct energy balance.

5. The intensity of the proton group was measured over a period of time. After normalizing to constant incident neutron flux, the intensity of the proton group was found to decrease with the expected 53 day half-life. This confirms the instability of the target material; the value of the half-life is further proof that the reaction studied is due to ^{7}Be.

2.2.2. *Results*

In fig. 1 are shown the pulse height distribution curves obtained when a thin sample of ^{10}B was bombarded with thermal neutrons, for gas filling pressures of 76 cm and 11 cm of mercury. The voltages applied to the chamber electrodes were adjusted to be proportional to pressure. A small shift occurs in pulse height; the main features are seen to be independent of pressure.

Fig. 2

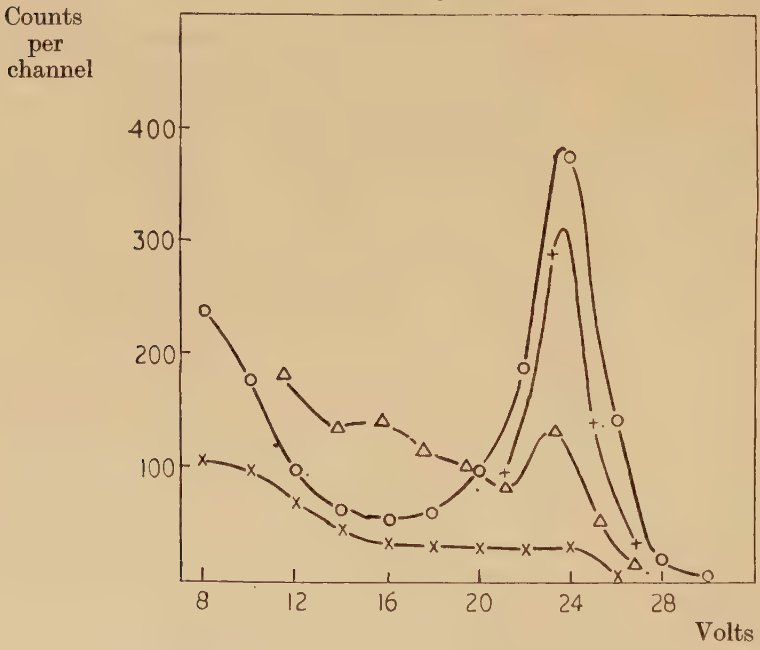

Pulse height spectra from neutron bombardment of ^{7}Be.
Curve 1 o 76 cm of mercury filling pressure
Curve 2 + 51 cm ,, ,, ,,
Curve 3 Δ 35 cm ,, ,, ,,
Curve 4 × 11 cm ,, ,, ,,

In fig. 2 are shown the pulse height distribution curves obtained when ^{7}Be was bombarded. Curve 1 was taken at 76 cm pressure when the range of protons of the peak energy is less than the minimum chamber dimension; curve 2, taken at 51 cm shows a reduction in the peak counting rate. Very few particles lose their full energy in the collecting volume at 35 cm pressure (curve 3). At 11 cm pressure (curve 4) a continuum remains, believed due to α-particles from the ^{10}B (n α) reaction emitted from depth in the chamber electrodes and walls. The collecting volume of the chamber is not well defined ; the shape of the pulse height spectrum from a group of monoenergetic particles of range greater than the minimum dimensions of the collecting volume cannot be calculated. It may be noted that in the geometry used the calculated value of the pressure required to stop a proton of energy 1·44 MeV from reaching the grid was 58 cm of mercury. The corresponding pressures for deuterons tritons and α-particles of the same energy were calculated to be 37, 30 and 10 cm respectively. At 35 cm some protons could lose their whole energy within the space bounded by the source and grid electrodes. At 11 cm pressure the maximum energy losses for protons, deuterons and tritons were calculated to be 0·43, 0·8 and 1·2 MeV respectively; α-particles could lose their whole energy. The distributions of fig 2 show that the main peak at 76 cm pressure is due to protons.

Fig. 3

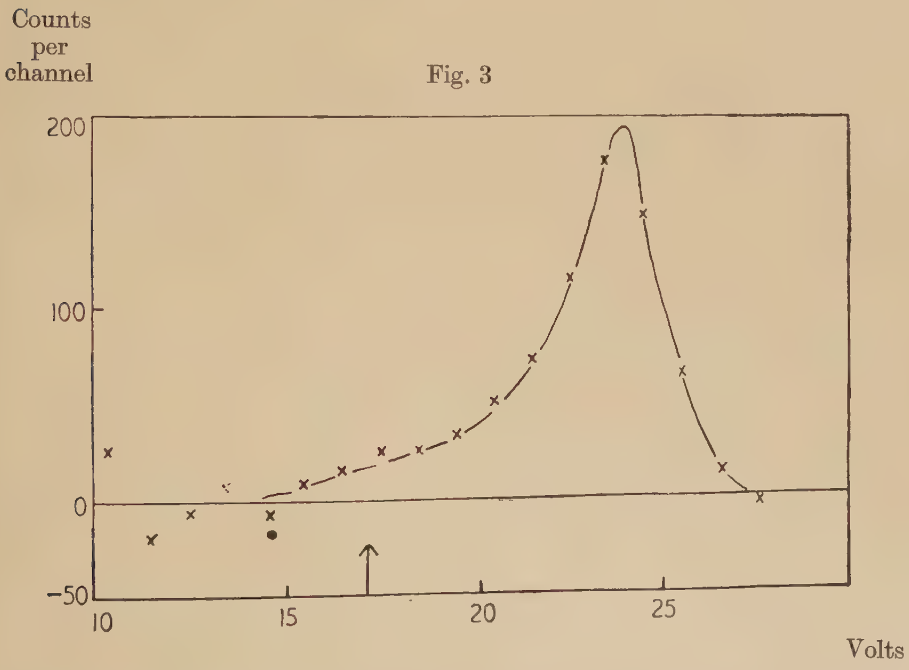

Pulse height spectrum of protons from the reaction ^{7}Be(n p)^{7}Li. The arrow indicates the pulse height expected from protons leaving the residual ^{7}Li nucleus in the excited state at 478 kev.

In fig. 3 the pulse height distribution is shown after the subtraction of background effects (e.g. particles from the ^{10}B (n α) reaction fast neutron recoils, radioactive contaminations etc.). Pulse height distributions were recorded for filling pressures of 76 cm and 11 cm of mercury pressure, with and without cadmium in the incident beam, and with the ^{7}Be deposit facing the collecting volume and reversed. A subtraction procedure yields a curve (fig. 3) which is the spectrum of pulses which can be attributed to protons emitted from the ^{7}Be as a result of slow neutron bombardment.

A sample of ^{233}U of the same physical dimensions could be substituted for the ^{7}Be deposit, and the fission counting rate determined as a measure of the neutron flux. Six measurements of the proton pulse height distribution and the corresponding fission rate were made over a period of time. A proton counting rate was obtained by summing over the spectrum between 1·1 and 1·8 MEV and normalizing to constant fission rate, i.e. to constant incident neutron flux. This normalized rate is plotted on a logarithmic scale against time in fig. 4. The half-life of the decay of the proton rate is 50±2 days. The instability of the target material is thus established and the value of the half-life is in fair agreement with that of ^{7}Be. Furthermore, if 10% of the initial proton rate were due to a background constant in time, the half-life would be reduced to 40 days and the fit to an exponential decay worsened. It seems certain that the proton rate does not include such a background, i.e. the procedure for evaluating the background is unlikely to give too high a value for the (n p) cross section.

Fig. 4

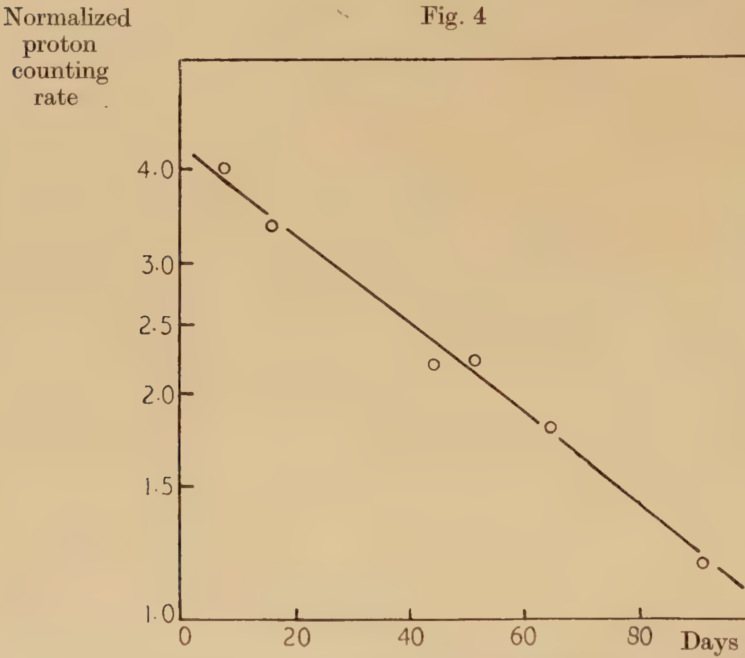

The decay of the ^{7}Be(np) proton counting rate with time.

Sufficient energy is available in the ^{7}Be (n p) reaction for protons of reduced energy to be emitted and the residual ^{7}Li nucleus left in the excited state at 478 kev. The arrow in fig. 3 indicates the position expected for the peak due to such ‘ excited state ’ protons. The proportion is less than 10% of the ground state group.

In fig. 4, and the spectra from the other five runs, there is an asymmetry and a broadening of the peak, relative to the peak from the ^{10}B (n α) reaction. The greater width of the proton distribution was shown to be due to the dependence of pulse height on collection time ; the contribution to the total proton counting rate of that portion of the spectrum below 1·1 MeV was estimated to be less than 7% from a study of the effect of collection time on pulse height distributions from α-particle sources. This method gives a better estimate than study of the pulse height distribution obtained by the subtraction procedure, where the statistical errors become large at the lower energies.

The relation between the neutron flux and the fission counting rate of the ^{233}U sample was determined in a subsidiary experiment in terms of the capture cross section of gold (97 ± 1 barns for neutrons of 0·025 ev energy). The accuracy of this measurement was $\pm 3\%$.

The cross section for the (n p) reaction in ^{7}Be leading to the ground state of ^{7}Li, calculated from the proton counting rate per unit fission rate and the mass of ^{7}Be is $5{\cdot}3 \pm 0{\cdot}8 \times 10^4$ barns. Of the 15% error, 10% occur in the determination of the mass of ^{7}Be because of the uncertainty in the branching ratio ; the other main source of error is in the interpretation of the proton spectrum. If the proportion of small pulses has its maximum value, the proton rate may be 7% too low ; on the other hand it may be 10% too high if the proportion of protons leaving ^{7}Li in its excited state has its maximum possible value.

2.3. *The* ^{7}Be (n α) *Reaction*

As was discussed in the introduction, the parity of ^{7}Be may be deduced from the relative magnitudes of the (n p) and (n α) reaction cross sections for neutrons incident with thermal energies.

Some 40 hours were spent in examining the region of the energy spectrum between 9 and 10 MeV with a gas filling pressure of three atmospheres. It is believed that traces of fissionable material were responsible for a background counting rate of 2 counts/hour/MeV energy interval. An upper limit of 1 barn can be assigned to the (n α) cross section on the assumption that a peak counting rate three times the standard deviation of the background rate would have been observed.

The (n p) reaction is therefore much more probable than the (n α) reaction, corresponding to odd parity for the ground state of ^{7}Be. The result is in accord with shell model predictions.

§ 3. DESTRUCTIVE IRRADIATION OF ^{7}Be

3.1. *Method*

In the presence of neutrons ^{7}Be nuclei are transformed by neutron capture as well as by K electron capture. The (n.p) cross section is so large that the increase of decay rate resulting from neutron bombardment gives a method of determining the neutron capture cross section. If the ratio of the activities of two ^{7}Be samples is measured to be y (>1 say) and the stronger is irradiated for a time t in a flux ν, the ratio of activities after irradiation will be reduced to $y^1=y \exp(-\sigma \int \nu \, dt)$, where σ is the cross section for all processes in which ^{7}Be is destroyed. For $\sigma=5\times10^{-20}$ cm^2, $\nu=10^{12}$ neutrons/cm^2/sec and $t=2{\cdot}6\times10^6$ sec (1 month) the change in relative activity $y/y^1-1=14\%$. The cross section can thus be measured in terms of a time integrated neutron flux and relative source strengths and does not depend on a knowledge of the ^{7}Be decay scheme.

3.2. *Results*

Two samples of ^{7}Be were sealed off in quartz tubes and their γ-activities compared with a scintillation detector. The value found for the ratio of activities (y) was $1{\cdot}112\pm0{\cdot}009$.

Fig. 5

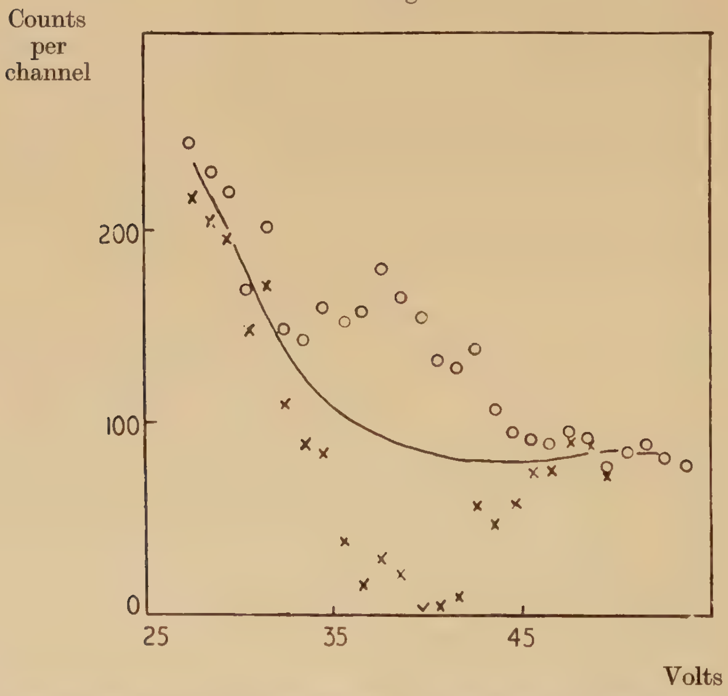

Difference spectra from ^{7}Be samples. x destruction of irradiated ^{7}Be assumed to be zero. o destruction of irradiated ^{7}Be assumed to be 10%. Full line radiation from ^{60}Co.

The stronger of the two sources, together with a similar quartz capsule containing 10·37 mg of cobalt wire, was irradiated for a period of 28 days in a high flux position in B.E.P.O

The irradiated ^{7}Be sample was found to have picked up a spurious activity of long life and γ-ray energy ~900 kev. The spectra of the irradiated and unirradiated ^{7}Be samples were studied with a sodium iodide scintillation detector and thirty channel pulse amplitude analyser covering the energy region 300–660 kev. The value of the ratio of the ^{7}Be activities, y^1, was determined as follows. The ordinates of the spectrum from the unirradiated sample were multiplied by factors x before subtraction from the irradiated sample's spectrum, to give 'difference spectra'. The value of x for which the corresponding difference spectrum could most closely be fitted by the spectrum from a source of cobalt 60 (γ-rays of 1·1 and 1·3 Mev) was taken as equal to y^1. Identical values were obtained by fitting the difference spectrum to a ^{56}Mn spectrum (γ-ray energy 850 kev) i.e. the value found for the ratio of ^{7}Be activities was insensitive to the exact energy assigned to the impurity radiation. Difference spectra are shown in fig. 5. The upper set of points correspond to a 10% destruction of ^{7}Be by neutron irradiation, the lower set to no destruction. The full line is due to cobalt radiation. From four sets of data taken over a period of weeks a consistent value of $y^1=1{\cdot}043\pm0{\cdot}005$ was found. The same value was found when data were taken with an organic crystal detector.

From the activity induced in the cobalt specimen the integrated flux ($\int\nu\,dt$) was found to be $1{\cdot}36\pm0{\cdot}10\times10^{18}$ neutron/cm^2.

Thus $y=1{\cdot}112\pm0{\cdot}009$, $y^1=1{\cdot}043\pm0{\cdot}005$, $\int\nu\,dt=1{\cdot}36\pm0{\cdot}10\times10^{18}$.

Hence $\sigma=4.8\pm0{\cdot}9\times10^{-20}$ cm^2.

If the spurious activity induced by neutron bombardment of the ^{7}Be sample included a body of long half-life emitting γ-rays not resolved from those of ^{7}Be the destruction of ^{7}Be will have been underestimated. If this possibility is admitted the quoted cross section must be regarded as a lower limit.

With stronger ^{7}Be sources and longer irradiation times the method is capable of considerably greater precision. The value found for the destruction cross section is in agreement with that measured for the (n p) reaction.

§ 4. APPLICATION OF THE RECIPROCITY THEOREM

4.1. *Introduction*

To deduce the spin of ^{7}Be from the reciprocity theorem (§ 1) it is necessary to determine the ^{7}Be (n p) and ^{7}Li (p n) cross section for energies of incident particles giving the same excitation of the compound nucleus in the two cases. This is not feasible experimentally ; a certain form of the energy dependence of the cross sections must be assumed.

From the reciprocity theorem it is evident that near the threshold of the ^{7}Li (p n) reaction, where the energy of the neutron is changing much more rapidly than that of the proton, a $1/v$ law dependence of the ^{7}Be (n p) cross section is equivalent to a ^{7}Li (p n) cross section proportional to $\sqrt{E_n}$ where E_n is the energy of the neutron in the centre of mass system. Taschek and Hemmendinger (1948) show a curve of $\sigma/\sqrt{E_n}$ versus $\sqrt{E_n}$ which falls steeply with increasing E_n. However, in the region $E_n=17$–30 kev, it appears that $\sigma/\sqrt{E_n}$ has reached a constant value of 0·045 barns/$\sqrt{}$kev. These results are shown in the circles of fig. 6. On the assumption that $\sigma/\sqrt{E_n}$ remains at this value as E_n is decreased to thermal energies, the (n p) cross section for neutrons incident on ^{7}Be with an energy in laboratory co-ordinates of 0·025 ev is $1{\cdot}6\times10^4$ barns, for a ^{7}Be spin of 3/2, or twice this value for a spin of $\frac{1}{2}$. The mean measured value of $5{\cdot}0\pm0{\cdot}8\times10^4$ barns corresponds to a spin of $0{\cdot}14\pm0{\cdot}15$. It appears that $\sigma/\sqrt{E_n}$ cannot be constant.

Fig. 6

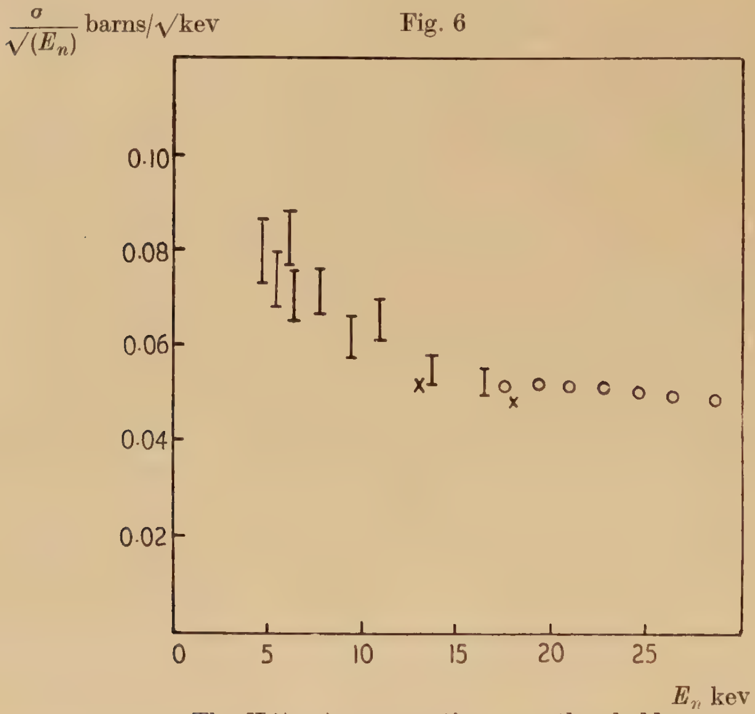

The ^{7}Li(p n) cross section near threshold.
o points due to Taschek and Hemmendinger
x points from ^{7}Be activation
I points from proton recoil counting

Three experiments have been made, with the proton beam of the Harwell electrostatic generator, in an attempt to clarify the situation: the absolute value of the ^{7}Li (p n) cross section has been determined at two energies near threshold, the energy dependence of the (p n) cross section has been studied to within 5 kev of threshold and some observations made on the inelastic proton scattering.

4.2. *Measurements on the System* ^{7}Li+p

For the absolute cross section determinations the ^{7}Be activity produced by bombardment with a measured charge of protons was compared with the activity of a source of ^{198}Au standardized by coincidence counting. The superficial masses of the thin targets used were found from the neutron yields far from threshold relative to the yields from targets thick enough to be weighed with accuracy. The values obtained for $\sigma/\sqrt{E_n}$ were $5{\cdot}2\pm0{\cdot}6\times10^{-26}$ cm$^2/\sqrt{}$ kev and $4{\cdot}8\pm0{\cdot}5\times10^{-26}$ cm$^2/\sqrt{}$ kev for values of E_n of 13 kev and 18 kev respectively. The major source of error arises from the uncertainty in the value of the branching ratio in ^{7}Be decay; the difference between the two values is probably significant.

To follow the variation of cross section with energy rather nearer to the threshold the neutron yield from a thin target was measured with a hydrogen filled proportional counter set at 0° to the proton beam (Tunnicliffe and Ward 1952). From the spectrum of proton recoils, the neutron energy in laboratory co-ordinates and the number of neutrons incident on the counter were determined. The neutron energy and the solid angle subtended by the counter in the centre of mass system were calculated therefrom. The total neutron yield was then derived on the assumption of isotropic emission of neutrons in the centre of mass system. The results are shown in fig. 6 and have been normalized to Taschek and Hemmendinger's values at the high energy end. The errors increase as threshold is approached largely because the ratio of solid angles in laboratory and centre of mass co-ordinates is a rapidly varying function of energy near threshold; here also the shape of the proton recoil spectrum becomes extremely sensitive to target thickness and proton energy resolution and the assignment of neutron energy and yield is untrustworthy.

From fig. 6 the value of $\sigma/\sqrt{E_n}$ is seen to be increasing as threshold is approached. The value of $\sigma/\sqrt{E_n}$ at threshold, determined from the ^{7}Be (n p) cross section on the assumption of a spin of 3/2, is 0·14 barns/$\sqrt{}$kev.

The yield of 478 kev γ-rays from inelastic proton scattering was studied near threshold. Below threshold there was no indication of a resonance; above threshold the yield decreases due to competition from the (p n) reaction. It is noteworthy that the decrease was more abrupt than would be expected from a (p n) cross section proportional to $\sqrt{E_n}$; a decrease of $\sigma/\sqrt{E_n}$ with increasing E_n near threshold is also required to account for the behaviour of the inelastic scattering cross section.

4.3. *Discussion*

From the rather imprecise data on the ^{7}Li (p n) reaction it is not possible to obtain by extrapolation a trustworthy value of $\sigma/\sqrt{E_n}$ as E_n tends to zero, i.e. the spin of ^{7}Be cannot be determined from the reciprocity theorem. Some conclusions are possible if the procedure is reversed; it is most likely that the mirror nuclei ^{7}Be and ^{7}Li have the same spin (3/2) in which case $\sigma/\sqrt{E_n}$ decreases by a factor 3 as E_n increases from 0 to 16 kev. If the variation of cross section is determined by a single level in ^{8}Be, E_0 kev below the threshold and of width Γ kev it follows from the Breit–Wigner formula that

$$3(E_0^2+\Gamma^2/4)=[(E_0+16)^2+\Gamma^2/4]$$

for s wave neutron emission. Hence Γ cannot exceed 30 kev, and the level must lie between 20 kev below the threshold and 2 kev above. The trend of $\sigma/\sqrt{E_n}$ with E_n suggests that the level is below threshold and of maximum width. Other levels may be contributing to the cross section, and neutron waves of higher angular momentum may be emitted at the higher energies. In the latter case neutron emission may not be isotropic and the derivation of the results of fig. 6 is invalidated. The effect of contribution from other levels, or from neutron waves other than s waves is that the value derived for the level width may be too large.

The existence of a level in ^{8}Be very close to the neutron threshold has been suspected for some time. Breit and Bloch (1948) suggested it in an analysis of the ^{7}Li (p n) results of Taschek and Hemmendinger. Bashkin and Richards (1951) found a variation in the ^{7}Li elastic proton scattering cross section which might be associated with such a level. More recently Newson and Gibbons (1954) have found more definite evidence for the level from a study of the ^{7}Li (p n) reaction. Their results, too, suggest that the level is below threshold.

From the absolute magnitude of the (p n) cross section and the total width it is possible to calculate the neutron width. The reduced neutron width, calculated on the assumption that only s wave neutrons are involved, is 50 kev for a (1 −) level and 90 kev for a (2 −) level; if the total width of the level is set equal to the proton width, the corresponding reduced proton width is found to be 20 kev. For a (p n) reaction between mirror nuclei the neutron and proton reduced widths are expected to be equal. Since systematic errors can arise in the extraction of reduced widths the agreement may be considered satisfactory.

The reduced widths found are of order one hundred times less than single particle widths; the level must involve a disturbance of the core, rather than result from the motion of an odd nucleon about the core. For a discussion of anomalously small reduced widths in the 1 p shell the reader is referred to a forthcoming publication by Lane and Thomas.

ACKNOWLEDGMENTS

The author is indebted to Dr. A. M. Lane for theoretical discussions and to Dr. F. D. S. Butement for preparation of the ^{7}Be samples.

REFERENCES

BASHKIN, S., and RICHARDS, H. T., 1951, *Phys. Rev.*, **84**, 1124.
BREIT, G., and BLOCH, I., 1948, *Phys. Rev.*, **74**, 397.
CAVANAGH, P. E., 1951, *Phys. Rev.*, **82**, 791.
LANE, A. M., and THOMAS, R. G., *Rev. Mod. Phys.* (to be published).
NEWSON, H. W., and GIBBONS, J. H., 1954, *Bull. Amer. Phys. Soc.*, **29**, No. 4, 52.
TASCHEK, R., and HEMMENDINGER, A., 1948, *Phys. Rev.*, **74**, 373.
TUNNICLIFFE, P. R., and WARD, A. G., 1952, *Proc. Phys. Soc.* A, **65**, 233.
TURNER, C. M., 1949, *Phys. Rev.*, **76**, 149.
WILLIAMSON, R. M., and RICHARDS, H. T., 1949, *Phys. Rev.*, **76**, 614.

XLVIII. *Further Evidence for the Electron-Decay of K-mesons*

By R. H. W. JOHNSTON and C. O'CEALLAIGH
Dublin Institute for Advanced Studies†

[Received December 13, 1954]

SUMMARY

An event is described in which a K-meson decays at rest to a particle at plateau ionization which has the properties of an electron of $p\beta c \sim 80$ MeV. This brings to three the number of K-mesons in which the charged decay product is apparently an electron.

§ 1. INTRODUCTION

DURING routine scanning of plates from Flight 30 of the Sardinia Flights of 1953, an event has been found which resembles those already described by Friedlander *et al.* (1954), and by Dahanayake *et al.* (1954). A heavy charged meson decays at rest. The charged secondary particle of ionization indistinguishable from the plateau value, had a visible range of 9 mm, passing through three plates before leaving the stack. The mean value of the scattering parameter $\bar{\alpha}$ was $0{\cdot}27°/100\,\mu$. This value will later be shown to be significantly different from that of a μ-meson of the observed ionization. Accordingly, the event was identified as being a further example of the electron-decay of K-mesons, the first evidence for the existence of which has recently been put forward by Friedlander *et al.* (1954). The following are the criteria (Friedlander *et al.* 1954) which must be satisfied by a K → e event:

(1) The estimate of mass of the primary particle must differ significantly from that of the π-meson and also from that of the proton;

(2) the ionization in the track of the secondary particle must be indistinguishable from the plateau value ($b^*=1$), while the estimate of $p\beta c$ must differ significantly from that of a μ-meson of plateau ionization; and/or

(3) if the track of the secondary particle is of sufficient length, there should occur a significant loss of energy by *bremsstrahlung*. In the present case no evidence was found for significant decrease of the energy of the secondary particle by *bremsstrahlung*, nor indeed would such be probable, since the visible length of trajectory is $\sim 1/3$ radiation length. For this reason, the identification of the secondary particle is based on the statistical argument (2).

§ 2. PRIMARY PARTICLE

The primary particle emerges from a star of type $10+4n$. Four black tracks and one heavy fragment ($Z \sim 3$) came to rest in the stack without visible secondary particles. Four grey tracks other than the K-particle, left the stack. No attempt was made to trace the lightly ionizing particles.

---

† Communicated by the Authors.

The primary particle passed through 3 plates before decay, having a mean range per plate $6640\,\mu$. From the estimated mean gap-length in the neighbourhood of the point of decay, it was concluded that the event occurred when the primary particle was at rest, or moving with negligible velocity. The total path traversed was 9·2 mm, corresponding, for mass $966\,m_e$, to an energy of emission of 37·8 MEV, and a time of flight $0{\cdot}11\times10^{-9}$ sec. Mass estimates were made using the techniques (1), scattering-range and (2), ionization-range.

2.1. *Scattering-range*

The mass estimates were made by the constant sagitta technique using the scattering scheme $\bar{D}_\pi=0{\cdot}5\,\mu$ of Fay *et al.* (1954). They give the following relationship which holds to a good approximation for singly-charged particles

$$M=273\times(0{\cdot}5\bar{D}_j)^N$$

where M is the value of the particle mass in terms of m_e, $\bar{D}_j$ is expressed in microns. The value of the exponent N given by Fay *et al.* is 2·32. We have, however, taken the value $N=2{\cdot}27$ as being more appropriate, as it takes into account variations in the value of the scattering constant, whereas the value $N=2{\cdot}32$ is based only on the assumed range–energy relationship. Extensive calibration work to check these and similar tables using identified protons and π-mesons is at present nearing completion (Bristol–Dublin Group).

Using the value $N=2{\cdot}27$ the mass of the primary particle was found to be

$$1010^{+190}_{-130}\,m_e.$$

2.2. *Mean Gap-Length–Range* ($\bar{G}$, R)

The mass of the primary particle was also measured using the $\bar{G}/R$ technique (O'Ceallaigh 1953, 1954, Menon and O'Ceallaigh 1954).

Two protons identified by δ-ray counts and one π-meson were used as calibration particles. The observations are shown in fig. 1 on a log–log plot. The results have been fitted by straight lines by the method of least squares. The estimates of mass* are :

From the π-meson $789\pm100\,m_e$.
From the protons $867\pm\ \ 80\,m_e$.

**Note added in proof.*—A normalized $\bar{G}$ calibration for the S.30 stack using methods analogous to those developed by Fowler and Perkins (private communication) has since been completed. Values have been found for the normalized parameter $\bar{G}^*=\bar{G}_0/\bar{G}_x$. $\bar{G}_0$ is the plateau mean gap-length determined by measurements on electrons, $\bar{G}_x$ the mean gap-length of protons and π-mesons of selected range. Use of this calibration yields a mass-estimate of the parent K-meson of $970\pm70\,m_e$.

These are in satisfactory agreement with those found for the range-scattering measurements.

Thus, the decaying particle satisfies criterion (1) and is assumed to be a K-meson.

Fig. 1

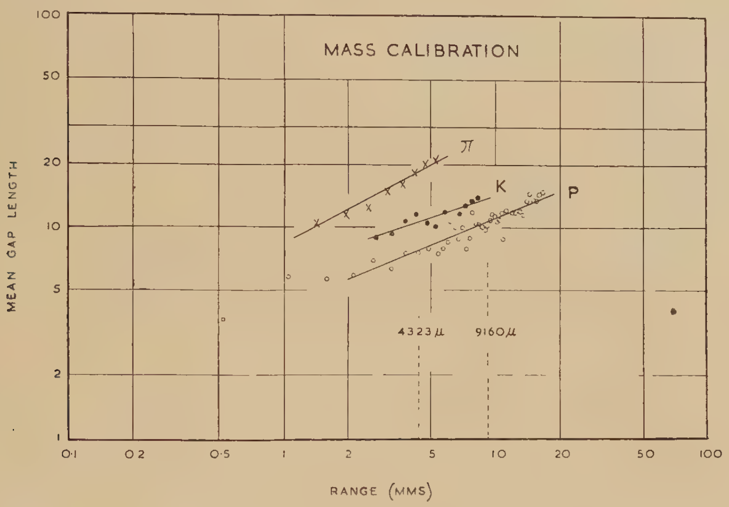

§ 3. Secondary Particle

The trajectory of the secondary particle was flat and had a total length in 3 plates of 9 mm. It left the stack through the processed edge of the fourth plate.

Since the plateau value of blob-density was very low (14 blobs/100μ), and the significance of the results depends on the accuracy of the follow through procedure, a very precise technique was necessary. This was similar to that at present employed in Bristol (1954). A C.T.S. M.4000 microscope was employed, having a rotating turntable carrying an accurately constructed jig secured by brass clamps. By use of this, the position of the track was fixed to within a few microns. It was orientated along the x-axis of the stage and the point of entry in the succeeding plate was calculated from the dip of the track. The spurious shift along the y-axis was found by examining under low power the displacement of steep neighbouring tracks. The stage was set in the calculated position, and the continuation of the track located. The identification was verified by comparison of the track characteristics, b, $\bar{\alpha}$ and dip angle. This operation was checked by several observers. Owing to the care taken, it is felt that the possibility of a mistaken identification is excluded.

3.1. *Influence of Distortion*

The scattering measurements were continued up to 1 mm from the edge of the third plate. It was necessary, therefore, despite the small dip of the track, to estimate the influence of distortion on the measured values of scattering parameter. In this plate, 7(*a*), the surface distortion vector component at right angles to the track was $\sim 30\,\mu$, corresponding for $150\,\mu$ cell, to a spurious sagitta of $0{\cdot}005\,\mu$ on a track of length $3500\,\mu$ in a $600\,\mu$ plate. This would lead to an overestimate of $\sim 1\%$ of the $\bar{\alpha}$ in this plate. In the other two plates, 6(*a*) and 5(*a*), both the distortion vector and dip are rather less than in plate 7(*a*). Accordingly, we may neglect the influence of distortion on the estimate of $p\beta c$ of the secondary particle.

Stage noise has been measured for the instrument used and shown to be negligible for cell sizes $< 500\,\mu$.

The results of the scattering and ionization measurements on the secondary particle are given in the following tables. The measurements have been made with coefficient of overlap $\lambda = 2$ and 3 but N throughout refers to the number of non-overlapping cells in each sample.

Table 1 contains details of measurements and characteristics of the individual segments of track.

Table 1

Plate	Projected length (μ)	Blobs/100 μ	Plateau blobs/100 μ	b^*	Cell sizes(μ)	$\bar{\alpha}$ 100 (0/100 μ)	N
5(*a*)	1820	14·4±0·7	13·82±0·21	1·04 ±0·05	75/25	0·311 ±0·056	20
6(*a*)	3547	12·8±0·6	13·19±0·26	0·97 ±0·05	100/25	0·300 ±0·042	33
7(*a*)	3536	12·6±0·6	13·29±0·27	0·95 ±0·05	150/50	0·304 ±0·055	20

Results of more extended measurements on the complete track using the ordinary method of noise-elimination (Fowler 1950) are given in table 2.

The weighted mean values of $p\beta c$ were as follows:

$$81 \pm 9 \text{ Mev } (\bar{\alpha}^{(2)}),$$

$$p\beta c \;\; 98 \pm 11 \text{ Mev } (\bar{\alpha}^{(3)}).$$

Appropriate values of scattering constant (Gottstein *et al.* 1951, fig. 1) have been used to calculate the values of $p\beta c$.

It will be observed that method of third difference yields consistently lower values of the estimate of $\bar{\alpha}_{100}$. It would appear doubtful, therefore, if an unbiassed estimate of second difference results from the division of the mean value of the third difference by the accepted factor $2^{1/2}$. Evidence obtained from extensive independent measurements, indicates that this factor should be decreased by $\sim 7\%$ (Appendix). It appears reasonable, therefore, to decrease the estimate of $p\beta c$ from $\bar{\alpha}^{(3)}$ to 90 ± 11 Mev.

Table 2

Cell sizes (μ)	150—100	N	150—50	N	100—50	N
(A) Rigorous 4 $\overline{D}$ cut-off						
$\bar{\alpha}^{(2)}$	0·311±0·035	52	0·324±0·035	52	0·268±0·024	80
$p\beta c$ (Mev)	76±8		73±8		86±8	
$\bar{\alpha}^{(3)}$	0·243±0·027	48	0·246±0·027	48	0·232±0·022	76
$p\beta c$ (Mev)	98±11		96±11		99±9	
(B) 4 $\overline{D}$ cut-off with replacement						
$\bar{\alpha}^{(2)}$	0·325±0·036	52	0·314±0·035	52	0·298±0·027	81
$p\beta c$ (Mev)	75·5±9		78·0±9		80·0±7	
$\bar{\alpha}^{(3)}$	0·249±0·029	49	0·249±0·029	49	0·260±0·023	81
$p\beta c$ (Mev)	98±11		98±11		92±8	
(C) No Cut-off						
$\bar{\alpha}^{(2)}$	0·313±0·035	52	0·320±0·036	52	0·294±0·027	81
$p\beta c$ (Mev)	83±9		81±9		86·5±8	
$\bar{\alpha}^{(3)}$	0·248±0·028	49	0·245±0·247	49	0·253±0·023	78
$p\beta c$ (Mev)	105±12		106±12		100±9	

3.2. *Calibration b^*–$p\beta c$*

In earlier work it has been customary to rely on the results of Daniel and Perkins (1954), Daniel *et al.* (1952) which give the relationship between g^* and $p\beta c$ for identified π-mesons and protons emergent from high-energy interactions. This work was carried out by simultaneous blob-counts and scattering measurements. The ‘ best π-line ’ of Daniel and Perkins was taken as standard, and it has been used to identify fast particles secondary to K-decay.

Recent work at Bristol has indicated, however, that the values of g^* for a given $p\beta c$ may differ significantly from stack to stack. Consequently, it has been felt necessary to establish experimentally this relationship for the present stack. This calibration has been carried out by making blob-counts on the tracks of long flat π-mesons which underwent π–μ–e decay or gave rise to characteristic σ-stars. Five such π-mesons were measured in the interval of residual range 0–8 cm corresponding to $p\beta c$ 0–120 Mev. The relationship between R and $p\beta c$ was taken to be that of Fay *et al.* (1954), points beyond the range 5·2 cm being found by graphical extrapolation. For each plate the blob-count corresponding to plateau was found by observation on long flat electrons from π–μ–e decay. This information was supplemented by counts on similar electrons from ρ–e decay, which were accepted when they did not differ significantly from each other, and from those from π–μ–e decays in the same plate. Observations were confined to those portions of the tracks which lay within 30μ from the surface and 10μ from the glass. Approximately 1500 blobs corresponding to 1 cm of track were counted in each plate. No attempt could be made to assess variations of b_0 with position in the plate, except that measurements were accepted only if made on segments of track more than 2 mm from the processed edges of the plate.

The results are given in fig. 2. They are well fitted for $120 \geqslant p\beta c \geqslant 20$ MeV by a straight line, $\log b^* = 1{\cdot}260 - 0{\cdot}5626 \log p\beta c$. The extrapolation of this line to cut the line $b^*=1$, yields an under-estimate of the value of $p\beta c$ at which a π-meson first reaches the plateau blob-count. The line agrees with the 'best line' of Daniel and Perkins, at the point $p\beta c = 100$ MeV, but appears to have a steeper slope. The μ-line was drawn in using the mass ratio $m_\pi/m_\mu = 1{\cdot}321$. The points of intersection of these lines with the line $b^*=1$ were found to be

$$p\beta c = 173 \text{ MeV},$$

$$p\beta c = 131 \text{ MeV}.$$

Fig. 2

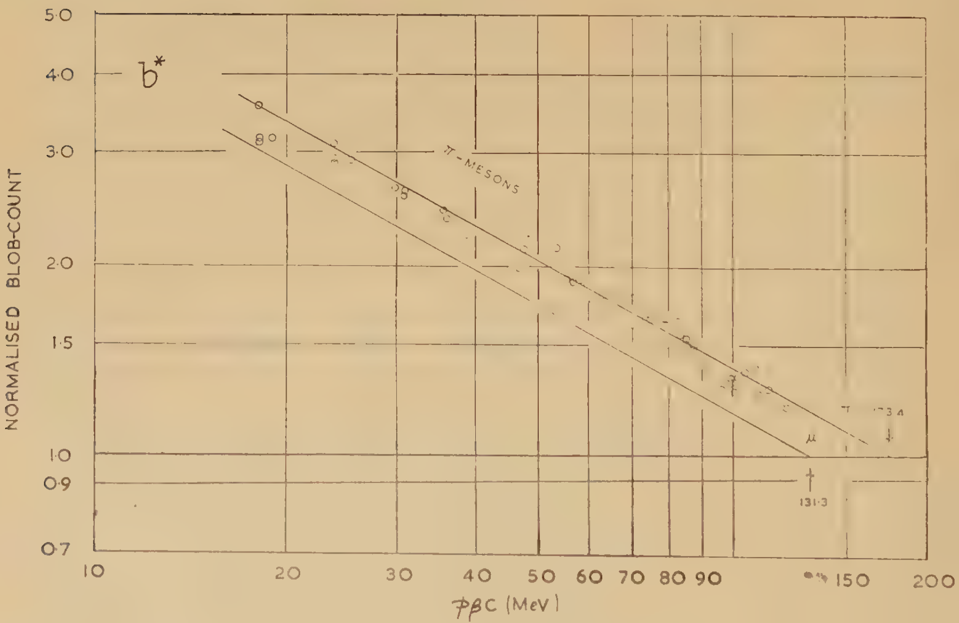

§ 4. Conclusions

As shown the value of $p\beta c$ for the secondary of the present event was 81 ± 9 MeV and is 6 standard deviations from the expected point. Thus, the probability is negligible that the secondary particle is a μ-meson. Even accepting the results of the estimate of $p\beta c$ by the method of third differences, the experimental $p\beta c$ is significantly different from that corresponding to a μ-meson. We may therefore conclude that the present example is to be identified as a case of K–e decay bringing the number of those identified at present to 3.

The observed value of $p\beta c$ agrees well with that found by Friedlander *et al.* but differs significantly from that found by Dahanayake *et al.* (49 ± 4 MeV). There is therefore good reason to suppose that in addition to the electron, at least two neutral particles are emitted as products of decay. This conclusion would be in agreement with the predictions of Michel (1952) based on the hypothesis of a universal Fermi interaction, analogous to the fundamental process of μ–e decay.

An event which from preliminary measurements appeared to be a second example of a K–e process has since been very carefully remeasured. The primary K-particle of estimated mass by scattering-range $970 \pm^{180}_{150}$ decays at rest to a secondary particle of blob-density indistinguishable from plateau. This was traced through 11 plates having average projected length $900\,\mu$ per plate. When however distortion corrections are applied, the estimate of $p\beta c$ of this particle becomes 120 ± 8 MeV. Thus, it appears as likely to be a μ-meson as an electron, although it is most improbable that it is a π-meson, and hence the reference (Dahanayake *et al.* 1954) requires modification.

ACKNOWLEDGMENTS

The authors wish to thank the Organizers and Team of the Sardinia Flights, 1953, for the exposures and for processing the plates. The event was found by Mrs. Mairin Johnston. We are grateful to her, to Miss Peggy O'Hea for assistance in carrying out the measurements and to Professor C. B. A. McCusker for reading the manuscript. For much helpful discussion we desire to thank Mr. D. Keefe and others of our Bristol colleagues. One of us (R. H. W. J.) thanks the Governing Board of the Dublin Institute for Advanced Studies for the award of a Research Scholarship.

APPENDIX

It has usually been assumed that an unbiassed estimate of $\bar{D}_2$ may be obtained from the experimental value of $\bar{D}_3$ by dividing by the factor $2^{1/2}$. This belief is founded on the assumption that the difference between two independent normally distributed variates is itself normally distributed with variance equal to the sum of the parent variances. However, the individual values of $\bar{D}_2$ taken even with coefficient of overlap $\lambda = 1$ are not independent, and also their distribution is only approximately normal.

Our measurements by the Cosyns–Vanderhaege method showed that the distortion of the secondary of the K-particle described in this paper was negligible. We have been led to suspect therefore, that the source of the discrepancy between the estimates of $\bar{\alpha}_{100}$ obtained from measurements of second and from third differences, might be a bias introduced by non-satisfaction of the conditions of normality and independence. Hence, the accepted value $2^{1/2}$ may be inappropriate to the experimental circumstances.

For these reasons we have investigated the matter experimentally using three groups of tracks with the results shown in table 3.

Table 3

Nature of tracks	No of cells	$\bar{D}_3/\bar{D}_2$
π-mesons (constant sagitta)	1806	$1{\cdot}26 \pm 0{\cdot}034$
Protons (constant sagitta)	612	$1{\cdot}25 \pm 0{\cdot}064$
105 MEV positrons from Cornell synchrotron	1449	$1{\cdot}35 \pm 0{\cdot}040$

From table 3 it would appear that the appropriate value of the divisor is lower than $2^{1/2}$, and we have adopted provisionally the value 1·32, corresponding to 7% bias. Investigation of this effect is being continued, because of the apparent discrepancy between the results for constant cell and constant sagitta.

REFERENCES

COSYNS and VANDERHAEGE, 1951, *Bull. du Cent. Phys. Nuc. Bruxelles*, **15**.
DAHANAYAKE, FRANCOIS, FUJIMOTO, IREDALE, WADDINGTON and YASIN, 1954, *Phil. Mag.*, **45**, 1219.
DANIEL and PERKINS, 1954, *Proc. Roy. Soc. Lond.*, **221**, 351.
DANIEL, DAVIES, MULVEY and PERKINS, 1952, *Phil. Mag.*, **43**, 753.
FAY, GOTTSTEIN and HAIN, 1954, *Nuovo Cim.*, **11**, Supplemento, 234.
FOWLER, 1950, *Phil. Mag.*, **41**, 169.
FRIEDLANDER, KEEFE, MENON and VAN ROSSUM, 1954, *Phil. Mag.*, **45**, 855.
GOTTSTEIN, MENON, MULVEY, O'CEALLAIGH and ROCHAT, 1951, *Phil. Mag.*, **42**, 708.
MICHEL, 1953, *Thèses*, Paris.
O'CEALLAIGH, 1953, *Bagnères Conference Report*; 1954, *CERN Standardisation Publication* B.S. 11.

XLIX. *Brillouin Zones of Some Intermetallic Compounds*

By P. J. BLACK
Royal Society Mr. and Mrs. John Jaffe Donation Student
Cavendish Laboratory, Cambridge*

[Received October 30, 1954]

SUMMARY

Data on Brillouin Zones for nine aluminium-rich compounds of iron have been obtained by x-ray analysis. For binary compounds and a ternary compound with nickel, the data can be correlated by assuming a reasonable electron absorption by iron, in agreement with previous results for alloys of cobalt and nickel. For ternary compounds containing copper and silicon, such correlation is not possible as the absorption required is obviously too high. Similar difficulties are encountered with some manganese compounds. It is suggested that the presence of a set of very strong x-ray reflexions at nearly the same spacings is not a sufficient criterion for classifying these complex phases as electron compounds.

§ 1. INTRODUCTION

THIS paper is concerned with the application of Brillouin Zone analysis to aluminium-rich intermetallic compounds of iron. Many intermetallic phases have been classified as electron compounds because it is believed that their stability is critically dependent on the filling of the zone by the free electron states. Brillouin Zone planes are related to strong x-ray reflexions (Jones 1934), and this relationship has been used to calculate volumes of Brillouin Zones for aluminium-rich compounds of the metals from chromium to nickel. It has been assumed that these are electron compounds and the electron–atom ratios derived from the volumes of the Brillouin Zones have been combined with the compositions of the compounds to give values for the 'valency' of the transition metal atoms. This analysis has been applied by Raynor and Waldron (1949), Douglas (1950), Robinson (1952 a, b, 1953), Robinson and Black (1953) and Black (1954) and these results and other work on these compounds have been reviewed by Taylor (1954). In general, valencies in approximate agreement with the electron absorption hypothesis of Raynor (1944) have been obtained. In the present work an attempt has been made to review an extensive set of such data for iron compounds.

---

* Communicated by W. H. Taylor.

§ 2. Analysis of the Data

It is necessary to consider precisely the significance of the data and this can best be done by reference to the work of Jones (1937) on the α/β phase boundaries, in which he analysed the role of the Brillouin Zone in determining the relative stability of these two phases. Curves of $N(E)dE$ against E (where E is the kinetic energy of the electrons) were computed and from them the electron–atom ratio at which the kinetic energy of free electrons is the same for both structures was found ; on either side of this value, one or other of the two structures would be the more stable because the electrons could be contained in the metal with a smaller total energy. The zones for the two structures are not good approximations to a sphere and their inscribed spheres contain only 64% and 78% of the full zone volumes. Jones' results show that each $N(E)$ curve falls sharply after the Fermi sphere first touches a plane of the zone, so that although both zones have a full volume corresponding to a ratio of two electrons per atom, the β-structure becomes more stable than the α when the latter has an electron–atom ratio of 1·41. In the present work, the largest inscribed spheres contain about 80% of the zone volume. The $N(E)dE$ curve will begin to fall after the Fermi surface first touches a plane of the zone, and some alternative structure should thus be more stable at an electron–atom ratio just above that required to fill the inscribed sphere. This latter value will be quoted here, together with the electron–atom ratio for a full zone—which should be an upper limit, for beyond this the electron distribution must overlap the zone faces and give a large increase in the energy of the electrons.

In most of the results given below, zone volumes have been calculated from the areas of the zone faces as determined graphically from drawings of the zone in projection. In other cases, an estimate of this volume has been made, and these figures are quoted in brackets. To each value of the electron–atom ratio derived from the zone, there corresponds a value for the number of electrons that each transition atom must absorb if the compound is to have this ratio and if normal valencies are assumed for aluminium, copper and silicon.

In all cases, the selected reflexions form an outstandingly strong group of approximately constant p-value. The p-values either are tabulated here or can be found in the original sources. In tables 1, 2 and 3, an approximate estimate is given, for each compound, of the ratio of the mean intensity of zone reflexions to the intensity of the strongest reflexion which appears at lower angles, i.e. inside the zone. In all cases, there are only one or two inner reflexions which are not very weak, and these do not form an approximately spherical zone. The figures may be compared with results for γ-brass, a complex structure for which it is generally accepted that the zone defines a stable electron concentration. In this case, the {222} reflexions lie within the zone formed by the {330} and {411} reflexions, and the ratios of the intensity of {222} to the intensities of {330} and {411} are approximately 1 : 9 and 1 : 3·5 respectively (Bradley and Thewlis 1926).* The zone reflexions themselves have unitary structure factors (Lipson and Cochran 1953, p. 251) of 0·7 and 0·3 for γ-brass: for $FeAl_3$, $FeCu_2Al_7$, Fe_2Al_5 and δ(AlFeSi) for which these unitary factors can be calculated, the values lie in the range 0·5 to 0·7. It seems that any criterion for restricting the application of zone analysis which is based on the relative or absolute intensity of zone reflexions cannot distinguish between these compounds and γ-brass.

§ 3

3.1. *The* (Al–Fe–Si) *System*

The existence of three 'α-phase' compounds has been reported (Armand 1952) and results for two of these have been discussed by Robinson and Black (1953). Chemical analyses by different workers of extracted crystals of the β-phase have given the following results:—

		Fe (wt. %)	Si (wt. %)
Dix and Heath	(1928)	27	15
Phragmen	(1950)	27·3	13·5
Pratt and Raynor	(1951)	26·7–27·3	13·8–14·9

The best approximate composition is $Fe_2Si_2Al_9$, which corresponds to 27·2 wt. % iron and 13·7 wt. % silicon.

Phragmen reported that the phase is monoclinic with $a=b=6{\cdot}12$ Å, $c=41{\cdot}5$ Å and $\beta=91°$. For the present work, crystals obtained by Pratt and Raynor were examined by Laue, oscillation and Weissenberg photographs, and were found to possess Laue symmetry $4/m$, with the following cell dimensions:—

$$a=6{\cdot}18\pm0{\cdot}06\text{ Å u.} \qquad c=42{\cdot}5\pm0{\cdot}5\text{ Å u.}$$

The Brillouin Zone was obtained from the following strong low-angle reflexions:—

Indices h	k	l	Multiplicity	$p=1/2d_{(hkl)}$ (Å^{-1})
2	2	0	4	0·229
1	1	18	8	0·241
0	2	16	8	0·248
1	3	2	8	0·257

The density, measured by a flotation method, is $3{\cdot}50\pm0{\cdot}10$ g/cm^3, which indicates 8·3 units of $Fe_2Si_2Al_9$ per cell. The Brillouin Zone data are summarized in table 1. The mean atomic volume is obtained from the measured density and chemical composition.

A third phase, the δ-phase, has been observed in this system by Gwyer and Phillips (1937), Janiche (1936) and Phragmen (1950). Phragmen calls it the *t*-phase ; he has measured the unit cell, which is tetragonal with $a=6{\cdot}12$ Å and $c=9{\cdot}48$ Å. According to Janiche, the composition is Al_4Si_2Fe. An approximate structure has been obtained by Spiegelberg (1954), which indicates the composition Al_3Si_2Fe, and from his results it has been calculated that the following low-angle planes give very strong reflexions :—

---

* Relative intensities are considered here, whereas Bradley and Thewlis list structure amplitudes.

Indices *h*	*k*	*l*	Multiplicity	$p=1/2d_{(hkl)}$ (Å^{-1})
2	2	0	4	0·231
1	1	4	8	0·241
1	3	0	4	0·258
2	0	4	4	0·267

The mean atomic volume is obtained from the structural data and unit cell dimensions.

The data for this system are summarized in table 1—results for the binary compound $FeAl_3$ are also included (Black 1954). The α_1–α_2–α_3 series might be considered in terms of an increase in silicon content being balanced by an increase in transition metal content to maintain a constant electron–atom ratio. The β and δ phases do not fit this trend and would have higher electron–atom ratios. This increase is not reflected in an increase of Brillouin Zone volume.

3.2. *The* (Al–Fe–Cu) *System*

The compounds occurring in this system have been investigated by Phragmen (1950) : there are two ternary compounds. Phragmen reported that the first of these is isomorphous with $MnAl_6$; its composition, in atomic percentages, is 83·2% aluminium, 4·2% copper and 12·5% iron, compared with 14·3% manganese and 85·7% aluminium in $MnAl_6$. A binary compound $FeAl_6$ has never been found and it is difficult to explain the role of copper in stabilizing a compound with a composition approximating to this. If the cell has the same size and symmetry, then there is not sufficient copper for complete replacement of aluminium or manganese on one particular site in the unit cell. Phillips (1954) has suggested that a compound $FeAl_6$ cannot be formed because the short Mn–Al distances of $MnAl_6$ are not possible for a transition metal which does not absorb as many electrons as manganese and that copper relieves this strain by replacing the aluminium. In $FeAl_3$, however, (Black 1954) the Fe–Al distances lie in the same range and can be as short as the Mn–Al distances of $MnAl_6$. The Brillouin Zone and corresponding electron–atom ratios for the compound can be calculated from the results for $MnAl_6$ (Nicol 1953) and the cell dimensions given by Phragmen ; his measured density, composition and cell size indicate that the mean atomic volume is almost the same as in $MnAl_6$. The data are given in table 2. Several compounds of this kind are related in such a way that isomorphous compounds have the same electron–atom ratio (β(AlMnSi) and Co_2Al_5—Robinson (1952 a), $FeNiAl_9$ and Co_2Al_9—Bradley and Taylor (1940)), but this type of explanation cannot apply to this case. Only if iron has about the same effective valency as manganese can these two compounds have the same electron–atom ratio.

The second ternary is of composition $FeCu_2Al_7$ and has been examined by Wiehr (1940) and Westgren (see Phragmen 1950). The unit cell is tetragonal with $a = 6{\cdot}32$ Å, $c = 14{\cdot}78$ Å. The structure was analysed by Westgren and the parameters have been published by Phragmen; from these the structure factors for all planes with $\sin \theta/\lambda < 0{\cdot}5$ have been calculated. The largest of these are listed below :—

Indices h	 k	 l	Multiplicity	$p = 1/2d_{(hkl)}$ (Å^{-1})
2	1	4	16	0·223
2	1	5	16	0·245
3	1	0	8	0·250
3	1	1	16	0·253
0	0	8	2	0·271

The mean atomic volume is obtained from the structural composition and the cell parameters.

The data for phases occurring in this system are reviewed in table 2. The trend of composition shows that the iron content is reduced by replacing both iron and aluminium by copper and this is consistent with a tendency to maintain a constant electron–atom ratio. $CuAl_2$ has been included for purposes of comparison. This structure gives strong low angle reflexions with values of p ranging from 0·211 to 0·263. It could not be classified as an electron compound—the normal Cu and Al valencies indicate that the electron distribution must overlap the Brillouin Zone planes.

3.3. Al-*Transition Metal Compounds*

Data for $FeAl_3$ have been presented elsewhere (Black 1954) and are quoted in table 1. The structure of another binary compound, Fe_2Al_5 has been determined by Schubert (1953), and Brillouin Zone data have been calculated from his results. The unit cell is orthorhombic, with $a = 7{\cdot}68$ Å, $b = 6{\cdot}40$ Å and $c = 4{\cdot}20$ Å and space group D_{2h}^{17}-Cmcm. The strong planes are as follows :—

Indices h	 k	 l	Multiplicity	$p = 1/2d_{(hkl)}$ (Å^{-1})
2	2	1	8	0·235
0	0	2	2	0·237
3	1	1	8	0·241
1	3	0	4	0·243
1	1	2	8	0·258
4	0	0	2	0·260

Tables 1–3

Compound	Composition atomic %		Mean atomic volume	e/a		Fe absorption		Ratio of mean intensity of zone reflexions to intensity of strongest reflexion lying within zone
	Fe	Si	Å^3	Inscribed sphere	Full zone	Inscribed sphere	Full zone	
$FeAl_3$	23·4	0	14·7	1·69	2·04	2·5	1·0	4 : 1
α_1	16·5	7	14·9	1·54	1·83	6·3	4·5	6 : 1
α_2	19	11	15·0	1·51	1·93	5·4	3·2	9 : 1
α_3	21	15	—	—	—	—	—	—
β	15	17	15·1	1·52	1·83	7·1	5·6	8 : 1
δ	17	33	14·8	1·53	(2·10)	7·8	4·4	4 : 1

Compound	Composition atomic %			Mean atomic volume	e/a		Fe absorption		Ratio of mean intensity of zone reflexions to intensity of strongest reflexion lying within zone
	Fe	Cu	Al	Å^3	Inscribed sphere	Full zone	Inscribed sphere	Full zone	
$(FeCu)\ (CuAl)_6$	12·5	4·2	83·2	15·1	1·35	(1·80)	9·5	5·9	4 : 1
$FeCu_2Al_7$	10	20	70	14·8	1·37	1·77	9·3	5·3	3 : 1
$CuAl_2$	—	33	67	14·8	1·6	(1·9)	$CuAl_2$ $e/a = 2·33$		1·7 : 1

Compound	Composition atomic %			Mean atomic volume	e/a		Fe absorption		Ratio of mean intensity of zone reflexions to intensity of strongest reflexion lying within zone
	Fe	Al	Ni	Å^3	Inscribed sphere	Full zone	Inscribed sphere	Full zone	
$FeAl_3$	23·4	76·6		14·7	1·69	2·04	2·5	1·0	4 : 1
Fe_2Al_5	28·6	71·4		14·0	1·61	1·98	1·9	0·6	5 : 1
Fe_3NiAl_{10}	17·7	73·6	8·7	13·8	1·50	(1·68)	3·2	2·7	2·5 : 1

Schubert's result indicates that the composition Fe_2Al_5 is attained by having some of the atomic positions only partially filled. The mean atomic volume is calculated from the structural data and so makes allowance for the effect of this. Bradley and Taylor (1940) have reported the existence of a compound Fe_3NiAl_{10}, which is isomorphous with Co_2Al_5 ; from calculations of the zone for this latter structure by Robinson (1952 a), and assuming the same cell parameters for the two compounds (Bradley and Taylor reported only small differences), the results of table 3 have been obtained. In estimating the iron absorption, it has been assumed that nickel absorbs two electrons less than iron, and the composition at the electron-rich limit of the Fe_3NiAl_{10} phase field has been taken.

§ 4. CONCLUSION

If it is assumed that a structure has all interatomic distances approximately equal, and high co-ordination so that each atom is completely surrounded by neighbours, then it can be shown that it must give a set of strong reflexion planes. The interplanar spacing of these can be related to the interatomic distance, by using the transformation which relates the intensity distribution in a powder pattern to the mean radial Patterson function (see formula (150) of Cochran and Lipson (1953)). It can then be calculated that for any structure of this type, the limiting Fermi sphere will contain 1·5–2·5 states per atom. Only general atomic packing conditions are assumed in deriving this, and the result is independent of the scale of the structure as the product (mean atomic volume × Brillouin Zone volume) is dimensionless. If empirical evidence from Brillouin Zone correlations is to be significant, it must show that the individual deviations within this mean range correspond to differences in the compositions of the compounds. In many cases, a detailed correlation of this type is not found.

Most of the results in 3.1 and 3.2 show that the empirical correlation of zone volumes on the basis of a reasonable assumed valency for the transition atoms is not possible ; the results of 3.3 might fit approximately with the Raynor hypothesis and in this respect they are in agreement with results for other transition metal–aluminium compounds. There are not enough data on the ternary compounds with copper or silicon of other transition metals to assess whether the discrepancies found here are peculiar to iron. Reference may be made to table 1 of Taylor (1954) for previous results : the data on an aluminium–manganese–zinc ternary compound and on the binary ($MnAl_6$) compound would both indicate a very large absorption for manganese. Of the two ternary compounds of manganese with silicon, the zone for the β-phase indicates an absorption of about 3 electrons for manganese, but the α-phase results again require a very much larger absorption (Robinson 1951). Jones (1953) has suggested that absorption to the extent of four electrons may be possible if this is compensated by a decrease in the free electron density in the neighbourhood of the atom.

It might be suggested that some of the compounds examined above do not belong to the same class as the aluminium-rich binary compounds. An attempt must then be made to define a criterion for distinguishing such compounds. The results given here suggest that ternary compounds containing silicon and copper do not belong to the same class as the binary compounds. An examination of their structures shows, however, that a distinction of this sort is not indicated by the inter-atomic distances and co-ordinations. It can be shown that the structures of several of the compounds discussed above are related, and that, in common with other compounds of manganese, cobalt and nickel, they all possess certain characteristic features. This will be discussed elsewhere (Black 1954).

The theoretical justification for extending the use of the Brillouin Zone theory to these complex compounds has been examined critically by Vousden (1954). At the same time, it seems that it is more reasonable to account for their stability in terms of a strong interaction between aluminium and transition metal atoms (e.g. $FeAl_3$, Black 1954), and Vousden has shown how this approach explains their characteristic properties (1954).

ACKNOWLEDGMENTS

I am grateful to Professor Raynor for supplying specimens, and I am indebted to Professor N. F. Mott and Dr. W. H. Taylor for provision of facilities and for their interest in the progress of this work. I wish to thank the Department of Scientific and Industrial Research and the Council of the Royal Society for financial support. I am grateful to Dr. Per Spiegelberg for permission to use unpublished results.

REFERENCES

ARMAND, M., 1952, *Comptes Rendus*, **235,** 1506.

BLACK, P. J., 1954, *Dissertation for Ph.D. Degree* (Cambridge) and *Acta Cryst.* (in press).

BRADLEY, A. J., and TAYLOR, A., 1940, *J. Inst. Met.*, **66,** 53.

BRADLEY, A. J., and THEWLIS, J., 1926, *Proc. Roy. Soc.* A, **112,** 678.

DIX, E. J., and HEATH, A. C., 1928, *Trans. Amer. Inst. Min. Met. Eng. Inst. Met. Div.*, p. 164.

DOUGLAS, A. M. B., 1950, *Acta Cryst.*, **3,** 19.

GWYER, A. J. C., and PHILLIPS, H. W. L., 1937, *J. Inst. Met.*, **38,** 29.

JANICHE, W., 1936, *Aluminium Archiv*, **5.**

JONES, H., 1934, *Proc. Roy. Soc.* A, **144,** 225 ; 1937, *Proc. Phys. Soc.*, **49,** 250 ; 1953, *Phil. Mag.*, **44,** 907.

LIPSON, H., and COCHRAN, W., 1953, *The Determination of Crystal Structures* (Bell : London).

NICOL, A. D. I., 1953, *Acta Cryst.*, **6,** 285.

PHILLIPS, H. W. L., 1954, *J. Inst. Met.*, **82,** 197.

PHRAGMEN, G., 1950, *J. Inst. Met.*, **77,** 489.

PRATT, J. N., and RAYNOR, G. V., 1951, *Proc. Roy. Soc.* A, **205,** 103.

RAYNOR, G. V., 1944, *J. Inst. Met.*, **70,** 531.

RAYNOR, G. V., and WALDRON, M. B., 1949, *Phil. Mag.*, **40,** 198.

Robinson, K., 1951, *Dissertation for Ph.D. Degree* (Cambridge) ; 1952 a, *Acta Cryst.*, **5,** 397 ; 1952 b, *Phil. Mag.*, **43,** 775 ; 1953, *Acta Cryst.*, **6,** 854.
Robinson, K., and Black, P. J., 1953, *Phil. Mag.*, **44,** 1392.
Schubert, K., 1953, *Naturwiss.*, **40,** 437.
Spiegelberg, P., 1954, private communication.
Taylor, W. H., 1954, *Acta Met.*, **2,** 684.
Vousden, P., private communication (in preparation for publication).
Wiehr, H., 1940, *Aluminium Archiv*, **31.**

L. *Thermal Acceptors in Germanium*

By R. J. Hodgkinson
Communication from the Staff of the Research Laboratories of the General Electric Co. Ltd., Wembley, England

[Received October 19, 1954]

Summary

Some results previously reported by the author are examined on the assumption that the thermal acceptors are copper atoms. A thermodynamic treatment of the solid solubility of copper in germanium is given in terms of the Principle of Lowest Free Energy, enabling a physical picture of the solubility to be given. This explains the approximately exponential dependence on inverse absolute temperature (below 800°c), which formerly led to the belief that thermal acceptors were lattice defects. An equation is derived which relates the concentrations of copper on the liquidus and solidus to the temperature. The experimental results are shown to obey this equation, which is equivalent to the one previously derived by Thurmond and Struthers, using a different approach.

---

§ 1. Introduction

It has long been known (Torrey and Whitmer 1946) that if a germanium specimen is heat treated at a high temperature, and then quenched rapidly to room temperature, the concentration of acceptor centres in it is increased. The concentration of these added acceptors, which are called ‘ thermal acceptors ’ is determined by the temperature of heat treatment.

There have been several publications (Fuller and Struthers 1952, Slichter and Kolb 1952, Seiler, Geist, Keller and Blank 1953) which suggest that the formation of thermal acceptors is associated with the diffusion of impurities into the germanium during heat treatment. In particular, copper has been suggested as being responsible for the observed heat treatment effects. Fuller and Struthers (1952) published measurements of the saturation concentration of diffused copper in germanium heat treated at various temperatures, and of the concentration of thermal acceptors in the same specimens. They found that within the limits of experimental error, the number of thermal acceptors was equal to the number of copper atoms. They therefore interpreted their results to mean that thermal acceptors were to be identified with copper atoms, and that the equilibrium concentrations of thermal acceptors were the saturation solid solubilities of copper in germanium at the temperatures in question. They found that the concentrations of thermal acceptors and of copper atoms were given by relations of the form (1), apart from those at the highest temperature of measurement (919°c), which were lower than this relation would predict.

$$n=A \exp\left(-\frac{W}{kT}\right) \qquad \dots\dots\dots \quad (1)$$

where n=concentration of thermal acceptors or copper atoms,
A=constant,
k=Boltzmann's constant,
T=absolute temperature,
W=constant (=28 000 cal/mol. or 1·24 ev/atom).

§ 2. EXPERIMENTAL WORK

Measurements of the concentrations of thermal acceptors have been carried out in this laboratory (Hodgkinson 1954), and have been extended up to 930°c.

Specimens of germanium about $0{\cdot}1\times0{\cdot}1\times2$ cm^3 were heat treated in evacuated silica capsules placed inside an electrical resistance furnace. At the end of a period of heat treatment, the silica capsule was pulled from the furnace into a beaker of water. The total time of quenching was of the order of a second or less. Concentrations of thermal acceptors were determined from electrical resistance measurements, carried out in a thermostat at 30°c.

2.1. *Results*

The results of the measurements are shown in fig. 1, where $\ln n$ is plotted against $1/T$. In the temperature range below 800°c, the concentrations of thermal acceptors are given by a relation of the form of eqn. (1). The values of W determined for the individual specimens vary from about 1·13 to 1·57 ev. Utilizing all of the measurements reported in this paper, $n=1{\cdot}61\times10^{22}\exp(-1{\cdot}31/kT)$. Above 800°c, the concentrations of thermal acceptors are lower than those given by eqn. (1), and above 880°c, the concentration of thermal acceptors decreases with rising temperature. The measurements at 919°c made by Fuller and Struthers are consistent with this decrease.

§ 3. THEORY

If thermal acceptors are copper atoms, it would be expected that their equilibrium concentration would be determined by equilibrium in the system copper–germanium. Figure 2 shows the copper–germanium phase diagram (Smithells 1949). The thermal acceptors would form a solid solution of copper in germanium at the right hand side of the diagram, but the saturation solubility is too small to be shown. It will be seen that above 650°c, the solid solution will be in equilibrium with the liquid phase. It would be expected that the solid solubility of copper in germanium would fall to zero as the melting point of pure germanium is approached. However, it is the retrograde solubility of copper in germanium at lower temperatures which is of main interest here.

Fig. 1

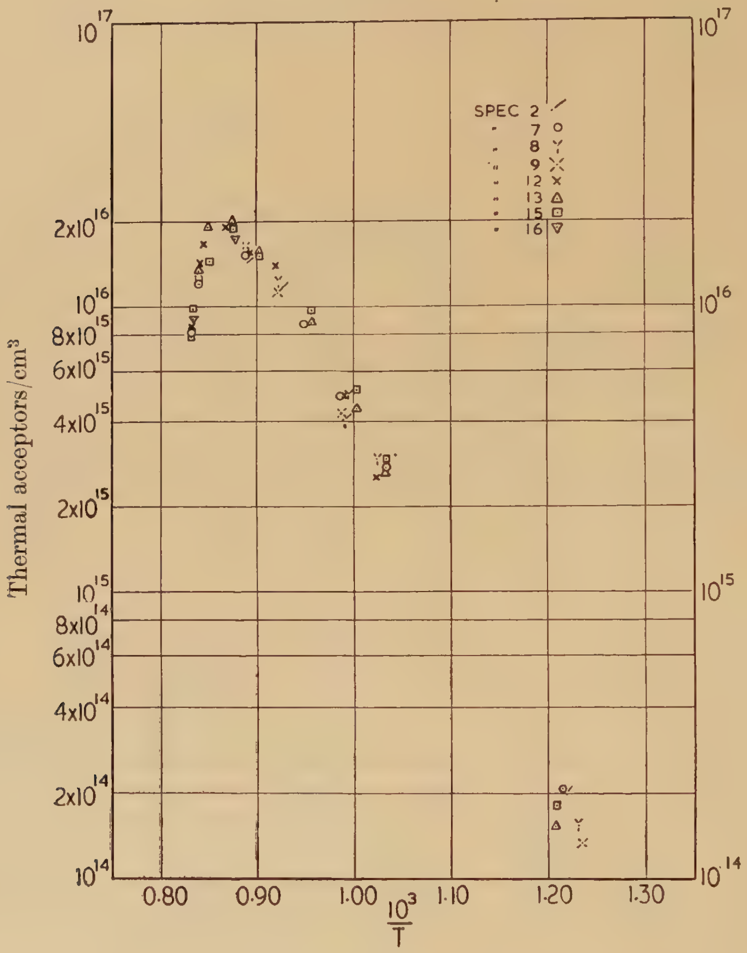

Experimental values of the variation of thermal acceptors with temperature.

3.1. *Previous Theoretical Treatment*

Recently, Thurmond and Struthers (1953) have treated the problem theoretically, by equating the partial free energy of copper in solid solution in germanium to that of copper in the liquid Cu–Ge phase in equilibrium with the solid. An expression is derived for the variation with temperature of K, the partition coefficient of copper between solid and liquid germanium.

$$\ln K = \frac{\Delta H_2^f - \overline{\Delta H_2^s}}{RT} + \frac{\sigma - \Delta S_2^f}{R} + \ln \gamma_2^l \quad . \quad . \quad . \quad (2)$$

where

K=ratio of concentration of copper on the solidus to concentration of copper on liquidus,

ΔH_2^f=heat of fusion of copper (assumed independent of temperature),

$\overline{\Delta H_2^s}$=partial molar heat of solution of solid copper in solid germanium,

σ=entropy term to account for changes of vibrational entropy of copper atoms on being transferred from a copper to a germanium crystal,

ΔS_2^f=entropy of fusion of copper (assumed independent of temperature),

γ_2^l=activity coefficient of copper in the liquid Cu–Ge phase,

R=gas constant/mole.

Fig. 2

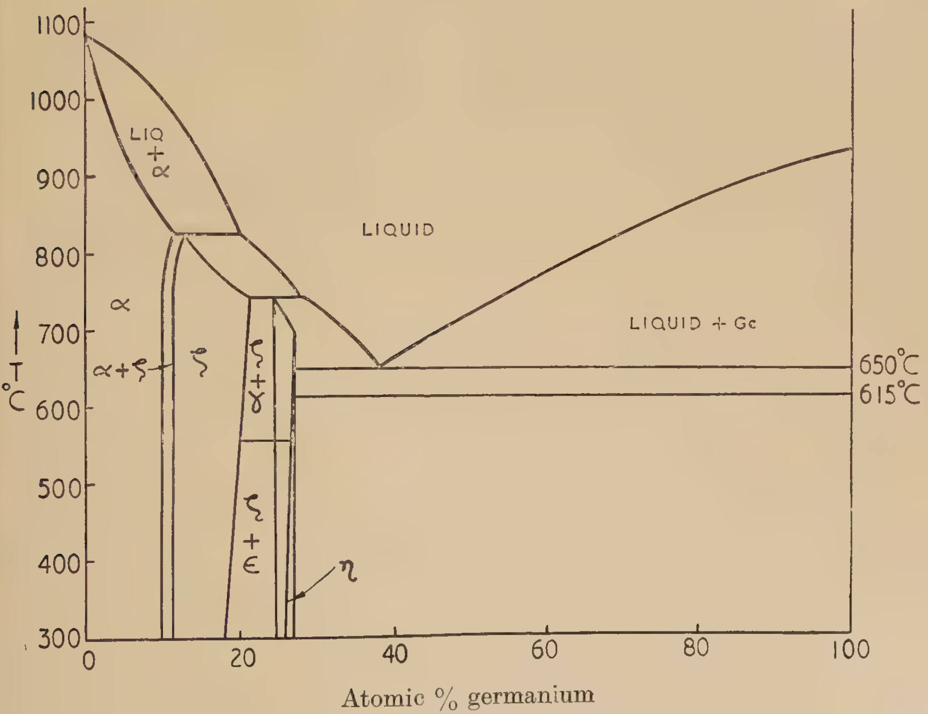

Cu–Ge phase diagram.

The solid is treated as a regular solution, and initially the liquid is treated as ideal. Later, the activity coefficient γ_2^l is introduced to take account of the departures from ideality of the liquid, and the term σ is introduced to take account of the change in vibrational energy of the copper atoms on being transferred from one medium to another.

Thurmond and Struthers conclude that $\ln K$ should be a smooth function of temperature. On plotting experimental values of $\ln K$ against $1/T$, a straight line is obtained. Extrapolation to T=melting point of pure germanium yields a value of $K=0{\cdot}98\times10^{-5}$, which is in good agreement with the value $1{\cdot}5\times10^{-5}$, found by other methods. On the assumption that $\ln \gamma_2{}^l$ has little effect on the slope of $\ln K$ v. $1/T$, the slope is equated to $\Delta H_2{}^f-\overline{\Delta H_2{}^s}$, from which $\overline{\Delta H_2{}^s}$ is calculated (=45 200 cal/g atom) since $\Delta H_2{}^f$ is known.

3.1.1. *Present Treatment*

The treatment presented here differs from that of Thurmond and Struthers, by considering the integral free energies of the solid and liquid phases. The principle of lowest free energy (Lipson and Wilson 1940, Cottrell 1948) is applied to obtain the equilibrium conditions. This enables a simple physical picture to be built up, which gives a qualitative explanation of the form of the solid solubility curve of copper in germanium. To apply the principle of lowest free energy, the variation of free energy with composition for the two phases is calculated. The theory is shown to be consistent with the experimental results.

3.2. *Principle of Lowest Free Energy*

Equilibrium conditions in an alloy system may be considered in terms of the principle of lowest free energy. To apply this principle the form and relative position of the free energy curves of the two phases in equilibrium must be known. These are now investigated for the solid solution of copper in germanium, and for the liquid copper–germanium phase.

3.3. *Free Energy Curve for the Solid Solution*

It will be assumed that the solid solution of copper in germanium is substitutional; however, the treatment for an interstitial solid solution will be similar, and the expression for the free energy will be of the same form.

The free energy, f, per atom of a dilute substitutional solid solution is given by an expression of the form (Mott and Jones 1936)

$$f=-\frac{kT}{N}\ln\frac{N\,!}{(N-n)\,!\,n\,!}+E(n)+\int_0^T C_v dT-T\int_0^T\frac{C_v dT}{T}\quad\ldots\quad(3)$$

where N=number of lattice sites/cm^3,

n=number of solute atoms/cm^3,

T=absolute temperature,

C_v=heat capacity per atom at constant volume,

$E(n)$=internal energy per atom at absolute zero of temperature.

The first term $k/N \ln N\,!/(N-n)\,!\,n\,!$ is the configurational entropy of mixing of the solvent atoms and the solute atoms.

For a very dilute solution, each solute atom will be surrounded completely by solvent atoms, and the energy increase of the solid due to the addition of one solute atom will be independent of n. $E(n)$ may therefore be written

$$E(n)=E_0+\frac{nE}{N},$$

where E_0 is the value of $E(n)$ for the pure solute, and E is the energy increase of the solution on introducing one solvent atom, substitutionally. In addition, in the case considered here, the solute atoms will be ionized, and an additional term will have to be added to the free energy (Goldberg 1952) in eqn. (3). Reiss (1953) has dealt with the problem of impurity atoms in semiconductors, and has shown that they may be treated as an ionized electrolyte.

At the temperatures considered here, the germanium will be intrinsic and the impurity atoms will all be ionized. The extra energy term will thus be independent of temperature. Suppose it is equal to ϵ, and suppose $E+\epsilon=W$. In addition, an entropy term $kT\ln 2$ must be added to account for the two possible spins of the electron in the impurity levels.

If it is assumed that germanium is an Einstein type solid, then for the pure solid (Mott and Jones 1936)

$$\int_0^T C_v dT-T\int_0^T \frac{C_v dT}{T}=\frac{3kT}{N}\ln\frac{h\nu}{kT}, \quad . \quad . \quad . \quad . \quad . \quad (4)$$

where ν is the vibration frequency of the atoms.

If n atoms of solute replace n germanium atoms, they will have a different vibration frequency ν' from the atoms they replace. Suppose that the vibration frequency of the x nearest neighbours to a solute atom is changed to ν'' along a line joining them to the solute atoms. Then eqn. (4) becomes (Mott and Gurney 1948)

$$\int_0^T C_v dT-T\int_0^T \frac{C_v dT}{T}=\frac{1}{N}\Big[\{3N-n(x+3)\}kT\ln\frac{h\nu}{kT} +3nkT\ln\frac{h\nu'}{kT}+nxkT\ln\frac{h\nu''}{kT}\Big]. \quad . \quad . \quad (5)$$

Thus, eqn. (3) becomes

$$f=-kT\ln\frac{N\,!}{(N-n)\,!\,n\,!}+E_0+\frac{Wn}{N}-\frac{nkT}{N}\ln 2 +\frac{1}{N}\Big[\{3N-n(x+3)\}kT\ln\frac{h\nu}{kT}+3nkT\ln\frac{h\nu'}{kT}+nxkT\ln\frac{h\nu''}{kT}\Big] \quad . \quad (6)$$

Applying Stirling's approximation to the first term on the right-hand side of eqn. (6), and differentiating with respect to n,

$$N\frac{\partial f}{\partial n}=kT\ln\frac{n}{N-n}+W-(x+3)kT\ln\frac{h\nu}{kT}-kT\ln 2+3kT\ln\frac{h\nu'}{kT} +xkT\ln\frac{h\nu''}{kT}=kT\ln\frac{n}{(N-n)}+W-kT\ln C-kT\ln 2 \quad . \quad . \quad (7)$$

where

$$C=\frac{\nu^{x+3}}{\nu'^3\nu''^x}.$$

For a minimum, $$\frac{\partial f}{\partial n}=0$$

i.e. $$n=2C(N-n)\exp\left(-\frac{W}{kT}\right)\doteqdot 2CN\exp\left(-\frac{W}{kT}\right).$$

Suppose $n=n_0$ at the minimum, then

$$n_0=A\exp\left(-\frac{W}{kT}\right) \qquad \text{. . . . . (8)}$$

where $$A=2C(N-n)\doteqdot 2CN=\text{const.}$$

To calculate the solid solubility curve of copper it is necessary to know the slope of the free energy curve i.e. $\partial f/\partial n$. This is most conveniently expressed by considering $n=\alpha n_0$ at any point on the curve. Thus eqn. (7) becomes

$$N\frac{\partial f}{\partial n}=kT\ln\frac{\alpha n_0}{N-\alpha n_0}+W+kT\ln C-kT\ln 2.$$

Now $$N-\alpha n_0\doteqdot N-n_0 \quad \text{since} \quad n\ll N \quad \text{and} \quad n_0\ll N.$$

Hence

$$N\frac{\partial f}{\partial n}\doteqdot kT\ln\alpha+\left[kT\ln\frac{n_0}{N-n_0}+W+kT\ln C-kT\ln 2\right].$$

But the term in brackets is zero, therefore

$$N\frac{\partial f}{\partial n}=kT\ln\alpha. \qquad \text{. . . . . . . (9)}$$

3.3.1. *Free Energy Curve for the Liquid Phase*

Unfortunately, the form of the free energy curve for the liquid phase is not known. Nor are the concentrations of copper in the liquid phase small. Thus the liquid cannot be considered a dilute mixture. However, it will be seen that if it be assumed that the liquid is ideal then the subsequent calculations agree fairly well with experiment.

For an ideal mixture, the heat of mixing will be zero, and the entropy of mixing ideal (Lumsden 1952).

Let

$F_{\mathrm{Cu}}{}^0$=free energy per atom of pure liquid copper at T°K.

$F_{\mathrm{Ge}}{}^0$=free energy per atom of pure liquid germanium at T°K.

Then the free energy per atom of a mixture of $(N-n)$ germanium atoms with n copper atoms will be

$$F_L=\frac{1}{N}[(N-n)F_{\mathrm{Ge}}{}^0+nF_{\mathrm{Cu}}{}^0]+\frac{kT}{N}\left[(N-n)\ln(N-n)+n\ln n-N\ln N\right]$$

therefore $$N\frac{\partial F_L}{\partial n}=(F_{\mathrm{Cu}}{}^0-F_{\mathrm{Ge}}{}^0)+kT\ln\frac{n}{N-n}$$

$$=\delta F^0+kT\ln\left(\frac{n}{N-n}\right). \qquad \text{. . . (10)}$$

3.4. *Practical Application*

3.4.1. *Physical Picture*

Before proceeding to the numerical calculation of the solid solubility curve of copper in germanium, a simple picture can be given which explains the shape of the curve, and gives physical meaning to the calculations. The solid solution will be referred to as the β-phase.

Figure 3 shows schematically the free energy curves of the liquid and β-phases at a fixed temperature T just above 650°C. Curve 1 is the free energy curve of the liquid phase, curve 2 that of the β-phase. The right-hand side of the diagram represents 100% Ge.

Fig. 3

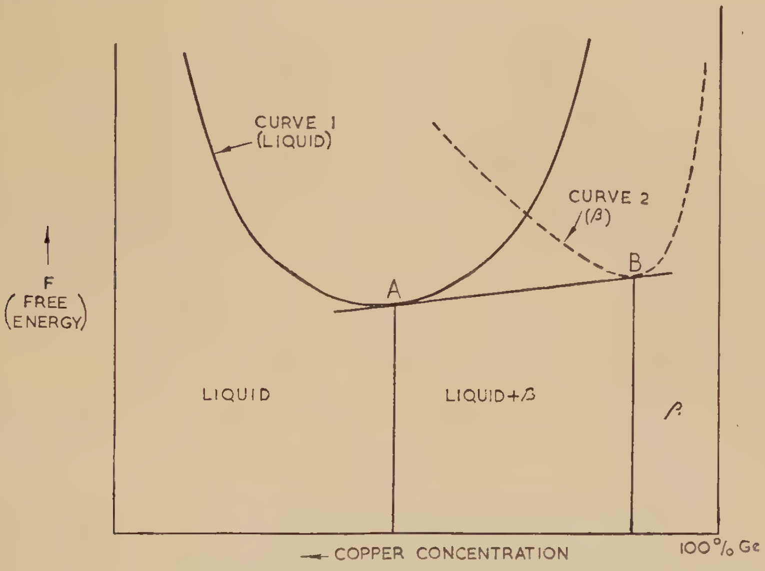

Variation of free energy of β and liquid phases with composition (T just>650°C).

The free energy curve of the β-phase is shown rising sharply as the concentration of copper tends to zero. This is because the configurational entropy term in the free energy decreases rapidly in this region.

From the principle of lowest free energy, the boundary points of the liquid and β-phases are given by the compositions at A and B respectively. In fig. 3, the tangent AB is drawn nearly horizontally, and the point B is thus nearly at the minimum of the free energy curve of the β-phase. If it is assumed that below a certain temperature this condition holds, then it would be expected that in this region $n_s \doteqdot n_0$ (see § 3.3) and that

$$n_s \doteqdot A \exp\left(-\frac{W}{kT}\right) \quad . \quad . \quad . \quad . \quad . \quad . \quad . \quad (11)$$

where n_s is the saturation concentration of copper atoms in the β-phase, i.e. the same form of temperature dependence is obtained as was found for thermal acceptors between 550°C and 800°C

As the temperature is raised curve 1 will sink relative to curve 2, and there will be a tendency for the point B to move to the right of the minimum. This tendency will be small until a limiting temperature is reached. Above this temperature, n_s will deviate strongly from the value given by eqn. (11), and eventually will decrease with rising temperature. This state of affairs is shown in fig. 4, where the notation is the same as in fig. 3. As the melting point of pure germanium is reached, the two points A and B will coincide at 100% Ge, i.e. the solubility will have become zero.

Fig. 4

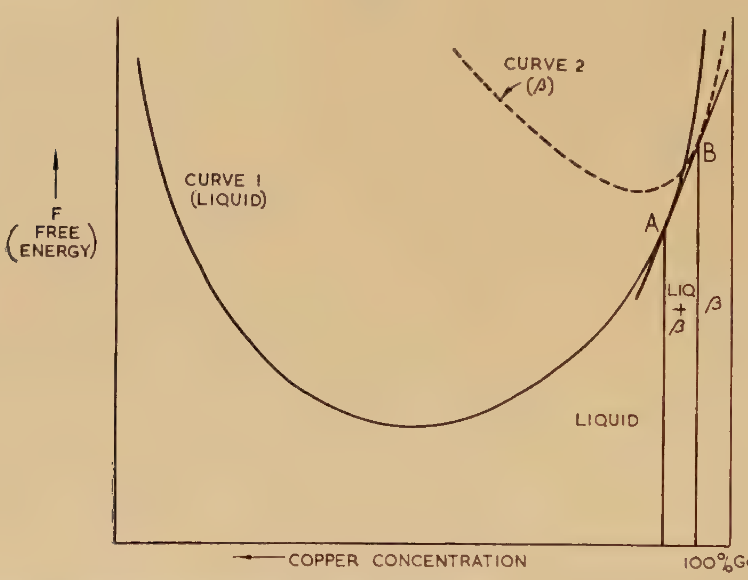

Variation of free energy of β and liquid phases with composition (high temps.).

3.4.2. *Numerical Calculation*

Now for a given temperature T,

$$\left(\frac{dF_L}{dn}\right)_{n=n_L}=\left(\frac{df}{dn}\right)_{n=n_s}$$

(see § 3.2) i.e. using eqns. (9) and (10)

$$kT\ln\alpha=\delta F^0+kT\ln\frac{n_L}{N-n_L}.$$

Hence
$$\frac{N-n_L}{n_L}=\frac{1}{\alpha}\exp\left(\frac{\delta F^0}{kT}\right).$$

But
$$\frac{n_s}{\alpha}=n_0$$

therefore
$$\left(\frac{N-n_L}{n_L}\right)n_s=n_0\exp\left(\frac{\delta F^0}{kT}\right)$$

i.e.
$$\left(\frac{N-n_L}{n_L}\right)n_s=A\exp\left(\frac{\delta F^0-W}{kT}\right). \quad . \quad . \quad . \quad . \quad (12)$$

By considering the quantities in this equation in terms of partial thermodynamic quantities, it can be shown to be equivalent to eqn. (2) apart from the term $\gamma_2{}^l$ since

$$n_0 = A \exp\left(-\frac{W}{kT}\right) \quad \text{(eqn. (8)).}$$

Fig. 5

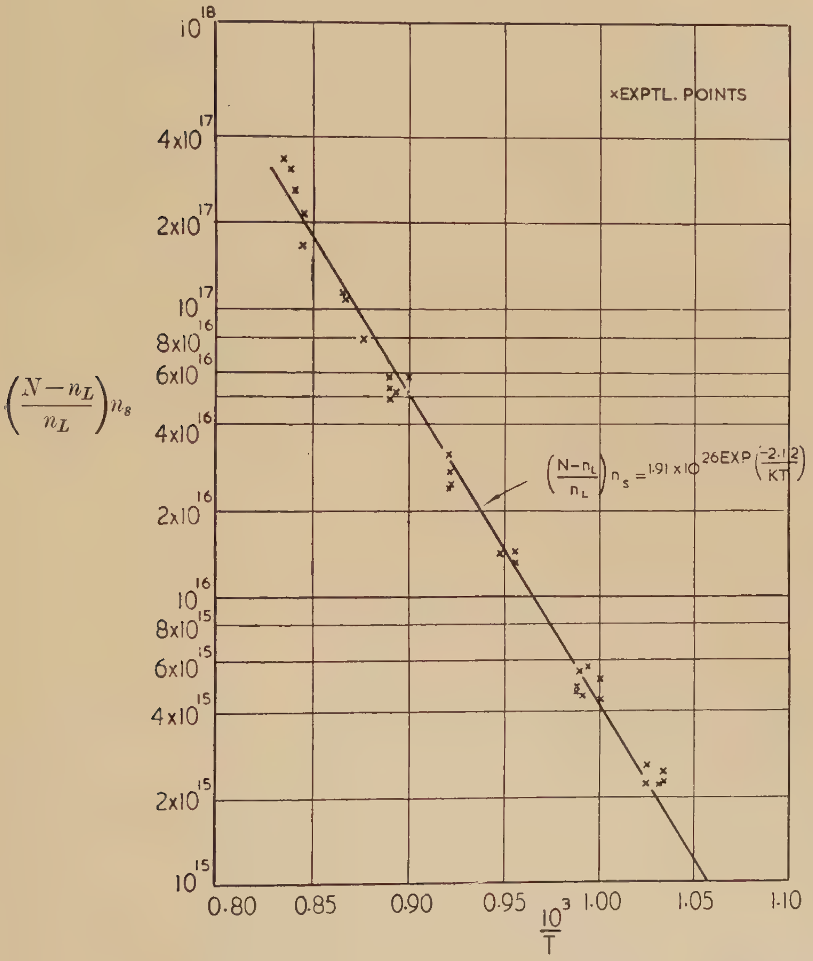

Plot of ln $\left(\frac{N-n_L}{n_L}\right)n_s$ against $\frac{10^3}{T}$ (values gained from expt. points for n_a).

Now, δF^0 would be expected to vary little with temperature, i.e. if $\ln[\{(N-n_L)/n_L\}n_s]$ is plotted against $1/T$, a straight line of slope $(\delta F^0 - W)/k$ should be obtained. These quantities have been plotted in fig. 5, where it can be seen that the linear relationship is obeyed fairly well, with

$$\delta F^0 - W = -2{\cdot}12 \text{ ev}$$

and

$$A = 1{\cdot}91\times10^{26}/\text{cm}^3.$$

In fig. 6, the $\ln n_s - 1/T$ curve corresponding to this line has been plotted, and compared with the experimental points.

Fig. 6

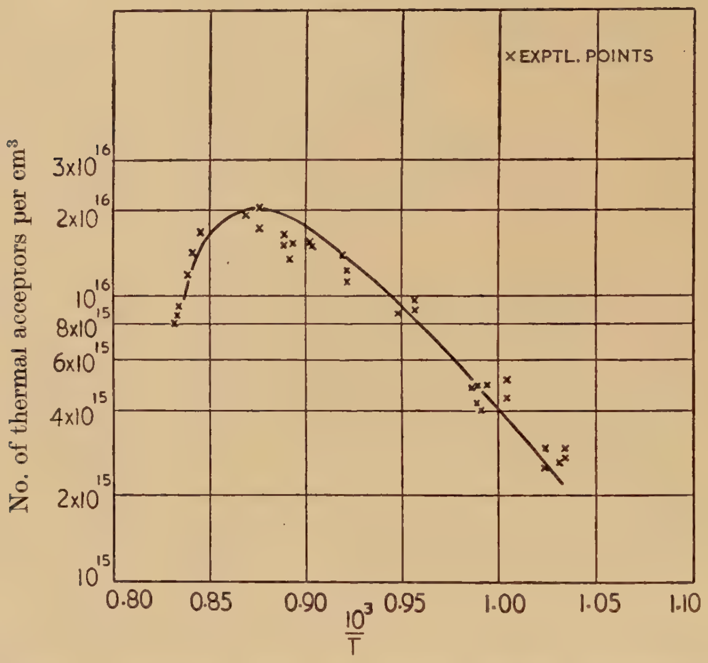

Comparison of theoretical curve for thermal acceptor concentration with experimental values.

§ 4. Discussion

It must be emphasized that the experimental values of n_s are concentrations of thermal acceptors, and not explicitly of copper atoms. Recently, van der Maesen and Brenkman (1954) have shown that nickel also diffuses rapidly in germanium. Their measurements of its solid solubility indicate that it is smaller than that of copper by a factor of 10 at 700°c, changing to a factor of 4 at 920°c. The effect of the presence of nickel on the measured values of n_s would thus be small except at the higher temperatures. The tendency of the plot of $\ln [\{(N-n_L)/n_L\}n_s]$ against $1/T$ to curve upwards at higher temperatures (fig. 5) may possibly be explained by the presence of nickel. However, there is good agreement between the values of n_s used in this paper, and the concentration of thermal acceptors found by Fuller and Struthers (1952). These, in turn, were in good agreement with the concentration of copper atoms diffused into the identical samples.

The variation of the solid solubility of nickel (van der Maesen and Brenkman 1954) with temperature follows the predictions made here, although the exponential low temperature region is small (above the eutectic temperature). The measurements also agree well with the type of variation given by eqn. (12).

The author wishes to express his thanks to Mr. R. W. Douglas for many helpful discussions.

REFERENCES

COTTRELL, A. H., 1948, *Theoretical Structural Metallurgy* (London : Arnold), p. 163.
FULLER, C. S., and STRUTHERS, J. D., 1952, *Phys. Rev.*, **87**, 527.
GOLDBERG, C., 1952, *Phys. Rev.*, **88**, 920.
HANSEN, M., 1934, *Der Aufbau der Zweistofflegierungen* (Berlin : Springer).
HODGKINSON, R. J., 1954, *G. E. C. Journal*, **21**, No. 1.
LIPSON, H., and WILSON, A. J. C., 1940, *Journ. Iron and Steel Inst.*, **142**, 107.
LUMSDEN, J., 1952, *Thermodynamics of Alloys* (London : Institute of Metals), p. 165.
VAN DER MAESEN, F., and BRENKMAN, J. O., 1954, *Phillips Res. Rep.*, (**9**) 3, 255.
MOTT, N., and GURNEY, R., 1948, *Electronic Processes in Ionic Crystals* (Oxford : University Press), p. 30.
MOTT, N., and JONES, H., 1936, *The Theory of the Properties of Metals and Alloys* (Oxford : University Press), p. 27.
REISS, H., 1953, *Journ. Chem. Phys.*, **21** (7), 1209.
SEILER, K., GEIST, D., KELLER, K., and BLANK, K., 1953, *Naturwiss.*, **40** (2), 56,
SLICHTER, W. P., and KOLB, E. D., 1952, *Phys. Rev.*, **87**, 527.
SMITHELLS, 1949, in *Metals Reference Book* (London : Butterworth).
TORREY, H. L., and WHITMER, C. A., 1946, *Crystal Rectifiers* (New York: McGraw Hill), p. 365.
THURMOND, C. D., and STRUTHERS, J. D., 1953, *Journ. Phys. Chem.*, **57**, 831.

LI. *A New Treatment of Anharmonicity in Lattice Thermodynamics : I*

By D. J. HOOTON
Department of Mathematical Physics, University of Edinburgh *

[Received November 6, 1954]

SUMMARY

Born has given a method by which the anharmonic vibrational motion of the atoms in a crystal can be approximated in terms of an adapted set of harmonic oscillations, these differing from the usual modes of vibration of harmonic lattice dynamics ; this method is here redeveloped from another standpoint and extended to give explicit results. The thermodynamical formulae of the anharmonic crystal can be given a simple form : they consist of the customary formulae for a set of harmonic oscillators, but now expressed in terms of new frequencies defined essentially from the quadratic *and* quartic terms in an expansion of the potential energy, plus correction terms which express the difference between the actual anharmonic motion and the harmonic approximation. For small anharmonicity the formulae reduce to those of the usual perturbation procedure (allowance for thermal expansion) with some extensions, but they also give a solution in the case of strong anharmonicity. This latter solution will later be used in a discussion of solid helium.

§ 1.

IN an attempt to establish the existence of intrinsic imperfections in a crystal at thermal equilibrium on the basis of lattice dynamics Born (1951 a) has paid critical attention to the anharmonicity of the atomic vibrations in a way which allows quite another type of problem to be dealt with. When the vibrational energy is large compared with the static cohesive energy the displacements of the atoms, say from regular lattice sites, may far exceed the limits of smallness implied by the use of the usual harmonic theory. For example, Domb (1952) has shown that in solid helium the zero-point energy (some 10–100 times larger than the thermal energy in the region 0–20°K) is such as to produce relative displacements of an order nearly three times as great as normally found (for example, in the other inert gas solids). Corresponding to this large energy, essentially anharmonic in nature, and one and a half times as great as the lattice potential, is a large vibrational expansion of the lattice as a whole. The usual harmonic lattice dynamics is characterized by a frequency proportional to $\sqrt{(d^2U/dV^2)}$, where $U(V)$ is the static lattice potential, say per

---

* Communicated by Professor M. Born, F.R.S.

mole, and V the molar volume; it is found for helium that d^2U/dV^2 goes over to negative values well within the experimental range of V so that the quadratic theory is inapplicable. Clearly, to describe such a solid we must pay proper attention to the anharmonic terms in the expansion of U and Born's considerations provide a direct means of approach. A similar situation may be met with near melting in an ordinary substance.

In the present paper general formulae will be developed by an alternative method to that of Born; the assumptions inherent in his treatment can then be clearly seen and it is possible to extend his results and to obtain explicit solutions. By suitable approximations these can be worked out to give a reasonable description of the properties of solid helium, and this application will be made in a later paper.

In general, the potential energy U of a vibrating molecular system is to be expressed as a polynomial expansion $U(x)$ in the individual atomic displacements $x_k - x_k^0$, with suitable reference positions x_k^0. The first point of Born's argument is to avoid the usual static condition $\partial U/\partial x_k^0 = 0$ as a definition* of the x_k^0, since the mean atomic positions $\langle x_k \rangle$ diverge increasingly from these static x_k^0 with increasing distance through the solid from any atom chosen as a fixed origin. Instead, the x_k^0 are defined as the $\langle x_k \rangle$ themselves; this preserves the idea of relatively small displacements $x_k - x_k^0$ so that the expansion of $U(x)$ is justified. The new definition may be expressed in terms of the first and third degree terms U_1, U_3 of the expansion taken together.

Naturally, if the x_k^0 are assumed to form an *infinite* lattice structure at the beginning the individual static conditions $\partial U/\partial x_k^0 = 0$ define only the relative basis vectors, being otherwise identically satisfied; they are in effect replaced by conditions $\partial U/\partial a_{\alpha\beta} = 0$ derived from the static part of the free energy (free crystal; $a_{\alpha\beta} = \mathbf{a}_\alpha \cdot \mathbf{a}_\beta$, the $\mathbf{a}_\alpha$ being the cell vectors, $\alpha, \beta = 1, 2, 3$). Born's expansion difficulty is avoided by the usual procedure of including the vibrational terms of the free energy ($\sim U_2$) in the definition (thermal expansion); the result is of course exactly equivalent to that of the new argument, which is in this case superfluous. Its relevance is to a *finite* lattice or a general molecular structure, and since the equations are non-linear there is the possibility of some irregular lattice solution; however, it now seems unlikely that such a solution, more stable than the regular lattice, will in fact exist.

In the following we shall retain the individual coordinates x_k^0 even though our interest is to develop a general description of strongly anharmonic vibrations in a regular lattice; the work is then symmetrical and no more complex, and may also be applied to other cases. For example, it is of some interest to study the linear monatomic chain, which can be solved explicitly; the theory shows exactly the trivial nature of the modifications in a finite but otherwise regular structure which occur at the free surface—a particular justification for the cyclic boundary condition—and will be given elsewhere.

---

* This definition is a necessary consequence of Born and Oppenheimer's general treatment (1927) of coupled atomic vibrations; however, Born (1951 b) has given an elegant generalization in which the static condition is no longer necessary.

The second, and in practice more important, aspect of Born's method is based on the necessity (for example, in solid helium) of considering that the atomic vibrations may have amplitudes which, though relatively small, are not so small that the corresponding frequencies can be specified by the quadratic terms U_2 alone. The new definition of the $x_k{}^0$ of course introduces a first change in the frequencies, arising from the third degree terms U_3, but does not affect their functional form. Obviously fourth degree terms must be included to make any functional difference, and it is generally true that essentially the terms of odd degree in $U(x)$ have to do with the structure of the crystal, the terms of even degree with its energy. The usual harmonic theory considers first and second degree terms together; any extension should clearly include third and fourth degree terms together (as we shall do here), and so on.

If the third and fourth degree terms in $U(x)$ represent only small corrections to the linear and quadratic, the explicit form of Born's results developed by the present author can be immediately expanded in a perturbation procedure (see Born 1952); this will be illustrated elsewhere for the linear chain. We may note here that the zero order solutions are simply the solutions of the usual harmonic theory, the equations

$$\partial U/\partial x_k{}^0 = 0,$$

$$\sum_{kk'} \partial U^2/\partial x_k{}^0\, \partial x_{k'}{}^0 \,.\, e_{kj}\, e_{k'j'} = \omega_j{}^2\, \delta_{jj'}, \qquad \ldots\ldots \qquad (1)$$

defining the $x_k{}^0$ together with the frequencies ω_j and modes e_{kj} of the proper vibrations. First order corrections $\delta x_k{}^0$ arise directly from the terms $\partial^3 U/\partial x_k{}^0\, \partial x_{k'}{}^0\, \partial x_{k''}{}^0$ of U_3, while the simultaneous corrections $\delta\omega_j$, δe_{kj} depend directly on the terms $\partial^4 U/\partial x_k{}^0\, \partial x_{k'}{}^0\, \partial x_{k''}{}^0\, \partial x_{k'''}{}^0$ of U_4 and are not given solely as the result of thermal (anharmonic) expansion expressed through the $\delta x_k{}^0$.

The nature of Born's approximation can be illustrated by the following simple example. In the problem of the vibrations of a molecule, one has to solve Schrödinger's equation for a potential well of shape (*a*).

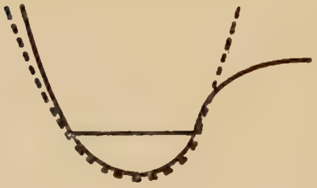

Shape (*a*).

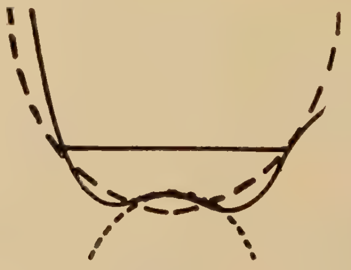

Shape (*b*).

When the vibrations are small (energy level as shown) only the bottom of the well comes in and the harmonic approximation (the dotted curve) is reasonable. If, however, the well is of a different shape (shape (*b*)) (consider, for example, an atom in the interior of a crystal, with large vibrational energy) this approximation breaks down completely (dotted curve). Nevertheless, a pseudo-harmonic approximation is still possible with a harmonic oscillator wave-function and the frequency parameter fitted by a variational principle equivalent to the fixing of average position and mean-square deviation mentioned above (dashed curve). Since the energy is always large in this case the central hump is of no consequence for the pseudo-harmonic vibration.

§ 2.

Following Born we write the Hamiltonian of a crystal containing N atoms ($k=1\ldots 3N$) in the form

$$\mathscr{H}=\tfrac{1}{2}\sum_k P_k^2/m_k+U(x), \qquad (2)$$

with

$$U(x)=U_0+U_1(x)+U_2(x)+\ldots,$$

$$U_r(x)=\frac{1}{r\,!}\sum_{(k)} U_{kk'}\ldots(x_k-x_k^0)(x_{k'}-x_{k'}^0)\ldots,\quad U_{kk'}\ldots=\partial^r U/\partial x_k^0\partial x_{k'}^0\ldots, \qquad (3)$$

the sum being over all sets of r indices k, and the x_k^0 having arbitrary values. As in the usual theory of normal coordinates, we make an orthogonal transformation of the form

$$\left.\begin{aligned} x_k-x_k^0&=\frac{1}{\sqrt{m_k}}\sum_j e_{kj}\,q_j,\\ P_k&=\sqrt{m_k}\sum_j e_{kj}p_j,\\ \sum_k e_{kj}\,e_{kj'}=\delta_{jj'},&\qquad \sum_j e_{kj}\,e_{k'j}=\delta_{kk'},\end{aligned}\right\} \qquad (4)$$

but now with arbitrary values for the e_{kj}. The potential $U(x)$ then goes over into a polynomial expansion

$$\left.\begin{aligned} &v(q)=U_0+v_1(q)+v_2(q)+\ldots,\\ &v_r(q)=\frac{1}{r\,!}\sum_{(j)} v_{jj'}\ldots q_jq_{j'}\ldots,\qquad v_{jj'}\ldots=\sum_{(k)}\frac{e_{kj}\,e_{k'j'}\ldots}{\sqrt{m_k\,m_{k'}\ldots}}U_{kk'}\ldots\end{aligned}\right\} \qquad (5)$$

(the sums being over all sets of r indices k, j) ; the energy (2) becomes

$$\mathscr{H}=\tfrac{1}{2}\sum_j p_j^2+v(q). \qquad (2')$$

In the *usual* theory the normal coordinates q_j are chosen by making the quadratic term $v_2(q)$ diagonal, and the motion is supposed to be one of small vibrations about the positions of static equilibrium :

$$v_2(q)=\tfrac{1}{2}\sum_j \omega_j^2\,q_j^2\,;\quad v_1(q)=0. \qquad (6)$$

The first condition defines the modes of vibration e_{kj}, together with harmonic frequencies ω_j, exactly as in (1), while the second defines the x_k^0 according to the static conditions $U_k=0$, also contained in (1). Generally the higher degree terms of $v(q)$ are ignored in (2′) or they may be treated as a small perturbation once the modes of vibration have been defined.

In the *present* theory we retain the transformation (4) but *drop the subsequent conditions* (6); further, the anharmonic terms of $v(q)$ (at least up to $v_4(q)$) are considered an essential part of the Hamiltonian of the actual crystal. This Hamiltonian (2′) can now be written out as

$$\mathscr{H}=\tfrac{1}{2}\sum_j p_j^2+U_0+v_1(q)+v_2(q)+v_3(q)+v_4(q)+\ldots, \qquad (7)$$

where $v_2(q)$ is no longer diagonal. Born's method is to compare this energy with that of an arbitrary set of harmonic oscillators,

$$H=\tfrac{1}{2}\sum_j p_j^2+U_0+\tfrac{1}{2}\sum_j \omega_j^2 q_j^2, \qquad (8)$$

new frequencies ω_j, together with *new* transformation parameters e_{kj} and *new* vibrational centres x_k^0, being chosen to make (8) the best possible approximation to (7). From (7), (8)

$$\left.\begin{aligned}\mathscr{H}&=H+H',\\ H'&=v_1(q)+\Big(v_2(q)-\tfrac{1}{2}\sum_j \omega_j^2 q_j^2\Big)+v_3(q)+v_4(q)+\ldots;\end{aligned}\right\} \qquad (9)$$

the statistical problem involved is to find the modification in, say, the free energy F (which corresponds to H) due to the perturbation H' under a suitable choice of the parameters ω_j, e_{kj}, x_k^0. This choice must in the first place allow such a perturbation to be made, so that the changes E_n', say, in the energy levels E_n of H are small by comparison with the E_n themselves. It must also agree with the condition $\langle x\rangle=x^0$ and, if the anharmonicity is neglected, lead to the customary ω_j, e_{kj}, x_k^0 defined in (1) or (6).

Instead of considering with Born the statistical density matrix $\rho(q, q')$ we shall work from its integral, the partition function

$$\left.\begin{aligned}\mathscr{Z}&=\int \rho(q, q)\, dq=\sum_n \exp(-\beta\mathscr{E}_n),\\ \mathscr{E}_n&=E_n+E_n', \quad \beta=1/kT.\end{aligned}\right\} \qquad (10)$$

Script letters will be used throughout to refer to the actual Hamiltonian (7). The partition function of the system of oscillators, together with the thermal average of the E_n', taken over the unperturbed energy levels E_n, will be written

$$Z=\sum_n \exp(-\beta E_n), \qquad E'=Z^{-1}\sum_n E_n' \exp(-\beta E_n); \qquad (10')$$

otherwise a bar will be used to denote the average value of any function of n, formed in respect to the partition function Z. Thus (10) becomes

$$\mathscr{Z}=Z\,\overline{\exp(-\beta E_n')}=Z\exp(-\beta E')\,\overline{\exp[-\beta(E_n'-E')]}. \qquad (11)$$

Supposing an expression can be found for the final term in (11), say*

$$\overline{\exp[-\beta(E_n'-E')]}=\exp(-\beta\Gamma), \qquad (12)$$

---

* More particularly, we could write $e^{+\beta^2\Gamma}$, since the odd terms in the expansion of (12) disappear on averaging.

we have at once for the free energy $\mathscr{F}$ of the anharmonic crystal

$$\mathscr{F}=-kT\log\mathscr{Z}=-kT\log Z+E'+\Gamma, \quad . \quad . \quad . \quad . \quad (13)$$

where it is well known that for the Hamiltonian (8)

$$-kT\log Z=U_0+kT\sum_j \log\left[2\sinh\left(\tfrac{1}{2}\hbar\omega_j/kT\right)\right]. \quad . \quad . \quad . \quad (14)$$

The thermodynamical properties of the anharmonic crystal can therefore not be described by an 'adapted' harmonic theory (with frequencies fixed anharmonically) alone; there remain the additional terms in (13) which represent a correlation between the auxiliary variables q_j. These terms, as well as the harmonic part of $\mathscr{F}$, are of course functions of the parameters ω_j, e_{kj}, $x_k{}^0$ and of the temperature.

Since for a lattice the $x_k{}^0$ replace the usual macroscopic parameters $a_{\alpha\beta}$ defined in § 1, the last remark suggests immediately that they should be chosen (simultaneously with the ω_j and e_{kj}) to give a minimum value of $\mathscr{F}$, in analogy to the minimum conditions usually imposed macroscopically. It is easily shown that to the $3N$ coordinates $x_k{}^0$, the $3N$ frequencies ω_j and the $\frac{1}{2}3N(3N-1)$ independent quantities e_{kj} there correspond just so many independent minimum conditions

$$\left.\begin{aligned} \frac{\partial\mathscr{F}}{\partial x_k{}^0}&=0, \qquad k=1-3N,\\ \frac{\partial\mathscr{F}}{\partial\omega_j}&=0, \qquad j=1-3N,\\ \sum_k\left(\frac{\partial\mathscr{F}}{\partial e_{kj_1}}e_{kj_2}-\frac{\partial\mathscr{F}}{\partial e_{kj_2}}e_{kj_1}\right)&=0,\ j_1\neq j_2=1-3N, \end{aligned}\right\} \quad . \quad . \quad . \quad (15)$$

by which to determine them. If there are external stresses they must of course be allowed for by writing the equivalent forces $-f_k$ on the right hand side of the first set of equations in (15). For a regular lattice these equations are equivalent (apart from a basis) to $\partial\mathscr{F}/\partial a_{\alpha\beta}=0$, subject, say, to a possible condition $\partial\mathscr{F}/\partial V=-p$. The relation between (15) and the conditions introduced by Born is discussed below.

The success of this formal development depends on our being able to calculate the average perturbation E' and the quantity Γ. It is clear that the energies $\mathscr{E}_n$, E_n, $E_n{}'$ are all proportional to N, the size of the system, wereas $\beta^{-1}=kT$ corresponds to the energy of one degree of freedom alone; thus to have any significance the exponentials in (11) should be written

$$[\exp(-\beta\eta_n)]^N, \quad \overline{\{\exp[-\beta(\eta_n-\eta)]\}^N}, \quad . \quad . \quad . \quad . \quad (16)$$

where $\eta_n=E_n{}'/N$, $\eta=E'/N$ are energy changes per oscillator. Thus for Γ the problem is to find the averaged Nth power of the exponential

$$\exp[-\beta(\eta_n-\eta)]=\exp[-\beta(\eta_n{}^T-\eta^T)]=1-\beta(\eta_n{}^T-\eta^T)+\ldots, \quad . \quad (17)$$

where we may split off the change in the zero energy E'_0 so that $\eta_n{}^T=(E_n{}'-E_0{}')/N$. The result itself should be put in the form of an Nth power since its logarithm appears in the free energy (13), and the latter is itself of order N. We have essentially to do with an expansion in powers of β, and the convergence depends on the order of magnitude of the thermal energy. For example, in solid helium the vibrational energy is $\sim 10^9$ erg/mol., the thermal energy 10^7–10^8 erg/mol.; at the solid helium temperatures in which we shall later be interested ($\sim 10^\circ$K) β is $\sim 10^{15}$ erg^{-1}, so that $\eta_n{}^T\beta \sim 10^{-1}$ ($N \sim 10^{23}$/mol.). Thus at such low temperatures an expansion in powers of β converges slowly and we can not expect that an accurate evaluation of Γ will be easily made. Instead we shall make a gross approximation by taking only the constant term in (17), which implies that $\Gamma = 0$: even for helium, however, this gives reasonable results.

To evaluate the remaining quantity E' we must express the various $E_n{}'$ by the usual perturbation formulae in terms of the matrix elements $H_{mn}{}'$ of H' with respect to the eigenstates of the oscillators (8). Going back to (9) we see that H' consists of a sum of homogeneous polynomial expressions in the oscillator amplitudes q_j. The $H_{mn}{}'$ may be written down at once from the well-known values of $(q_j q_{j'} \ldots)_{mn}$, and from them the energy perturbations $E_n{}'^{(1)}, E_n{}'^{(2)}, \ldots$, and so the thermal averages $E'^{(1)}, E'^{(2)}, \ldots$, in successive orders. Thus,

$$\left.\begin{aligned}
E'^{(1)} &= \frac{1}{Z} \sum_n \exp(-E_n\beta)\, H_{nn}{}' \\
&= \frac{1}{Z} \sum_n \exp(-E_n\beta)\, \{v_2(q) - \tfrac{1}{2} \sum_j \omega_j{}^2 q_j{}^2 + v_4(q) + \ldots\}_{nn} \\
&= \tfrac{1}{2} \sum_j \overline{q_j{}^2}\, \{\tilde{v}_{jj} + \tfrac{1}{2} \sum_{j'} v_{jjj'j'}\, \overline{q_{j'}{}^2} + \ldots\} - \tfrac{1}{8} \sum_{jj'} \overline{q_j{}^2}\,\overline{q_{j'}{}^2}\, v_{jjj'j'} \ldots, \\
\tilde{v}_{jj'} &= v_{jj'} - \omega_j{}^2 \delta_{jj'}, \quad \overline{q_j{}^2} = \frac{1}{Z} \sum_n \exp(-E_n\beta)\, (q_j{}^2)_{nn};
\end{aligned}\right\} \quad . \quad . \quad (18)$$

all odd order terms vanish by symmetry, and we have used the fact that $\overline{q_j{}^4} = 3\overline{q_j{}^2}{}^2$. For the (non-degenerate) zero-energy perturbation $E_0{}'$ (which is in fact all that is needed in the helium problem to be discussed later) it is found that in the second order

$$\left.\begin{aligned}
E_0{}'^{(2)} &= \sum_n{}' \, |H_{0n}{}'|^2/(E_0 - E_n) \\
&= -\frac{1}{\hbar} \sum_j \frac{a_j{}^2}{\omega_j} \{v_j + \tfrac{1}{2} \sum_{j'} v_{jj'j'} a_{j'}{}^2 + \ldots\}^2 - \frac{1}{\hbar} \frac{1}{2!} \sum_{jj'} \frac{a_j{}^2 a_{j'}{}^2}{\omega_j + \omega_{j'}} \times \\
&\qquad \{\tilde{v}_{jj'} + \tfrac{1}{2} \sum_{j''} v_{jj'j''j''}\, a_{j''}{}^2 + \ldots\} - \frac{1}{\hbar} \frac{1}{3!} \sum_{jj'j''} \frac{a_j{}^2 a_{j'}{}^2 a_{j''}{}^2}{\omega_j + \omega_{j'} + \omega_{j''}} v_{jj'j''}{}^2 \\
&\quad - \frac{1}{\hbar} \frac{1}{4!} \sum_{jj'j''j'''} \frac{a_j{}^2 a_{j'}{}^2 a_{j''}{}^2 a_{j'''}{}^2}{\omega_j + \omega_{j'} + \omega_{j''} + \omega_{j'''}} v_{jj'j''j'''}{}^2 \ldots, \\
a_j{}^2 &= \tfrac{1}{2}\hbar/\omega_j = \lim_{T \to 0} \overline{q_j{}^2}.
\end{aligned}\right\} . \quad (19)$$

But since $E_0{}'^{(2)} = \lim\limits_{T \to 0} E'^{(2)}$ we may infer that $E'^{(2)}$ is to be got from (19) by writing $\overline{q_j{}^2}$ instead of its limit $a_j{}^2$. The general form to be expected in the higher orders is then clear from (18), (19): appropriate powers of the curly brackets plus some remainder terms. The latter diminish rapidly in magnitude (see below) and as a further simplification we shall neglect them in the second and higher orders.

If now (14), (18) and the generalized form of (19) are put into (13), together with the approximation $\Gamma=0$, and the minimum conditions (15) applied, some lengthy but straightforward calculation shows that a solution can be obtained by setting the curly brackets equal to zero :

$$\left.\begin{aligned} v_j+\tfrac{1}{2}\sum_{j'} v_{jj'j'}\,\overline{q_{j'}{}^2}&=0,\\ \tilde{v}_{jj'}+\tfrac{1}{2}\sum_{j''} v_{jj'j''j''}\,\overline{q_{j''}{}^2}&=0\,; \end{aligned}\right\} \quad . \quad . \quad . \quad . \quad . \quad (20)$$

here terms of the fifth degree in q are dropped, since we are considering only a first correction (terms v_3, v_4) in the anharmonicity. The eqns. (20) for the parameters $x_k{}^0$, ω_j, e_{kj} also ensure that we have a proper perturbation procedure : the brackets in (18), (19) and the higher orders vanish, and since the average effect of fourth degree terms is in general to be treated as equivalent to that of the quadratic, the order of magnitude of the remainder terms, for example in E_0, is given by

$$\tfrac{1}{8}\sum_{jj'} \overline{q_j{}^2}\,\overline{q_{j'}{}^2}\,v_{jjj'j'} \sim \tfrac{1}{4}\sum_j \overline{q_j{}^2}\,\tilde{v}_{jj} \sim \tfrac{1}{4}\sum_j (\tfrac{1}{2}\hbar/\omega_j)\omega_j{}^2=\tfrac{1}{4}E_0,$$

$$\frac{1}{\hbar}\,\frac{1}{4\,!}\sum_{jj'j''j'''}\frac{a_j{}^2a_{j'}{}^2a_{j''}{}^2a_{j'''}{}^2}{\omega_j+\omega_{j'}+\omega_{j''}+\omega_{j'''}}\,v_{jj'j''j'''} \sim \frac{1}{\hbar 4\,!}\sum_j \frac{a_j{}^4}{4\omega_j}\Big[\sum_{j'} a_{j'}{}^2\,v_{jjj'j'}\Big]^2 \sim \frac{1}{48}E_0,$$

and similar fractional expressions. Transforming (20) according to the reciprocal of (4) we get

$$\left.\begin{aligned} U_k+\sum_{k'k''} U_{kk'k''}\,A_{k'k''}&=0,\\ \sum_{kk'}\frac{e_{kj}\,e_{k'j'}}{\sqrt{m_k\,m_{k'}}}\Big\{U_{kk'}+\sum_{k''k'''} U_{kk'k''k'''}\,A_{k''k'''}\Big\}&=\omega_j{}^2\,\delta_{jj'},\\ A_{kk'}&=\tfrac{1}{2}\sum_j \frac{e_{kj}\,e_{k'j}}{\sqrt{m_k\,m_{k'}}}\,\overline{q_j{}^2}, \end{aligned}\right\} \quad . \quad . \quad (21)$$

an immediate extension of the old definitions (1). In the case when U_3, U_4 are small compared to U_1, U_2 (21) may obviously be solved by successive approximations.

Just these relations (21) have also been found by the present author as the explicit expression of the general conditions originally developed by Born (1951 a) from the equations

$$\langle q_j\rangle=0, \quad \text{or} \quad \langle x_k\rangle=x_k{}^0, \quad \langle q_jq_{j'}\rangle=\overline{q_j{}^2}\,\delta_{jj'}, \quad . \quad . \quad . \quad (22)$$

as definitions of the parameters $x_k{}^0$, ω_j, e_{kj} ; $\langle\ \rangle$ denotes the thermal average under the Hamiltonian (7). Born's development is based on an expansion of the density matrix ρ in (10) according to the expression

$$\rho=\sigma g, \qquad g=1+g_1+g_2+\dots,$$

where $Z = \int \sigma(q, q)\, dq$, and g_r is a polynomial of degree r in the coordinates q; by comparison with (11) it is clear that

$$1+\bar{g}_1+\bar{g}_2+\ldots=\exp(-\beta E')\exp(-\beta \Gamma)=(1-\beta E'+\ldots)\times$$
$$(1+\tfrac{1}{2}\beta^2\,\overline{(E_n'-E')^2}+\ldots).$$

Thus the polynomials g_r, like the E', are of the order N, and to make a properly convergent expansion we should have to write

$$\rho=\sigma(g')^N, \quad g'=1+g_1'+g_2'+\ldots, \quad \ldots \ldots \quad (23)$$

which destroys the relative simplicity of Born's equations. However, as his method stands, the expression for $\bar{g}$ got from the first few polynomials g_r turns out to be the same as the leading terms of $1-\beta E'^{(1)}$. No higher powers of β are obtained before the work becomes prohibitive, so that in practice the term in Γ, which requires the use of (23), is automatically excluded, nor is there any contribution from the $E'^{(2)}$ or higher orders. Born's treatment by successive polynomials of course implies that the $v_r(q)$ are of successive orders of magnitude and so gives the terms of $1-\beta E'^{(1)}$ only in successive approximations. The present treatment is not so restricted and allows, in particular, v_4 to be equivalent in its effect to v_2; the simplifications which exclude the higher orders and the term in Γ are thus of more general significance than Born's method would imply. The approximate identity between the results of (15) and (22) confirms that the present method of specifying the parameters x_k^0, ω_j, e_{kj} has a good physical meaning as discussed in § 1 above.

§ 3.

A solution of (21) in which the anharmonic terms are not regarded as small corrections is evidently connected with the presence of large vibrational energies; the determination of the frequencies is thus the main problem and the exact form of the crystal (x_k^0) and of the modes of vibration (e_{kj}) is relatively unimportant. Whatever the x_k^0, we may isolate the effect of the new vibrational energies (frequencies) from the second set of equations in (21) by assuming that the e_{kj} have the customary form defined by the non-diagonal equations ($j \neq j'$) in (1). Of course this implies that $U_{kk'}$ has been made diagonal, and we now write the diagonal equations of (1) as

$$\sum_{kk'} \frac{e_{kj}\, e_{kj}}{\sqrt{m_k m_{k'}}} u_{kk'} = \omega_j^{0\,2} \quad \ldots \ldots \quad (1')$$

to avoid confusion with the new frequencies ω_j. The assumption refers only to the *non*-diagonal equations in (21):

$$\sum_{kk'} \frac{e_{kj}\, e_{k'j'}}{\sqrt{m_k m_{k'}}} U_{kk'}\{1+\sum_{k''k'''} U_{kk'k''k'''} A_{k''k'''}/U_{kk'}\}=0 \; (j \neq j'). \quad (24)$$

and the approximation implies that the last term in the bracket (though not small) is largely independent of k, k'. The diagonal equations remain, and may now be written

$$\omega_j^2=\omega_j^{02}+\tfrac{1}{2}\sum_{j'} v_{jjj'j'}\,\overline{q_{j'}^2}, \qquad j=1-3N. \quad . \quad . \quad . \quad . \quad (25)$$

Although there is no necessity for the ω_j^{02} to be positive (roughly speaking, they are positive only for atomic spacings less than the inflexion distance of the interatomic potential) that no longer prevents a description of the vibrational energy being made, so long as the whole expression (25) leads to positive ω_j^2.

The eqns. (25) are non-linear, since

$$\left.\begin{aligned}&\overline{q_j^2}=E_j/\omega_j^2,\\ &E_j=\tfrac{1}{2}\hbar\omega_j \coth\left(\tfrac{1}{2}\hbar\omega_j/kT\right),\end{aligned}\right\} \quad . \quad . \quad . \quad . \quad . \quad . \quad . \quad (26)$$

the latter being the thermal average of the energy of the jth oscillator alone. Thus (25) must be solved by iteration or approximation. At low temperatures, or for large zero-point energy, the use of a_j^2 as in (19) leads to

$$\omega_j^2=\omega_j^{02}+\tfrac{1}{4}\hbar\sum_{j'} v_{jjj'j'}/\omega_{j'}; \quad . \quad . \quad . \quad . \quad . \quad . \quad . \quad (27)$$

the equations in this form can be solved explicitly for the linear chain, and the resulting solutions will later be used to give an approximation by which the helium problem can be discussed.

Going back to (13) we see that, subject to the approximations that have been made, the free energy of the anharmonic crystal is to be written

$$\left.\begin{aligned}&\mathscr{F}=U_0+F-\tfrac{1}{4}\sum_j f_j\,E_j,\\ &f_j=1-\omega_j^{02}/\omega_j^2;\end{aligned}\right\} \quad . \quad . \quad . \quad . \quad . \quad . \quad (28)$$

$F=\Sigma_j F_j$ now refers to (14), or (8), without the constant U_0, while the final term of $\mathscr{F}$ expresses the remainder of (18) with due regard to (20), (25).

Some care is needed in general in applying the formulae of thermodynamics to (28) since the new frequencies ω_j, solutions of (25), are explicitly T-dependent as well as being functions of the x_k^0; the ω_j^0 and e_{kj} are functions of the x_k^0 alone by (1) or (1′). In a lattice the x_k^0 are equivalent to the macroscopic lattice parameters, and in any case they specify the molar volume V; thus, excluding any relative variation of the x_k^0 with T at constant V, we may write

$$\left(\frac{\partial}{\partial T}\right)_V=\left(\frac{\partial}{\partial T}\right)_{\omega,\,V}+\sum_j\left(\frac{\partial\omega_j}{\partial T}\right)_V\frac{\partial}{\partial\omega_j}.$$

For example, the entropy, energy, and specific heat at constant volume follow from (28) according to

$$\left.\begin{aligned}&\mathscr{S}=S+\tfrac{1}{4}\sum_j f_j\,C_j+\sum_j s_j,\\ &\mathscr{E}=U_0+E+\tfrac{1}{4}\sum_j f_j\,(C_jT-E_j)+\sum_j e_j,\\ &\mathscr{C}=C+\tfrac{1}{4}\sum f_j\,T\left(\frac{\partial C_j}{\partial T}\right)_{\omega_j,\,V}+\sum c_j;\end{aligned}\right\} \quad . \quad . \quad . \quad . \quad . \quad (29)$$

the final terms contain all the variation of ω at constant V, while the $S=\Sigma_j S_j$, $E=\Sigma_j E_j$, $C=\Sigma_j C_j$ are the usual oscillator functions. It is to be noted that the latter are derived from (28) by the operator $(\partial/\partial T)_{\omega V}$ *alone*: operations at constant volume in the ordinary oscillator thermodynamics imply that the frequencies are held constant, and corresponding oscillator relations must be used here in the same sense.

In practice it is to be expected that the anharmonic properties of the crystal will depend mainly on volume, so that the temperature dependence of the energy (frequencies) at constant volume is a small correction; that is certainly the case for solid helium, for which the eqn. (27) may be used, and the terms in s_j, e_j, c_j may then be safely ignored.

The whole problem is now to describe the new vibrational spectrum ω_j, and from it the f_j of (28), in any particular example. By (25) or (27) this spectrum is to be got from the fourth degree terms in the expansion of $U(x)$ as well as from the quadratic and the solution can not be simple. For practical purposes we might hope to make an adaptation of the well known Debye approximation and this will be discussed in a following paper.

ACKNOWLEDGMENTS

I should like to thank Professor Max Born for suggesting this problem to me and for continued helpful discussion throughout. The work was supported by a Mr. and Mrs. John Jaffe Donation from the Royal Society. I am also indebted to the Referees for helpful criticism and comment, and in particular for the formulation of the example given in the first section.

REFERENCES

BORN, M., 1951 a, *Fest. d. Akad. Wiss. Göttingen* (Math.-Phys. Kl.), "Die Gültigkeitsgrenze der Theorie der idealen Kristalle und ihre Überwindung"; 1951 b, *Nach. d. Akad. Wiss. Göttingen* (Math.-Phys. Kl.), "Kopplung der Elektronen- und Kernbewegung in Molekeln und Kristallen"; 1952, *Comptes Rendus 2^e Réunion Chimie Physique*. Paris

BORN, M., and OPPENHEIMER, R., 1927, *Ann. Phys.*, **84**, 457.

DOMB, C., 1952, *Comptes Rendus 2^e Réunion Chimie Physique*. Paris.

LII. *A New Treatment of Anharmonicity in Lattice Thermodynamics: II*

By D. J. Hooton
Department of Mathematical Physics, University of Edinburgh*

[Received November 6, 1954]

Summary

The thermodynamical formulae of the previous paper are worked out with the help of an adaptation of Debye's continuum approximation; in particular, the specific heat at constant volume is put into a form suitable for numerical calculation. This formula contains, however, a factor which expresses the (possibly strong) volume dependence of the relation between the new frequency spectrum and that of the customary lattice dynamics; the factor appears in addition to the Debye characteristic temperature θ and must be estimated in any particular application—for example, in the following consideration of solid helium it will be approximated from a linear chain model. The meaning of a Debye characteristic temperature in the anharmonic theory is discussed, and the place of an empirical Debye temperature, determined by fitting specific heat measurements to a theoretical specific heat formula, is also considered. A discussion of this fitted Debye temperature (due to Domb and Salter) is adapted to the anharmonic theory in order to give later a correct application to solid helium.

§1

In a previous paper (referred to as I) a method originally due to Born for treating anharmonicity in a crystal has been given explicit form in a way suited to the discussion of problems involving large vibrational energy. In this paper we shall deal with the application of Debye's continuum approximation in the new theory. The theoretical definition of the Debye characteristic temperature θ gives a result of the same form as proposed by Domb (1952) in connection with solid helium by fitting the Debye specific heat formula to experimental measurements. Such an empirical parameter, whose variation at constant volume is useful as a guide to the exact lattice spectrum, can also be defined in the new theory, and the justification of Domb's formula will be discussed.

The results obtained here will be illustrated elsewhere for the example of a linear monatomic chain, which can be solved explicitly; they also provide a basis for the thermodynamical discussion of solid helium to be made in a following paper.

---

* Communicated by Professor M. Born, F.R.S.

§ 2

The x_k^0 of I are assumed to form a regular cyclic lattice in what follows, and for simplicity we shall deal with a monatomic lattice only; there would be no essential difficulty in treating 'optical' vibrations in addition to the 'acoustic' vibrations discussed here. With the x_k^0 replaced by lattice parameters $a_{\alpha\beta}$, the first set of equations (I, eqn. (21)) is to be replaced by conditions* $\partial\mathscr{F}/\partial a_{\alpha\beta}=0$ (free crystal; otherwise external 'forces' must be written on the right-hand side, for example—and this is important for helium—$\partial\mathscr{F}/\partial V=-p$). The remaining equations (I, eqn. (21)), approximated according to (I, eqn. (24)), namely

$$\left.\begin{aligned} &\omega_j^2=\omega_j^{02}+\tfrac{1}{2}\sum_{j'} v_{jjj'j'}\overline{q_{j'}^2}, && j, j'=1-3N, \\ &\sum_{kk'}\frac{e_{kj}\,e_{k'j'}}{\sqrt{(m_k m_{k'})}}\,U_{kk'}=\omega_j^{02}\delta_{jj'}, && k, k'=1-3N, \end{aligned}\right\} \quad . \quad . \quad (1)$$

give simultaneously new harmonic frequencies ω_j which are functions of the $a_{\alpha\beta}$ and of T, while the ω_j^0 and e_{kj} are the well-known harmonic lattice frequencies and plane-wave vectors, functions of the $a_{\alpha\beta}$ alone. By (1) there is a 1 : 1 correspondence between the ω_j and the ω_j^0 and it may be shown that ω_j and ω_j^0 vanish together; we may therefore speak of three acoustic branches to the new frequency spectrum. However, although the corresponding vibrations have the usual form (in this approximation), there are no longer any linear wave equations by which to determine their frequencies.

Failing an exact solution of the non-linear eqns. (1) we can apply the well-known Debye approximation, most simply in the isotropic form. Thus the density of vibrations in the continuous Debye spectrum,

$$\left.\begin{aligned} &dz=\frac{9N}{\omega^{D^3}}\,\omega^2\,d\omega=\frac{9NT^3}{\theta^3}\,\xi^2\,d\xi, \\ &\xi=\frac{\hbar\omega}{kT}, \qquad \theta=\frac{\hbar\omega^D}{k}, \end{aligned}\right\} \quad . \quad . \quad . \quad . \quad . \quad (2)$$

replaces the unknown dz of (1). Here the cut-off frequency ω^D, or the characteristic temperature θ, is strongly volume-dependent, with in general a T-dependence at constant volume;† the latter is to be ignored when the corresponding property of the ω_j is ignored, as mentioned at the end of I.

The thermodynamical functions (I, eqns. (28), (29)) of the anharmonic lattice depend on the frequencies ω_j through the usual oscillator functions derived from F_j (the free energy), but as well contain additional terms which provide corrections to the new harmonic approximation. Thus, for example,

---

* See, for example, M. Born (1939).

† This of course has nothing to do with the empirical T-dependence at constant volume of a 'fitted' θ, got from specific heat values, which expresses the 'non-Debye' nature of the actual spectrum.

$$\left.\begin{aligned} \mathscr{E}&=U_0+E-\tfrac{1}{4}\sum_j f_j(E_j-TC_j)+\sum_j e_j, \\ e_j&=-T\left(\frac{\partial\omega_j}{\partial T}\right)_V\frac{\partial}{\partial\omega_j}(F_j-\tfrac{1}{4}f_jE_j), \qquad f_j=1-\omega_j^{02}/\omega_j^2, \end{aligned}\right\} \quad . \quad . \quad (3)$$

where E_j is the energy and C_j the specific heat at constant volume of an oscillator of frequency ω_j, as defined in the usual theory.

The Debye approximation (2) can only be applied directly to functions of the frequencies ω_j which do not depend otherwise on the index j, and this excludes terms containing f_j or the derivatives of ω_j such as appear in (3). It is not difficult to show that all the terms in (I, eqns. (28), (29)) which are not functions of the ω_j alone are of the form $\Sigma_j\tau_j\Omega_j$, where Ω_j *is* such a function, and τ_j is equal to $(\partial\omega_j/\partial T)_V$, $(\partial\omega_j/\partial T)_V{}^2$, $(\partial^2\omega_j/\partial T^2)_V$, the product of these with f_j, or f_j itself. To get any further we must replace these τ_j by quantities which are constant along the spectrum, which is similar to Grüneisen's approximation, that all $\partial\omega_j{}^0/\partial V$ are the same, in treating thermal expansion. Strictly speaking, we should replace the vibrational index j by the reciprocal lattice indices

$$\binom{h}{j}, \qquad h=1-N, \qquad j=1-3$$

(acoustic branches); the τ_j might then be averaged for each branch of the spectrum separately. However, to use the isotropic Debye density (2) we need overall values of the τ and need not introduce the separate indices. So far as f_j is concerned, the assumption that $\omega_j{}^{02}/\omega_j{}^2$ is roughly constant along each branch is not an unlikely one, it being shown elsewhere that in the linear chain model f_j *is* constant along the spectrum. We have already noted that the T-dependence of the ω_j is most probably a small effect, if not to be ignored, so the averaging of the derivatives $(\partial\omega_j/\partial T)_V$ is unimportant.

Thus, $$\sum_j\tau_j\Omega_j\rightarrow\frac{9NT^3}{\theta^3}\,\tau\int_0^{\theta/T}\Omega(\xi)\xi^2\,d\xi,$$

in which τ is strongly volume-dependent and has also, in general, a small T-dependence at constant volume. The formulae (I, eqns. (28), (29)) then go over into Debye integrals such as (from (3))

$$\begin{aligned} \mathscr{E}=U_0+\frac{9NT^3}{\theta^3}\int_0^{\theta/T}\Bigg[&(1-\tfrac{1}{4}f)E(\xi)+\tfrac{1}{4}fTC(\xi) \\ &-\frac{\hbar}{k}\left(\frac{\partial\omega}{\partial T}\right)_V\left\{\frac{\partial F(\xi)}{\partial\xi}-\tfrac{1}{2}(1-f)\frac{E(\xi)}{\xi}-\tfrac{1}{4}f\frac{\partial E(\xi)}{\partial\xi}\right\}\Bigg]\xi^2\,d\xi, \\ &\tau=f, \text{ on } \left(\frac{\partial\omega}{\partial T}\right)_V, \end{aligned} \quad . \quad . \quad . \quad . \quad (4)$$

which are readily integrated in the usual way. For the application to solid helium we shall drop the terms in $(\partial\omega/\partial T)_V$ throughout. In that case (4) becomes

$$\mathscr{E}=U_0+(1-\tfrac{1}{4}f)E^D(\theta/T)+\tfrac{1}{4}fTC^D(\theta/T)\,; \quad \ldots\ldots \quad (5)$$

we may also write down the specific heat at constant volume from (I, eqn. (29)), or by differentiating (5):

$$\mathscr{C}=(1+\tfrac{3}{4}f)C^D(\theta/T)-\tfrac{3}{4}fC^E(\theta/T). \quad \ldots\ldots \quad (6)$$

Here E^D, C^D are the usual Debye formulae, and C^E the Einstein formula for the molar specific heat, defined as follows:

$$\left.\begin{aligned} &E^D(\theta/T)=3RTD(\theta/T), \qquad C^D(\theta/T)=3R\{4D(\theta/T)-3P(\theta/T)\},\\ &C^E(\theta/T)=3RQ(\theta/T)\,;\\ &D(\theta/T)=\frac{3T^3}{\theta^3}\int_0^{\theta/T}\{\tfrac{1}{2}\xi+P(\xi)\}\xi^2\,d\xi,\\ &P(\xi)=\xi/(e^\xi-1), \qquad Q(\xi)=P(\xi)-\xi\frac{dP(\xi)}{d\xi}. \end{aligned}\right\} \quad . \quad (7)$$

We see from (6) that in this adaptation of the Debye theory there is no longer a universal specific heat function in the variable θ/T alone; an explicit volume dependence remains through the quantity f.

The problem of finding the new harmonic spectrum in any particular example is now replaced by that of determining θ and the quantities f, $(\partial\omega/\partial T)_V$, ... Of the latter, only a suitable average f is of real importance, and it may be possible to simplify its determination by the use of symmetry properties of the lattice—but now the symmetry of fourth degree terms is in question rather than that of the usual quadratic terms alone. In applying the theory to solid helium we shall use as an approximation to f the value derived for a linear chain of helium atoms; this exhibits the strong volume dependence which is the new factor in the theory.

For θ we might follow the empirical practice of fitting the specific heat formula of the Debye approximation—now given essentially by (6)—to experimental values; it is necessary to distinguish the resulting ‘ fitted ’ parameter θ from what would be got by the *usual* empirical fitting of the Debye formula C^D alone. The latter, say θ', is discussed for helium by Domb (1952) and by Dugdale and Simon (1953) but has no real place in the anharmonic theory since the properties of a strongly vibrational solid can not be regarded as those of a set of harmonic oscillators *alone*. θ and θ', as empirical parameters, are related by the equation

$$\mathscr{C}(\theta/T)=C^D(\theta'/T). \quad \ldots\ldots\ldots \quad (8)$$

§ 3

From a theoretical standpoint Debye's approximation must be made so that the long elastic waves which it introduces are identical with the long (acoustic) lattice vibrations, clearly elastic in character, that they have to replace. For the present Debye theory the harmonic 'lattice vibrations' in question are fictitious, being those of Born's adapted harmonic approximation *alone*; they are not in themselves the actual (anharmonic) lattice vibrations of the crystal, and the intrinsic energy of the Debye continuum is not the same as the internal energy $\mathscr{E}$ given by (3). The parameter θ is in fact to be defined through the velocity of the plane waves e_{kj} of the new harmonic approximation in the long wave limit $j \rightarrow 0$ (or the averaged velocity over the three branches in the limit $\binom{h}{j} \rightarrow \binom{0}{j}$, $j=1, 2, 3$):

$$\theta = \frac{\hbar}{k}\omega^D = \frac{2\pi h}{k}\sqrt[3]{\left(\frac{3N}{4\pi V}\right)} \cdot c, \qquad c = c_l. \quad \ldots \quad (9)$$

(9) is the usual relation between θ and the average isotropic elastic velocity c of the Debye continuum, and we write c_l for the limiting 'lattice' velocity of the harmonic approximation. In the usual theory c can be made equal to c_l by a comparison between the linear wave equations of the continuum and those of the lattice; that is not possible here, since we no longer have any linear wave equations in the frequencies ω_j. To find c_l it is necessary to solve the ω_j-spectrum itself near the origin of the wave-number space, and an explicit example of this calculation is given elsewhere for the linear chain.

Of course, when macroscopic (i.e. experimental) elastic properties of the crystal are defined in the usual way—for example, an adiabatic compressibility κ—they must contain all effects of the actual state of anharmonic vibrational motion, whatever it may be. Nevertheless, their definition implies that there are at least *long* elastic-type waves actually present which are harmonic in character; this is not unreasonable, since most of the vibrational energy lies in the short-wave region, outside which the anharmonicity can be neglected. The corresponding macroscopic elastic velocity is essentially

$$(\rho\kappa)^{-1/2} = \frac{V}{M^{1/2}}\sqrt{\left(\frac{\partial^2 \mathscr{E}}{\partial V^2}\right)}. \quad \ldots \ldots \quad (10)$$

($\mathscr{F}$ would replace $\mathscr{E}$ for isothermal compressions; (10) is an isotropic average.) But it is clear that this concept of an effective harmonic continuum can not be extended to the short-wave region, and so used to define a Debye approximation (which refers to *all* vibrations), since the microscopic, and more energetic, part of the lattice motion *must* be regarded as anharmonic; we can see that harmonic Debye formulae *alone* can not give a sufficient description of the whole anharmonic motion since harmonic *lattice* formulae are not of themselves sufficient, even when the frequencies are anharmonically defined.

The present Debye velocity therefore satisfies a relation of the form* (10),

$$c \approx \frac{V}{M^{1/2}} \sqrt{\left(\frac{\partial^2 \epsilon}{\partial V^2}\right)} \quad . \quad . \quad . \quad . \quad . \quad . \quad . \quad . \quad (11)$$

(a relation of this form must be true in any harmonic continuum), but with the elastic energy ϵ equated to the energy U_0+E of the new harmonic approximation itself. This energy *is* the energy of a complete set of harmonic vibrations, and differs from $\mathscr{E}$ by the final terms of (3). In the anharmonic theory the vibrational part E of ϵ is essential; the equivalence of c and c_l then implies that the energy of the long waves e_{kj} $(j \rightarrow 0)$ is strongly dependent on that of the short waves, and such a relation is in fact contained in the eqns. (1). In the usual harmonic theory (relatively small vibrational energy) only U_0 appears; the elastic velocity (11) is then

$$c_0 \approx \frac{V}{M^{1/2}} \sqrt{\left(\frac{\partial^2 U_0}{\partial V^2}\right)}, \quad . \quad . \quad . \quad . \quad . \quad . \quad . \quad (12)$$

in immediate agreement with the velocity c_l of the usual plane waves of frequencies $\omega_j{}^0$. If correction terms $E(\omega_j{}^0)$ are included, the change δc_0 corresponds to the $\delta\omega_j{}^0$ given by the equations (I, eqn. (21)).

From (9), (11) the volume dependence of θ is clear; there is also a temperature dependence at constant volume, through the energy term E, and this has already been mentioned as representing the corresponding property of the ω_j-spectrum. Compared to the variation of θ with volume (for example, in solid helium θ ranges from 40–160°K when V goes from 20–10 cm^3), the temperature dependence is unimportant; whenever (1) is approximated by the zero-vibrational form (I, eqn. (27)) E is to be replaced by the zero energy E_0 in (11) and this (theoretical) temperature dependence drops out.

θ, or c, is only formally determined by (11) since E itself depends on the unknown ω_j and must be approximated by the Debye formula $E^D(\theta/T)$; thus we have an approximate differential equation for θ, non-linear and of the second order: it is given essentially by the zero-energy form

$$\theta = \text{const}\, \frac{N^{1/3}V^{2/3}}{M^{1/2}} \sqrt{\left(\frac{\partial^2 U_0}{\partial V^2} + \frac{9}{8} R \frac{\partial^2 \theta}{\partial V^2}\right)}. \quad . \quad . \quad . \quad (13)$$

---

* For this form, and for (9), see for example M. Born (1923). (10) corresponds to elastic deformations from a state of vanishing initial stresses, as is usual in elasticity theory. When, for example, an isotropic pressure is necessarily present—as it is for solid helium—we may expect a modification in the macroscopic elastic velocity of the type

$$\sqrt{(\partial^2\mathscr{E}/\partial V^2)} \rightarrow \sqrt{(\partial^2\mathscr{E}/\partial V^2 + fn\,(p/V))}.$$

It is reasonable that such a modification should also be made in (11); the energy of the anharmonic lattice under external stresses is then approximated with the help of harmonic oscillations in a Debye continuum under corresponding stresses.

Such a relation can not be avoided in the strongly anharmonic theory, whereas in the usual case (with or without the correction δc_0) it does not appear. A formula of the type (13) has been postulated by Domb (1952) to account for the Debye parameter, called θ' in §2, got by fitting Debye's formula C^D as in (7) to the measured specific heat of solid helium. We shall next see how the analysis of Domb and Salter (1952) on which this is based is to be modified in the anharmonic theory, and whether it is of any significance for solid helium.

§4

Domb and Salter have considered the almost constant values of the Debye parameter θ' found in many lattices at relatively high temperatures and any given volume when the specific heat formula C^D is fitted to experimental results, and have given an expansion in powers of

$$x=\hbar\omega_m/kT$$

for the correspondingly small T-dependence (ω_m is the maximum lattice frequency); the variable x is $\sim\theta'/T$ and will in general be smaller than unity. In the same paper it is shown that the Debye zero-energy $\frac{9}{8}R\theta'$, written in terms of the constant limiting value of θ', is a good approximation to the actual zero-energy of the lattice, which is rather surprising, since the consideration is based on (relatively) high temperatures while the zero-energy characterizes the opposite limit of large values of x. We shall see below that in both the usual and the new theory the functional form of the constant limiting fitted Debye parameter as given by Domb and Salter's method is just that of the theoretical expressions (12) or (13), as must be the case if this θ or θ' is to express correctly other thermodynamical properties, such as the zero-energy, at different volumes; only the constant factor is new. Moreover, the simple Debye formula $\frac{9}{8}R\theta'$ as quoted above will be found to retain a certain validity in the new theory.

θ' is defined by equating the Debye formula $C^D(\theta'/T)$ to the experimental specific heat values. Instead of using an integral expression such as (7) for the molar specific heat, Domb and Salter use an expansion formula* due to Thirring:

$$\left.\begin{aligned} C&=3Nk\left\{1+\sum_n(-1)^n B_n\frac{2n-1}{2n\,!}I_{2n}\left(\frac{\hbar\omega_m}{kT}\right)^{2n}\right\},\\ I_k&=\frac{\mu_k}{\omega_m{}^k},\qquad \mu_k=\frac{1}{3N}\sum_j\omega_j{}^k. \end{aligned}\right\}\quad . \quad . \quad . \quad (14)$$

C is the specific heat corresponding to any spectrum of independent oscillators of frequencies ω_j and maximum frequency ω_m. C^D is got by writing in μ_k^D, ω^D corresponding to the Debye spectrum; the experimental specific heats are represented when the proper μ_k, ω_m of the actual lattice spectrum is used. By equating the two expansions so found, and developing θ' in powers of $\hbar\omega_m^0/kT$, Domb and Salter obtain the formula

---

* The factor $2n-1$ is missing in Domb and Salter's paper, although their numerical values are correct. Their formula for θ', by comparison with (15), is also evidently in error. The B_n are the Bernoulli numbers, $\frac{1}{6}$, $\frac{1}{30}$, ...

$$\theta'=\frac{\hbar}{k}\sqrt{\left(\frac{5\mu_2^0}{3}\right)}\left\{1-\frac{1}{40}\left(\frac{\hbar\omega_m^0}{kT}\right)^2\left(I_4-\frac{25}{21}I_2^2\right)^0\Big/I_2^0+\ldots\right\}; \quad . \quad (15)$$

the indices ^{0} are introduced to correspond to the lattice spectrum ω_j^0 of the harmonic theory. Since $\mu_2^0 \simeq \alpha/m$, where α is the force constant of the lattice, and with $\alpha \simeq \partial^2\phi/\partial a^2$, $U_0=N\phi$, $V=Na^3$, $M=Nm$, the constant term of (15) is clearly*

$$\theta' \approx \frac{1}{m^{1/2}}\sqrt{\left(\frac{\partial^2\phi}{\partial a^2}\right)} \approx \frac{N^{1/3}V^{2/3}}{M^{1/2}}\sqrt{\left(\frac{\partial^2 U_0}{\partial V^2}\right)}; \quad . \quad . \quad . \quad (16)$$

(16) is in immediate agreement with (9) and (12).

In the anharmonic case the specific heat given in (I, eqn. (29)) is no longer represented by (14), but by

$$\mathscr{C}=3Nk\left\{1+\sum_n(-1)^nB_n\frac{(2n-1)(1-\frac{1}{2}fn)}{2n\,!}I_{2n}\left(\frac{\hbar\omega_m}{kT}\right)^{2n}\right\}, \quad . \quad (17)$$

ω_j and ω_m being the frequencies of the new harmonic approximation. Since θ' is still defined by Debye's formula, or (14), Domb and Salter's method will now give

$$\theta'=\frac{\hbar}{k}\sqrt{\left(\frac{5\mu_2}{3}(1-\tfrac{1}{2}f)\right)}\left[1-\frac{1}{40}\left(\frac{\hbar\omega_m}{kT}\right)^2\frac{2(f-1)}{f-2}\right.$$
$$\left.\times\left\{I_4-\frac{25}{21}\frac{(f-2)^2}{4(f-1)}I_2^2\right\}\Big/I_2+\ldots\right]. \quad . \quad (18)$$

On the other hand, if we fit the proper Debye temperature θ of the new theory by equating $\mathscr{C}(\theta/T)$ from (6) to the lattice expression (17) we get

$$\theta=\frac{\hbar}{k}\sqrt{\left(\frac{5\mu_2}{3}\right)}\left\{1-\frac{1}{40}\left(\frac{\hbar\omega_m}{kT}\right)^2\frac{2(f-1)}{f-2}\left(I_4-\frac{25}{21}I_2^2\right)\Big/I_2+\ldots\right\}; \quad . \quad (19)$$

(18) and (19) are in agreement with (8). The constant term of (19) is the direct extension of (16), but no longer refers to the empirical θ' at all; the slightly different temperature dependences in (18), (19) are unimportant to the present discussion. Although in practice θ and θ' are not very different, it is clear from the earlier discussion that the simple Debye formula $C^D(\theta'/T)$ has no real place in the anharmonic

---

* If there is an external pressure p it is readily shown that

$$\frac{\partial^2\phi}{\partial a^2} \rightarrow \frac{\partial^2 U_0}{\partial V^2}-\frac{2}{3}\frac{p}{V};$$

(16) is then still in agreement with the theoretical value—cf. footnote to (11).

theory (and from this analysis an empirical θ' has no meaning when f exceeds 2). If f is small enough that $\sqrt{(1-\frac{1}{2}f)}$ can be expanded we have for the constant terms of (18) and (19)

$$\theta' \approx \theta(1-\tfrac{1}{4}f).$$

Domb and Salter's expression for the zero energy, $\frac{9}{8}R\theta'$, with θ' the constant limiting value, now corresponds to the use of the constant limiting θ in (5):

$$\mathscr{E}_0=\tfrac{9}{8}R\theta(1-\tfrac{1}{4}f) \approx \tfrac{9}{8}R\theta'.$$

Thus if the empirical $\frac{9}{8}R\theta'$ is still a good approximation to the zero energy it is because the limiting θ is a good approximation to the new Debye parameter, and does not indicate that the customary Debye formulae retain their validity.

The new second moment can not be found from a force constant $\varkappa$ as before since we have no linear wave equations for the ω_j; instead, by (1), we may write formally

$$\mu_2=\mu_2{}^0+\frac{1}{6N}\sum_{jj'} v_{jjj'j'}\overline{q_{j'}{}^2} \approx \frac{\partial^2 U_0}{\partial V^2}+\chi; \quad . \quad . \quad . \quad . \quad (20)$$

χ clearly depends on the vibrational energy, so that (19) is of the same type as the theoretical formula (13) for θ.

For helium, Domb has replaced U_0 in (16) by the energy at 0°K, which includes the essential part of the vibrational term χ; thus (19) with (20) gives the basis for his result in the new theory, provided θ' is replaced by the proper θ—and provided we may work from the first few terms only of (14) or (17) as a good approximation in this particular case. Certainly for solid helium the parameter x of the above analysis is by no means small—for the range of T ($\sim$ 10°K) to be studied in the following paper $\theta'/T \sim$ 7–20. But Domb and Salter show that for a face-centred cubic lattice x may be as large as 6 and yet the first terms of their expansion be adequate, a result[*] depending on relations between the higher order moments of the lattice spectrum $\omega_j{}^0$. We might assume a face-centred cubic structure for helium without much thermodynamical error, and possibly the moments of the new harmonic spectrum ω_j (which depend on the fourth degree terms in the lattice potential as well as on the terms of second degree) will have similar properties. In that case the larger values of $\xi_j=\hbar\omega_j/kT$ which occur in the helium spectrum would be of little effect, even though the exact expression

$$k(\tfrac{1}{2}\xi_j/\sinh \tfrac{1}{2}\xi_j)^2$$

---

[*] The radius of convergence of this expansion, or of that quoted below, is 2π; yet no question of convergence really arises since in any case only a few terms would be used. Domb and Salter quote for the coefficient of $(\hbar\omega_m^0\ kT)^2$ in (15) a value of the order 10^{-4}, even though $I_2{}^0$, for example, is equal to $\frac{1}{2}$—a change in order of magnitude which is very surprising.

for the specific heat of the jth oscillator (~ 0 for $\xi_j \sim 10$ or more) may obviously differ for such values from the first few terms of the expansion

$$1-\frac{1}{12}\xi_j^2+\frac{1}{240}\xi_j^4-\ldots$$

which underlies (14). But nothing very useful can be said without further knowledge of the new moments μ_k, and the possibility of Domb and Salter's analysis remains very doubtful in this particular case. For helium, then, we must regard (13) as essentially a theoretical formula for which the empirical parameter θ (got by fitting the integral expression (6) to experimental specific heats) provides an approximate solution.

ACKNOWLEDGEMENTS

I must again thank Professor Max Born for his interest in this work, and also Dr. R. Haag for some very helpful discussions. The work was done under a Royal Society maintenance grant.

REFERENCES

BORN, M., 1923, *Atomtheorie des festen Zustandes* (Leipzig: Teubner); 1939, *J. Chem. Phys.*, **7**, 591.
DOMB, C., 1952, *Comptes Rendus* 2^e *Réunion Chimie Physique, Paris.*
DOMB, C., and SALTER, L., 1952, *Phil. Mag.* (7), **43**, 1083.
DUGDALE, J. S., and SIMON, F. E., 1953, *Proc. Roy. Soc.* A, **218**, 291.

LIII. CORRESPONDENCE

Paramagnetic Resonance in Sodium and Potassium Superoxides

By J. E. Bennett, D. J. E. Ingram and M. C. R. Symons
University of Southampton

and P. George and J. Stanley Griffith
Department of Colloid Science, Cambridge

[Received February 3, 1955]

The superoxides of sodium and potassium, NaO_2 and KO_2, are of interest because the O_2^- ion has an unpaired electron (Neumann 1934 and Kassatochkin *et al.* 1936). Such compounds should give rise to paramagnetic resonance absorption, and we have recently detected this in both salts.

The pale yellow sodium peroxide, available commercially, was investigated first. Chemical and physical tests show that this substance contains about 10% of the higher oxide NaO_2 (George 1942); and it can thus be used directly as a magnetically dilute sample of the O_2^- ion, the other anions present being diamagnetic. The amorphous mixture was placed in a dried cavity resonator, and its absorption studied at 90°K. A broad asymmetrical line was obtained, having a maximum intensity at high fields, and falling off to a marked shoulder at low fields. Measurements were made at 9000 Mc/s, 23 000 Mc/s and 36 000 Mc/s, and the separation between the low-field shoulder and the high-field maximum was found to be accurately proportional to the frequency used. This shows that the spread of the absorption line is due to a g-value variation, and not an energy level splitting. The g-values obtained were $g_{\parallel}=2{\cdot}175\pm0{\cdot}005$ and $g_{\perp}=2{\cdot}002\pm0{\cdot}005$. Within the larger experimental error of $\pm0{\cdot}05$, the values obtained from the potassium superoxide, prepared by passing oxygen over the heated distilled metal, were identical. Complete disappearance of the signal, when the superoxides were treated with water, confirmed that it was due to the O_2^- ions.

We may interpret these results in terms of the electronic structure of the ground state of the O_2^- ion. In molecular orbital notation this is expected to be

$$(\sigma_g\ 1s)^2\ (\sigma_u\ 1s)^2\ (\sigma_g\ 2s)^2\ (\sigma_u\ 2s)^2\ (\sigma_g\ 2p)^2\ (\pi_u\ 2p)^4\ (\pi_g\ 2p)^3\ \text{(Massey 1938).}$$

As with nitric oxide, the free ion would be in a $^2\Pi$ state, the spin-orbit coupling giving a $^2\Pi_{1/2}$ and $^2\Pi_{3/2}$ state. In nitric oxide $^2\Pi_{1/2}$ lies below $^2\Pi_{3/2}$; O_2^-, being one electron short of the closed shell of F_2, will have the multiplet inverted with $^2\Pi_{3/2}$ below $^2\Pi_{1/2}$. However in the solid at low temperatures we expect the symmetry about the molecular axis to be removed (Zhdanov and Zvonkova 1952), one of the π_g 2p orbitals having a higher energy than the other. The magnetic properties of the ion will then depend upon the ratio, μ, of this energy difference to the spin–orbit coupling constant. Assuming the ion is not free to rotate, we distinguish two limiting cases for the lower state of the ion. For μ zero we have the free ion with $g_{\parallel}=4$, $g_{\perp}=0$; for μ infinite the orbital contribution is completely quenched giving $g_{\parallel}=g_{\perp}=2$; and for intermediate values $2<g_{\parallel}<4$, $0<g_{\perp}<2$. The detailed theory gives $g_{\perp}=1{\cdot}99$ when $g_{\parallel}=2{\cdot}175$, in reasonable accord with the results quoted above. Within the experimental error, μ is the same for NaO_2 as for KO_2 which is a little surprising because they probably differ in crystal structure (Templeton and Dauber 1950, Zhdanov and Zvonkova 1952).

Preliminary measurements on potassium ozonate give a symmetrical absorption line with a much smaller g variation, centred on the free-spin value. In contrast to this and the superoxides, the absorption obtained from frozen solutions of chlorine dioxide is shifted to lower field values, and hyperfine components due to interaction with the chlorine nuclei are resolved in the wings. This is to be expected as the unpaired electron moves over the whole molecule in this case. Further measurements are in progress on all these compounds, and the theory and results will be reported in detail in the near future.

REFERENCES

GEORGE, P., 1942 a, *Discussions of Faraday Society*, No. 2, 203, 218; 1942 b, *J. Chem. Soc.* (in the press).

KASSATOCHKIN, W., and KOTOW, W., 1936, *J. Chem. Phys.*, **4,** 458.

MASSEY, H. S. W., 1938, *Negative Ions* (Cambridge: University Press), p. 27.

NEUMAN, E. W., 1934, *J. Chem. Phys.*, **2,** 31.

TEMPLETON, D. H., and DAUBEN, C. H., 1950, *J. Amer. Chem. Soc.*, **72,** 2251.

ZHDANOV, G. S., and ZVONKOVA, Z. V., 1952, *Doklady. Acad. Nauk. S.S.S.R.*, **82,** 743. (See *Chemical Abstracts*, 1952, 6893 h.)

The Decay of 175 *and* 177 *Ytterbium*

By H. de Waard
Nobel Institute for Physics, Stockholm*

[Revised MS. received February 16, 1955]

The only spectroscopical measurements on the β^--active isotopes of ytterbium hitherto reported are those of Cork *et al.* (1950) on ^{175}Yb and those of McGowan (1951) on ^{177}Yb. These authors have not observed the rotational levels found by Temmer and Heydenburg (1954) in lutetium by Coulomb excitation. A part of the β-decay from the ground states of 175 and 177 ytterbium should lead to the first rotational states in the lutetium daughter nuclei and γ-rays de-exciting these states should therefore be found in the decay of these ytterbium isotopes. Such γ-rays were indeed observed in the present investigation.

1. ^{175}Yb (4·2 d). 99·8% pure Yb_2O_3 was irradiated for one week at Harwell. A part of the active material was then further purified by ion exchange chromatography. The γ-spectrum of this activity was studied with a scintillation spectrometer, conversion and β-spectra were taken with a double focussing and an intermediate image magnetic spectrometer, respectively. β–γ and e^-–γ coincidences and delayed coincidences were measured in the intermediate image spectrometer with a γ-recording NaI(Tl)-crystal placed directly behind the source. An oscilloscope+multiplier arrangement resembling that described by Hofstadter and McIntyre (1950) was used for recording coincidences between selected lines of the γ-spectrum and electrons focussed by the magnetic lens on the detector Geiger counter. The results obtained from these measurements are summarized in tables 1 and 2.

Table 1. γ-rays in the Decay of ^{175}Yb

γ-ray	γ-energy (kev)	conv. ratios	conv. coeff.	rel. int. γ-rays
γ_1	113·0±0·3	$K/(L+M+N)=2{\cdot}5\pm0{\cdot}5$	$\alpha_K=2{\cdot}25\pm0{\cdot}5$	$\gamma_1/\gamma_2=0{\cdot}5\pm0{\cdot}05$
γ_2	281±1	$K/L>4$		
		$K\gamma_2/K\gamma_3=0{\cdot}3\pm0{\cdot}04$		$\gamma_2/\gamma_3=0{\cdot}5\pm0{\cdot}05$
γ_3	395·1±0·3	$K/L=5{\cdot}9\pm0{\cdot}7$		
		$L/(M+N)=4{\cdot}3\pm1$		

The decay scheme of ^{175}Yb, given in fig. 1(*a*) could be determined unambiguously from the experimental results. The first excited level of ^{175}Lu is undoubtedly identical with the first rotational level observed by Heydenburg and Temmer and must therefore be assigned 9/2+. The conversion and intensity data of γ_2 and γ_3 show that these γ-rays very probably are both mixtures of $E1+M2$-radiation (with

---

* Communicated by Professor Manne Siegbahn.

$M2/E1 = 4 \pm 2\%$ for γ_2 and $M2/E1 = 26 \pm 7\%$ for γ_3), in which case a 7/2— or 9/2— assignment must be made for the second level. A measurement of the angular correlation between γ_1 and γ_2, described in the accompanying letter (Hartmann *et al.* 1955), show that a 9/2— assignment is most probable.

Table 2. β-components in the Decay of ^{175}Yb

β-comp.	max. en. (kev)	rel. int. (%) (approx.)	log fT	in coinc. with
β_0	463 ± 3	87	$6{\cdot}25 \pm 0{\cdot}05$	
β_1		3	$7{\cdot}3 \pm 0{\cdot}2$	γ_1
β_2	72 ± 3	10	$4{\cdot}8 \pm 0{\cdot}2$	γ_2, γ_3

Fig. 1

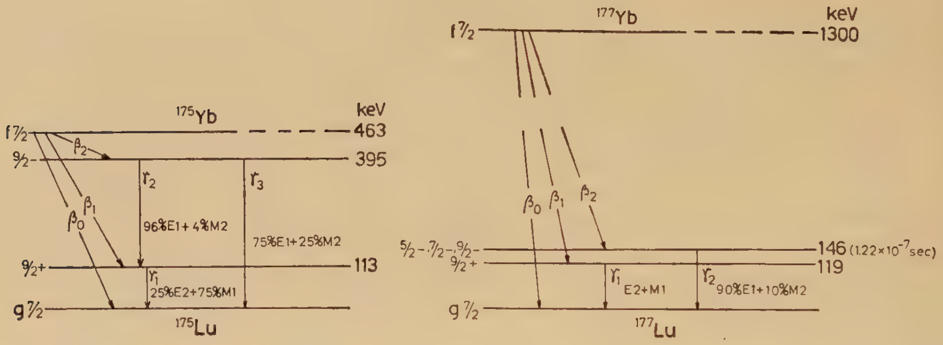

(*a*) (*b*)

Disintegration schemes of ^{175}Yb (*a*) and ^{177}Yb (*b*). The index numbers of the β- and γ-rays refer to tables 1 and 2 (^{175}Yb) and 3 and 4 (^{177}Yb).

From delayed coincidence measurements performed both with the coincidence arrangement mentioned above and with a fast delayed coincidence circuit of similar construction as one described earlier (de Waard 1952), upper limits of 6×10^{-8} sec for the half life of the 395 kev level and of 2×10^{-9} sec for that of the 113 kev level could be determined.

2. ^{177}Yb (1·8 h). This activity was produced by fast neutron irradiation of the 99·8% pure Yb_2O_3 in the big cyclotron of this Institute. The activated oxide was used without further purification. The γ-spectrum of this activity was studied with a scintillation spectrometer, conversion and β-spectra were taken in an intermediate image magnetic spectrometer. β–γ coincidence and delayed coincidence measurements were made with scintillation detectors for both β- and γ-rays, utilizing the oscilloscope coincidence arrangement used also for the measurements on ^{175}Yb. From delayed coincidence plots a half life of $0{\cdot}122 \pm 0{\cdot}005$ μsec was deduced for the state at 146 kev in ^{177}Lu, in good agreement with the value of $0{\cdot}13 \pm 0{\cdot}02$ μsec found by McGowan (1951). Further results obtained from the measurements are given in tables 3 and 4,

The decay scheme of ^{177}Yb, given in fig. 1(*b*), follows from the experimental results. The first excited state of ^{177}Lu must be the first rotational level of that nucleus (9/2+). The conversion data of γ_2 seem to be in accordance only with a 90% $E1+10\%$ $M2$ character for this ray. The 146 kev level should therefore have a negative parity and a spin 5/2, 7/2 or 9/2.

Table 3. γ-rays in the Decay of ^{177}Yb

γ-ray	γ-energy (kev)	conv. ratios $(K/L+M)$	conv. coeff.	rel. int. γ-rays
γ_1	119 ± 1	3^{+3}_{-1}		
γ_2	146 ± 1	$3{\cdot}5^{+1{\cdot}5}_{-0{\cdot}5}$	$\alpha_K=0{\cdot}63\pm0{\cdot}08$	$\gamma_1/\gamma_2=0{\cdot}18\pm0{\cdot}04$

Table 4. β-components in the Decay of ^{177}Yb

β-comp.	max. en. (MEV)	rel. int. (%) (approx.)	log fT
β_0	$1{\cdot}30\pm0{\cdot}05$	88	$6{\cdot}20\pm0{\cdot}05$
β_1		3	$7{\cdot}55\pm0{\cdot}2$
β_2		·9	$7{\cdot}05\pm0{\cdot}2$

From the character of γ_2 and the lifetime of the 146 kev level follows a square of nuclear matrix element $|M|^2\sim1$ for de-excitation of this level by $M2$ radiation and $|M|^2\sim5\times10^{-6}$ for de-excitation by $E1$ radiation ($|M|^2$ is expressed in ‘ Weisskopf units ’). Such very slow $E1$ transitions have also been found by Sunyar (1955).

A more extensive report on the work summarized here will be published in *Arkiv för Fysik*.

The author is much indebted to Professor Manne Siegbahn for the privilege to work at The Nobel Institute for Physics, to Mr. W. Forsling for making the chemical separations and to Mr. H. Atterling for arranging the cyclotron irradiations.

A stipend of the Netherlands Organization for Pure Research is gratefully acknowledged.

REFERENCES

CORK, J. M., BRANYAN, C. E., RUTLEDGE, W. C., and STODDARD, A. E., 1950, *Phys. Rev.*, **78,** 95.
DE WAARD, H., 1952, *Physica*, **18,** 1151.
Referred to by: GOLDHABER, M., and SUNYAR, A. W., 1955, chapter XVI, “ Beta and Gamma-Ray Spectroscopy ”, edited by K. Siegbahn, Amsterdam (to appear shortly).
ÅKERLIND, L., HARTMANN, B., and WIEDLING, T., 1955, *Phil. Mag.*, **46,** 448.
HOFSTADTER, R., and MCINTYRE, J. A., 1950, *Rev. Sci. Instr.*, **21,** 52.
MCGOWAN, F. K., 1951, *ORNL-report*, 952.
TEMMER, G. M., and HEYDENBURG, N. P., 1954, *Phys. Rev.*, **94,** 1399.

Angular Correlation of Gamma Rays in ^{175}Lu

By L. Åkerlind, B. Hartmann and T. Wiedling
Laboratory of Physics, University of Stockholm, Sweden

[Received February 16, 1955]

As a complement to a β-spectroscopic investigation of ^{175}Yb reported by De Waard (1955) we have made an investigation of the angular correlation of the two cascaded gamma rays of 281 kev and 113 kev energies in ^{175}Lu following the β-decay of ^{175}Yb.

The investigation was made with two scintillation spectrometers coupled in coincidence. One spectrometer accepted only the full energy photopeak of the 113 kev gamma ray. The 53 kev x-ray peak of Lu was suppressed by shielding the NaI(Tl) crystal in the front with 1·3 mm tin. The discriminator in the other channel was put just below the 281 kev photopeak. About 0·7 mm lead was placed in front of this NaI(Tl) crystal. With the exception of the lines mentioned above and the cross-over line at 395 kev no other lines belonging to the decay of ^{175}Yb were found resolved by the scintillation spectrometers.

Pile irradiated Yb_2O_3 was chemically purified by ion exchange chromatography. The correlation measurements were performed on a source of $Yb(NO_3)_3$ dissolved in water. The volume of the solution was about 6×10^{-3} cm^3. Coincidences were collected for every fifteen degrees between 90° and 180°.

A least squares fit of the experimental points to the function $W(\theta)=1+\Sigma A_{2L}P_{2L}(\cos\theta)$, corrrected for the finite angular resolution of the counters, was made yielding a normalized experimental correlation function $W(\theta)=1+(0{\cdot}202\pm0{\cdot}012)P_2(\cos\theta)$. A small A_4 coefficient with a value of about $-0{\cdot}004$ was found, too.

The ground state of ^{175}Lu is known to have spin 7/2 (Mack 1950). The first excited state of ^{175}Lu has been identified as a rotational level and must therefore be assigned 9/2 (De Waard 1955). Conversion data seems to characterize this transition as a mixture of electric quadrupole and magnetic dipole radiation, $E2/M1=0{\cdot}33\pm0{\cdot}10$, and further the 281 kev gamma ray as a mixture $M2/E1=(4\pm2)\%$ so that the 395 kev level must probably be assigned 7/2— or 9/2— (De Waard 1955).

We therefore tried the two following spin sequences: $9/2\rightarrow9/2\rightarrow7/2$ and $7/2\rightarrow9/2\rightarrow7/2$. It is immediately found that pure character of both cascaded γ-rays is not consistent with the correlation measurement (Biedenharn and Rose 1953). Assuming a spin 9/2 for the excited state at 395 kev and a pure character of the transition leading from that state to the first excited state our correlation measurement gives a mixing ratio $E2/M1=(17\pm1)\%$ for the rotational transition to the ground state while a spin 7/2 and pure character of the first transition yields $E2/M1=(3{\cdot}1\pm0{\cdot}5)\%$. Both values lie outside the limits of error of the conversion measurements.

When both transitions are mixed a knowledge of one mixing ratio is required to find the mixing ratio of the other (Rose 1954). Using the ratio given by De Waard for the second transition the spin sequence $9/2 \rightarrow 9/2 \rightarrow 7/2$ gives a mixing ratio of 2% for the first transition and $A_4 = -0{\cdot}002$. The mixing ratio is here very insensitive to variations in the mixing ratio of the 113 kev gamma ray.

The spin sequence $7/2 \rightarrow 9/2 \rightarrow 7/2$ gives a mixing ratio of 14% and $A_4 = 0{\cdot}012$. A comparison with spectroscopic results shows that the spin sequence $9/2 \rightarrow 9/2 \rightarrow 7/2$ is most probable.

By making new and more accurate measurements we hope to be able to draw more definite conclusions about the spins and transitions of ^{175}Lu.

REFERENCES

BIEDENHARN, L. C., and ROSE, M. E., 1953, *Rev. Mod. Phys.*, **25**, 729.
DE WAARD, H., 1955, *Phil. Mag.*, **46**, 445.
MACK, J. E., 1950, *Rev. Mod. Phys.*, **22**, 64.
ROSE, M. E., 1954, *Phys. Rev.*, **93**, 477.

Interaction of Dislocations and F-Centres in Sodium Chloride Single Crystals

By S. Amelinckx, W. Van der Vorst, R. Gevers and W. Dekeyser
Laboratorium voor Kristalkunde, der Rijksuniversiteit, Rozier, 6, Gent (Belgium)

[Received February 8, 1955]

Hedges and Mitchell (1952) have given the first direct evidence for the existence of networks of dislocations. They have shown that photolytic silver aggregates along certain lines in AgBr single crystals during the ' print out ' process and they identified these lines as dislocation lines.

We have now succeeded in revealing dislocation lines in the interior of melt grown and natural rock salt crystals. This was achieved by additive coloration by means of sodium metal and by the precipitation of small additions of $BaCl_2$.

For the coloration of the crystals by sodium metal, we used, in a slightly modified form, a technique described by Rexner (1932).

This method consists essentially in enclosing a certain quantity of sodium metal in a cavity made in the crystal. After a suitable heat treatment colloidal sodium metal seggregates out along certain surfaces and along certain lines within the crystal.

Photograph 1 (photographs 1–4, Plate 6) is an example of a set of very low angle grain boundaries as observed in a well annealed ' single crystal ' by means of the ultra microscope, at low magnification (100 ×). The heavy lines correspond to grain boundaries which are practically normal to the plane of observation. The lines of intersection of these inner boundaries with the cleavage plane correspond exactly to the pattern of etchpits which is revealed after etching with methyl alcohol (Amelinckx 1954). In many cases the inner surfaces visibly consist of networks of lines, as can be seen on photograph 4 (500 ×).

Observations on polygonized specimens prove still more conclusively that the observed pattern is due to dislocations. The visible inner surfaces (photograph 2, 100 ×) have exactly the orientation of the walls of dislocations built up during the polygonization of bent specimens. Photograph 3 gives at higher magnification (500 ×) an example of a pattern obtained from such a specimen. The walls have the orientations (110) and $(1\bar{1}0)$ i.e. normal to active glide planes. Some of them (e.g. AB) visibly consist of well separated dots. When focusing lower and lower into the crystal, the location of these dots does not change appreciably, suggesting that they mark parallel dislocation lines normal to the plane of observation.

Similar results as described above can be obtained by the addition of a small quantity of $BaCl_2$ (0·002 to 0·003 g $BaCl_2.2H_2O$ per 1 g NaCl) to the NaCl-melt. On slow cooling, the impurity ($BaCl_2$ or a mixed

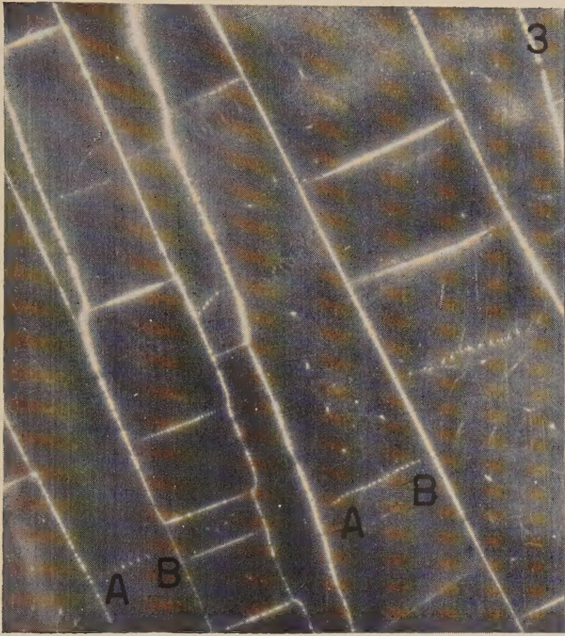

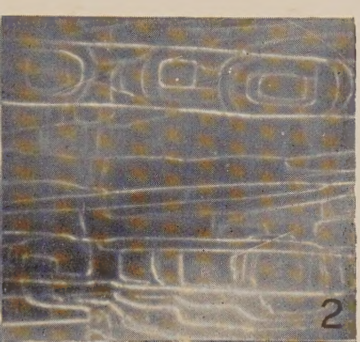

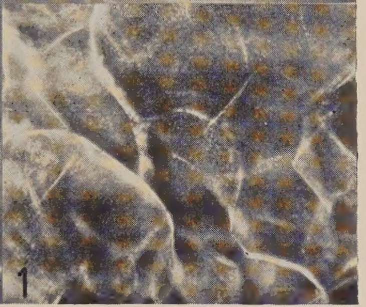

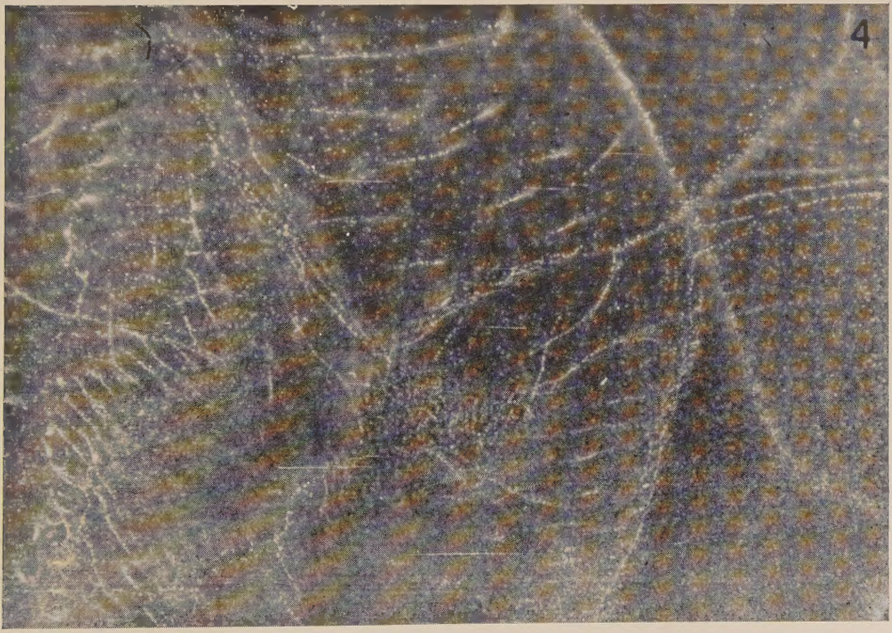

Photograph 1

Inner surfaces in NaCl single crystal revealed by additive coloration with sodium metal (100 ×).

Photograph 2

Dislocation walls due to the polygonization of a bent NaCl single crystal (100 ×).

Photograph 3

Dislocation walls due to polygonization of a bent NaCl single crystal (higher magnification, 500 ×). Some of the walls (AB) visibly consist of separated lines perpendicular to the plane under observation.

Photograph 4

Inner surfaces in deformed and annealed NaCl single crystal (higher magnification, 500 ×).

LIV. REVIEWS OF BOOKS

Isotope Geology. By K. Rankama. (London: Pergamon Press Ltd.) [Pp. 535.] Price £3 15*s*. 0*d*.

'Isotope Geology' is defined by Rankama as "investigation of geological phenomena by means of stable and unstable isotopes of elements and of changes in their abundance". Such geological phenomena include determination of geological age, generation of heat by radioactivity, measurement of paleotemperatures, origin of coal, calcite etc. The appearance of 'Nuclear Geology' (H. Faul, Editor (John Wiley)) close on the heels of 'Isotope Geology' and which covers some of the same field, together with the possibility of a third book, all testify to the intense activity which has recently developed in the field covered by 'Isotope Geology'.

Rankama points out that most of the research has in the past been carried out by physicists and chemists and the first part of the book (chapters on Atoms, Nuclei and Nuclides, Radioactivity, Mass Analysis, Isotope Fractionation, Properties of Nuclear Radiation) is addressed essentially to geologists. The second part (Natural Science of Nuclides) represents the heart of the book. Here a chapter is devoted to each element. Literature coverage is unusually thorough and in all some 1244 entries appear in the bibliography. One is impressed by the enormous disparity in the amount of investigation which has been carried out on different elements. Carbon in particular, has been intensely investigated and some 330 C^{12}/C^{13} ratios are listed.

Although addressed primarily fo the geologist, 'Isotope Geology' will be of interest to a much wider audience and all those seeking either general information in the field of isotope geology, a thorough reference source, or a guide to problems awaiting investigation—and these indeed are many—will find the book invaluable.

L. H. A.

Introduction to Atomic and Nuclear Physics. By Henry Semat. (London: Chapman and Hall Ltd.) Price 50*s*. net.

This is a very useful American book for a reader who wants to look up hurriedly the evidence for the existence for a neutrino, the properties of the V particle or the difference between the various types of particle accelerator. So far as the reviewer can see it is reliable and completely up-to-date. Inevitably in a book that covers all atomic and nuclear physics in 500 pages the treatment is superficial, and at times it is not completely clear; for instance in the discussion of fission (p. 404) it is not stated whether the critical energy for fission is a quantity that has been observed or calculated.

As a minor criticism: is it still necessary to include an appendix on the evaluation of the integrals $\int p\,dq$ which occur in the old quantum theory? And one might wish that an author of a text book would set a good example on how to write formulae in a way that makes as little use of hand-setting as possible. On page 380 we find

$$\mathrm{e}^{-\frac{2}{\hbar}\int_{R}^{r_1}\sqrt{2M(U-\epsilon_\alpha)}\,dr}$$

which offends against almost every rule that the editors of the *Philosophical Magazine* would commend to their contributors.

N. F. M.

[*The Editors do not hold themselves responsible for the views expressed by their correspondents.*]